Abstract

Since the innovator speech of Nobel laureate Richard Feynman in the early 1959, the progress of nanotechnology has been a succession of inventions and developments. One of those is the invention in 1986 of the Atomic Force Microscope.

In this work is explained in the first two chapters an historical introduction over Scanning Tunneling Microscopy and in particular over Atomic Force Microscopy. Following with a detailed description of the physics behind it.

After that, this work continues describing the equipment used for imaging. Due to mayor access in the design and specifications of two AFM manufacturers, we decided to make a comparison of our equipment with other AFM manufacturer evidencing pros and contras in: design, performance and specifications.

Even the big steps done and discoveries made in this field there are a lot of unknown parameters that sometimes are correlated simply or in a complex way. For this, the use of an AFM isn't a simple task that can be learned easily. A short users manual for imaging with Cervantes Nanotec is present in chapter 4.

Meanwhile the biological applications have a bigger impact. For this that a big part of my work is dedicated to image bacterial samples and the results achieved were satisfactory.

First, it was achieved imaging and mechanical characterization of biofilms. Second, it was possible to image in liquid environment bacterial samples and biofilm connections.

Another big achievement was using the AFM as a nanomanipulating tool, able to modify the sample surface. The idea is using tip, in the lithography section for moving, grasping breaking bacteria membranes while forces exerted are calculated during manipulation.

In conclusions we propose in which direction it should continue the study of manipulating, and is proposed another way in calibrating lateral forces.

Resumen

Desde el discurso innovador del premio Nobel Richard Feynman en los principios de 1959, el progreso de la nanotecnología ha sido una sucesión de invenciones y desarrollos. Uno de estas invenciones es el Microscopio a Fuerzas Atómicas (AFM) en el 1986 por Binning.

En éste trabajo se explica en los primeros dos capítulos una breve historia sobre las Scanning Tunneling Microscopy y más en particular sobre el AFM, seguido de una descripción detallada de las leyes físicas que están detrás de esta invención.

Después de esto, se continua con una descripción del equipo usado y debido a mayor acceso en el diseño y las especificaciones de dos productores de AFM, se ha decidido hacer una comparación entre los dos evidenciando los pros y los contras sobre el diseño, actuación y especificaciones.

Aunque la grande invención, hay muchos parámetros que aún no se sabe como están relacionados entre ellos, algunos sencillamente y otros en manera más complicada. Por esto que se ha pensado de hacer un pequeño manual de uso para los principiantes, que es el capítulo 4.

Mientras que las aplicaciones biológicas del AFM tienen un mayor impacto debido a la cantidad de información que se puede sacar. En el capítulo 5 se han conseguido dos resultados muy buenos. Primero, se ha hecho posible hacer imágenes y caracterizar mecánicamente biofilms. Segundo, se ha conseguido hacer imágenes en ambiente liquido de biofilms.

Otro gran resultado es el utilice del AFM como una herramienta para la manipulación de superficies y membranas. Básicamente ha sido usada la punta de AFM como una nano-herramienta capaz de mover, rascar y romper membranas de bacterias.

En conclusión, proponemos unas futuras direcciones de estudio, y una innovadora manera de calibrar la fuerza lateral.

General Index pp.3

Chapter 1: Introduction

On the evening of December 29, 1959, Nobel Laureate Richard Feynman [1] delivered a visionary 7000 word after-dinner talk to a meeting of the American Physical Society at the California Institute of Technology. It was entitled "There's Plenty of Room at the Bottom". It was the defining moment for nanoscience and the future of nanotechnology.

"I would like to describe a field in which little has been done, but in which an enormous amount can be done in principle…What I want to talk about is the problem of manipulating and controlling things on a small scale." Richard Feynman.

In the course of his lecture, Feynman made this prediction: "In the year 2000, when they look back at this age, they will wonder why it was not until the year 1960 that anybody began seriously to move in this direction." But there's a simple reason people didn't immediately begin working at the nanoscale. They didn't have the tools. The scanning tunneling microscope and the atomic force microscope were the two most important tools at the beginning of the nanoscale revolution, but now there's an expanding toolkit of devices used to observe, measure, and manipulate nanoscale structures. And as we learn more about the nanoscale world, we'll be able to make even better tools. We had to wait till 1981 that Nobel Laureate Binning, invents Scanning Tunneling Microscope; a modern tool for studying the morphology and the local properties of the solid body surfaces with a high spatial resolution.

In chapter 2 we are going to speak about the physics that stays behind the SPM and more in particular of Atomic Force Microscope. Through some simple passages we will discover the forces that stays behind and some simplified models of AFM feedback and cantilever motion equations.

Instead in chapter 3 we discuss the state of art in manufacturing AFM. And more in particular on *Nanotec Electrónica* and *Nanonics*. The first one is the producer of our own microscope and the second one are the manufacturers of *Multiprobe 4000* explained more in detail further.

Chapter 4 is a short AFM manual for beginners. Briefly introducing WSxM (software controlling AFM electronics), we describe how to use the microscope in the three main modes: contact (DC), dynamic (AC) and Jumping (JM). The equivalent open source code is named GxSM, and in this chapter we describe another open source solution to SPM.

Chapter 5 includes a good biological study over two main types of bacteria: Pseudomonas aeruginosa and Escherichia Coli as among the most popular and of relevant study interest. We pass through an optical phase, later a topographical and mechanical characterization of their

membranes. The main interest in characterizing these two groups of bacteria is: their ability to survive in extreme conditions (good for our experiments in air), their ability to form biofilms presenting resistance to antibiotics (as different studies have been observing).

We conclude this chapter with two main achievings:

1. Mechanical and topographical characterization of biofilm over Pseudomonas and E.Coli.
2. Topographical characterization of biofilms in liquid environment.

Chapter 6 gives another optics of AFM. Till now we have been customized to see at an AFM as a proximity microscope; good for discovering rigid body surface properties. But here we use AFM probes for manipulating surfaces, moving bacteria, breaking links between them and more important is the ability to record forces the probe is experimenting during manipulation.

In this chapter are exposed some simple manipulations like: grasping surface, moving bacteria, breaking membranes, calculating forces exerted over the probe. Some simple tasks but really important regarding information we get. Till now, only few research groups have been able to measure forces exerted over bacterial membranes using AFM.

"Are you having trouble imagining a nanometer? If you are, don't feel bad. You aren't alone."

Chapter 2: Introduction over Scanning Probe Microscopy **pp.9**

Chapter Index

2.1 Introduction to SPM

The concept of the atom has been around in one form or another since the ancient Greeks. Yet at the beginning of the twentieth century, there were still some scientists who doubted the atom's existence. To them, an atom was simply a useful fiction. It took Albert Einstein, in a 1905 paper, to explain the indirect evidence for the existence of atoms and to show that the sizes of atoms and molecules could be determined. Nonetheless, scientists doubted that we'd ever be able to observe an atom, or anything else smaller than a few hundred nanometers, because of diffraction limits imposed by the nature of the light, until (SPM)invention in 1981.

The Scanning Probe Microscopy (SPM) is one of the powerful modern research techniques that allow investigating the morphology and the local properties of the solid body surface with high spatial resolution. During last decades the scanning probe microscopy has turned from an exotic technique accessible only to a limited number of research groups, to a widespread and successfully used research tool of surface properties. Currently, practically every research in the field of surface physics and thin-film technologies applies the SPM techniques. The scanning probe microscopy has formed also a basis for development of new methods in nanotechnology, i.e. the technology of creation of structures at nanometric scales.

The Scanning Tunneling Microscope (STM) is the first in the probe microscopes family; invented in 1981 by the Swiss scientists G. Binnig and H. Rohrer [2][3]. In their works they have shown, that this is a quite simple and rather effective way to study a surface with spatial resolution down to atomic one. Their technique was fully acknowledged after visualization of the atomic structure of the surface of some materials and, particularly, the reconstructed surface of silicon. In 1986, G. Binnig and H. Rohrer were awarded the Nobel Prize in physics for invention of the tunneling microscope.

After the tunneling microscope creation, Atomic Force Microscope (AFM), Magnetic Force Microscope (MFM), Electric Force Microscope (EFM), Scanning Near-field Optical Microscope ($SNOM$) and many other devices having similar working principles and named as scanning probe microscopes have been created within a short period of time.

Working principle: By using specially prepared tips in the form of needles is performed the analysis of a surface and of its local properties. The size of the working part of such tips (the apex) is about ten nanometers. The usual tip - surface distance in probe microscopes is about 0.1 – 10 nanometers.

Various types of interaction of the tip with the surface are exploited in different types of probe microscopes. For example the tunnel microscope is based on the phenomenon of a tunneling current between a metal needle and a conducting sample.

2.2 Basic stages in SPM development and the established types

Since 1981, there have been developed several techniques and here bellow we are going to list the most important ones in a chronologic order.

1981 - *Scanning tunneling microscope*. G. Binnig, H. Rohrer.
Atomic resolution images of conducting surfaces.

1982 - *Scanning near-field optical microscope*. D. W. Pohl.
Resolution of 50 nanometers in optical images.

1984 - *Scanning capacitive microscope*. J. R. Matey, J. Blanc.
500 nm (lateral resolution) images of capacitance variation.

1985 - *Scanning thermal microscope*. C. C. Williams, H. K. Wickramasinghe.
Resolution of 50 nm in thermal images.

1986 - *Atomic-force microscope*. G. Binnig, C. F. Quate, Ch. Gerber.
Atomic resolution on non-conducting (and conducting) samples.

1987 - *Magnetic-force microscope*. Y. Martin, H. K. Wickramasinghe.
Resolution of 100 nanometers in magnetic images.
"Frictional"force microscope. C. M. Mate, G. M. McClelland, S. Chiang.
Atomic-scale images of lateral (″frictional″) forces.
Electric force microscope. Y. Martin, D. W. Abraham, H. K. Wickramasinghe.
Detecting of single charges on a sample surface.
Inelastic tunneling STM spectroscopy. D. P. E. Smith, D. Kirk, C. F. Quare.
Detection of phonon spectra of molecules in *STM*.
Laser driven STM. L. Arnold, W. Krieger, H. Walther.
Imaging by non-linear mixing of optical waves in *STM*.

1988 - *Ballistic electron emission microscope*. W. J. Kaiser.
Schottky barriers investigation with nanometer resolution.
Inverse photoemission microscope. J. H. Coombs, J. K. Gimzewski, B. Reihl et al
Detection of luminescence spectra on nanometer scales.

1989 – *Near-field acoustic microscope*. K. Takata, T. Hasegawa, S. Hosaka, S. Hosoki.

Low-frequency acoustic measurements with the resolution of 10 nm.

Scanning noise microscope. R. Moller A. Esslinger, B. Koslowski.

Detection of tunnel current without voltage bias.

Scanning spin - precession microscope. Y. Manassen, R. Hamers, J. Demuth

Visualization of spin in a paramagnetics with 1 nm resolution.

Scanning ion-conductance microscope. P. Hansma, B. Drake, O. Marti, S. Gould

Imaging in electrolyte with 500 nm resolution.

Scanning electrochemical microscope. O. E. Husser, D. H. Craston, A. J. Bard.

1990 - *Scanning chemical potential microscope.* C. C. Williams, H. K. Wickramasinghe.

Atomic scale images of chemical potential variation.

Photovoltage STM. R. J. Hamers, K. Markert.

Photovoltage images on nanometer scale.

1991 - *Kelvin probe force microscope*.N. Nonnenmacher, M. P. O'Boyle

1994 – *Apertureless near-field optical microscope*.

F. Zenhausern, M. P. O'Boyle, H. K. Wickramasinghe.

Optical microscopy with 1 nm resolution.

Many other microscopy techniques have been developed based upon *SPM*. The followings are the established types:

- (*AFM*) Atomic force microscopy consists of a micro scale cantilever with a sharp tip at its end that is used to scan the specimen surface.
- (*BEEM*) Ballistic electron emission microscopy, studies ballistic electron transport through variety of materials and material interfaces.
- (*EFM*) Electrostatic force microscopy plots the locally charged domains of the sample surface; similar to how *MFM* plots the magnetic domains of the sample surface.
- (*ESTM*) Electrochemical scanning tunneling microscopy, studies the structure of the electrochemical processes at molecular or atomic level.
- (*FMM*) Force modulation microscopy, is an extension of *AFM* imaging that includes characterization of a sample's mechanical properties. Like *LFM* and *MFM*, *FMM* allows simultaneous acquisition of both topographic and material-properties data.
- (*KPFM*) Kelvin probe force microscopy is based on the measurement of the electrostatic forces between the small conducting *AFM* tip and the sample.

- (MFM) Magnetic force microscopy, measures magnetic force between the tip and sample.
- ($MRFM$) Magnetic resonance force microscopy combines the ideas of magnetic resonance imaging (MRI) and AFM.
- ($NSOM$) Near-Field scanning optical microscopy or ($SNOM$), breaks the far field resolution limit by exploiting the properties of evanescent waves.
- (PDM) Phase detection microscopy, is another technique that can be used to map variations in surface properties such as elasticity, adhesion, and friction.
- ($PSTM$) Photon scanning tunneling microscopy.
- ($PTMS$) Photothermal microscopy is derived from two parent instrumental techniques: infrared spectroscopy and AFM.
- ($SECM$) Scanning electrochemical microscopy.
- (SCM) Scanning capacitance microscopy, images spatial variations in capacitance by inducing a voltage between the tip and the sample. Characterizes sample surface using information obtained from electrostatic capacitance changes between surface and probe.
- (SGM) Scanning gate microscopy, with an electrically conductive tip used as a movable gate that couples with a capacitance the sample and probes electrical transport.
- ($SICM$) Scanning ion-conductance microscopy, maps local ion currents above the surface.
- ($SPSM$) Spin polarized microscopy.
- ($SThM$) Scanning thermal microscopy, measures sample's surface thermal conductivity.
- (STM) Scanning tunneling microscopy studies local electronic structure of a sample.
- (SVM) Scanning voltage microscopy is based in obtaining an electric potential map of the raster surface with the use of conductive probes.
- ($SHPM$) Scanning Hall probe microscopy helps creating a magnetic induction map by coupling STM with a semiconductor Hall sensor.

2.3 Scanning Tunneling Microscopy

Historically, the first microscope in the family of probe microscopes is the scanning tunneling microscope. The working principle of STM is based on the phenomenon of electrons tunneling through a narrow potential barrier between a metal tip and a conducting sample in an external electric field.

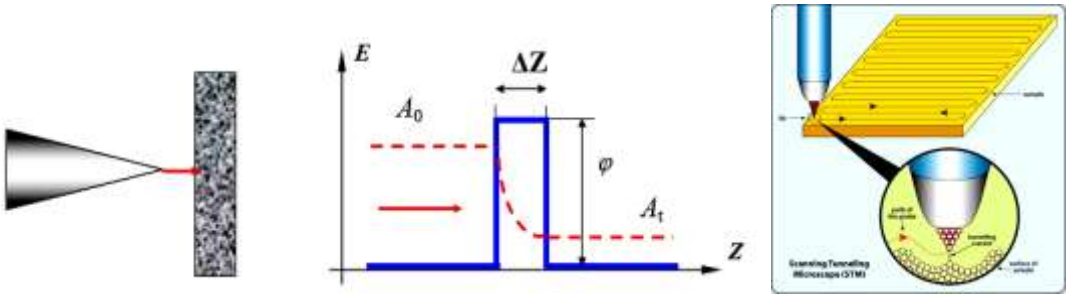

Image 2.1 Scheme of electrons tunneling through a potential barrier in STM.

Here's the basic concept: The STM has a metal needle that scans a sample by moving back and forth over it, gathering information about the curvature of the surface. The STM tip approaches the sample surface to distances of several $\mathring{A}\,ngstroms$. This forms a tunnel transparent barrier, whose size is determined mainly by the values of the work function for electron emission from the tip (φ_T) and from the sample (φ_S). A rectangular shape with effective height equal to the average work function φ^* can approximate the barrier [4]:

$$\varphi^* = \frac{1}{2}(\varphi_T + \varphi_S). \qquad \textit{Eq.2.1}$$

Basically, electrons with energy near the Fermi level E_F participate in the tunneling process. In case of contact of two metals the expression for the tunneling current density (in one-dimensional approximation) is [5], [6]:

$$j_t = j_0\left[\varphi^* \exp(-A\sqrt{\varphi^*}\Delta Z) - (\varphi^* + eV)\exp(-A\sqrt{\varphi^* + eV}\Delta Z)\right] \textit{Eq.2.2}$$

where (ΔZ) is the tunneling distance and j_0 and A are set by the following expressions:

$$j_0 = \frac{e}{2\pi h(\Delta Z^2)} \text{ and } A\frac{4\pi}{h}\sqrt{2m}, \textit{Eq.2.3,2.4}$$

For small values of the bias voltage $(eV < \varphi)$, the current density can be approximated by a simpler expression and in the final formula the exponential dependence is very strong, an even simpler formula is frequently used for estimations and qualitative reasoning:

$$j_t = j_0(V)e^{-\frac{4\pi}{h}\sqrt{2m\varphi^*}\Delta Z}, \textit{Eq.2.5}$$

in which the value $j_0(V)$ is assumed to be not dependent on the tip-sample distance.

The exponential dependence (Equation 2.5) of the tunneling current on distance (ΔZ)

allowsadjusting the tip-sample distance in a tunneling microscope with high accuracy. The STM is an electromechanical system with a negative feedback. The feedback system FS keeps the tunneling current value at the constant level (I_0), selected by the operator. The control of the tunnel current value, and consequently of the tip-sample distance, is performed by moving the tip along Z_{axis} with the help of a piezoelectric element (Image 2.2).

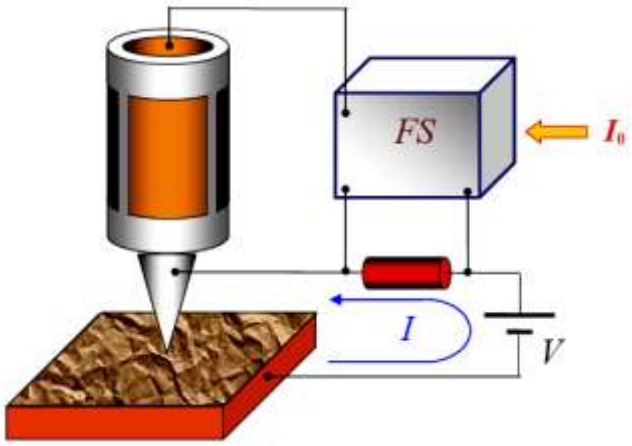

Image 2.2Simplified block-diagram of the feedback in STM.

2.4 Atomic Force Microscope

Atomic Force Microscope $(AFM)$was invented in 1986 by G. Binnig, C. F. Quate and C. Herber [7] The AFM working principle is the measurement of the interactive force between a tip and the sample surface using special probes made by an elastic cantilever with a sharp tip on the end (Image 2.3). The force applied to the tip by the surface, results in bending of the cantilever. Measuring the cantilever deflection, it is possible to evaluate the tip–surface interactive force and surface topography.

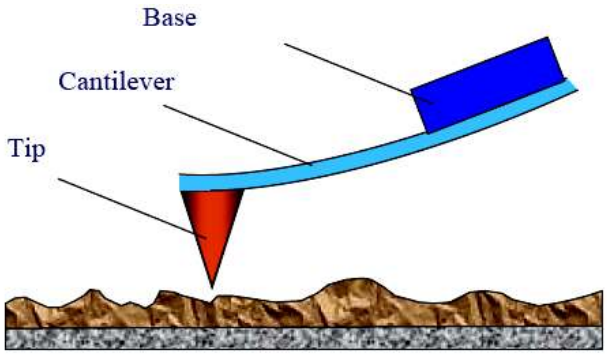

Image 2.3 AFM probe schematic picture.

The AFMprobe is a flexible cantilever, we can think of it as a diminutive diving board with a tip attached to its underside. As the tip scans the sample, the force between them is monitored. To keep the force constant, the cantilever is moved up and down. In addition to gathering information about the topography of a sample, the AFM can measure the friction between the tip and the sample, and it can also measure the elasticity, or softness, of a sample.

2.4.1 Forces in the "*NanoWorld*"

The first and the mayor force that all AFM take in account are the Van der Waals forces [8]. The Van der Waals potential energy of two atoms, located at a distance r from each other, is approximated by the exponential function - Lennard-Jones potential:

$$U_{LD}(r) = U_0\left\{-2\left(\frac{r_0}{r}\right)^6 + \left(\frac{r_0}{r}\right)^{12}\right\}, \qquad Eq.2.6$$

The first term of the sum describes the long-distance attraction caused, basically, by a dipole-dipole interaction and the second term takes into account the short-range repulsion due to the Pauli exclusion principle. The parameter r_0 is the equilibrium distance between atoms, the energy value in the minimum.

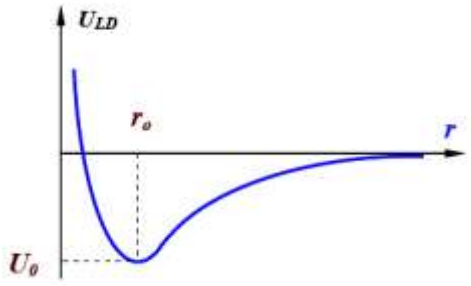

Image 2.4Lennard-Jones potential qualitative form.

Lennard-Jones potential allows estimating the interaction force of a tip with a sample [9], [10]. The energy of the tip-sample system can be derived, adding elementary interactions for the entire tip and sample atoms.

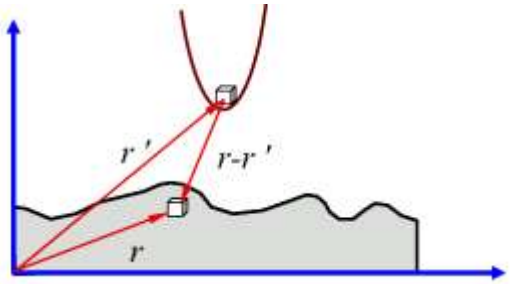

Image 2.5 How to calculate the energy of interaction between tip and sample atoms.

Then for the energy of interaction we get:

$$W_{PS} = \iint_{V_P V_S} U_{LD}(r - r')n_P(r')n_S(r)dVdV', \qquad Eq.2.7$$

where $n_S(r)$ and $n_P(r')$ are the densities of atoms in the sample and in the tip. Accordingly, the force affecting the tip from a surface can be calculated as follows:

$$\vec{F} = -grad(W_{PS}), \qquad Eq.\ 2.8$$

Generally this force has both a component normal to the sample surface and a lateral component (laying in the plane of the sample surface). Actual interaction of a tip with a sample has more complex character; however, the basic features are the same: the AFM tip is attracted by the sample at large distances and repelled at small distances.

Acquisition of a AFM surface topography consists in recording the small deflections of the elastic cantilever. For this purpose optical methods (Image 2.6) are widely used in atomic force microscopy (the technique named *beam-bounce*).

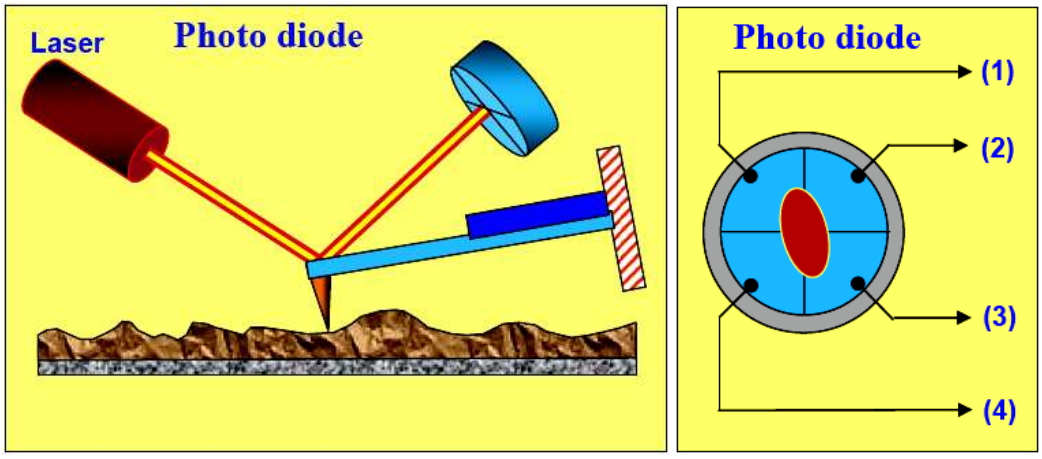

Image 2.6Schematic description of the optical system to detect the cantilever bending.

The optical system is aligned so that the beam emitted by a diode-laser is focused on the cantilever, and the reflected beam hits the center of a photodetector. Four-section split photodiodes are used as position-sensitive photodetectors.

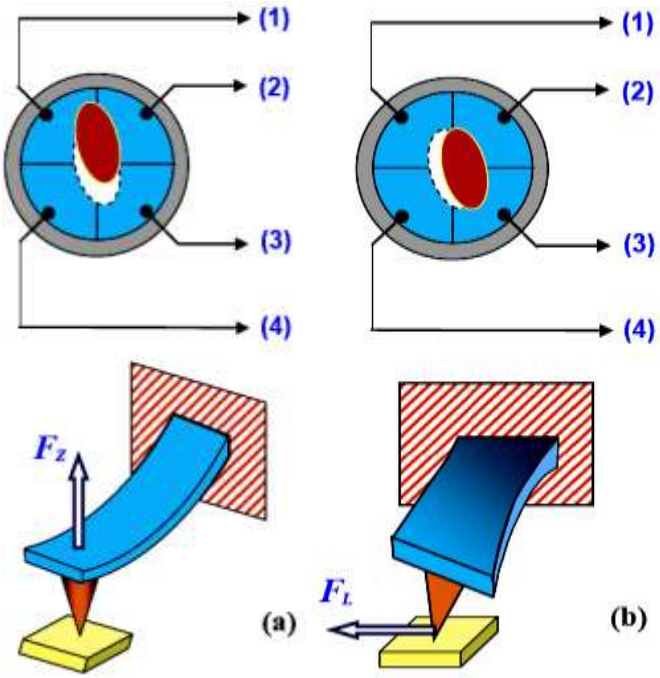

Image 2.7Relation between the types of the cantilever bending deformations (Bottom) and the change of the spot position on the split photodiode (Top).

Two quantities may be measured by the optical system: the cantilever bending due to attractive or repulsive forces (F_Z) and the cantilever torsion due to lateral components (F_L) of the tip-surface interaction forces. If reference values of the photocurrent in the photodiode sections are designated as $I_{01}, I_{02}, I_{03}, I_{04}$, and I_1, I_2, I_3, I_4 are the current values after change of the cantilever position, then differential currents from various sections of the photodiode $\Delta I_i = I_i - I_{0i}$ will characterize the value and the direction of the cantilever bending or torsion. In fact, the following current difference

$$\Delta I_Z = (\Delta I_1 + \Delta I_2) - (\Delta I_3 + \Delta I_4), \qquad Eq.2.9$$

is proportional to the cantilever bending due to a force normal to the sample surface (Image 2.7 (a)), and the following combination of differential currents,

$$\Delta I_L = (\Delta I_1 + \Delta I_4) - (\Delta I_2 + \Delta I_3), \qquad Eq.2.10$$

characterizes the cantilever bending due to lateral forces (Image 2.7(b)).

The ΔI_Z value is used as an input parameter in a feedback loop of the atomic force microscope (Image 2.8). The feedback system (FS) keeps $\Delta I_Z = const$ with the help of a piezoelectric

transducer (scanner), which controls the tip-sample distance in order to make the bending ΔZ equal to the value ΔZ_0 preset by the operator.

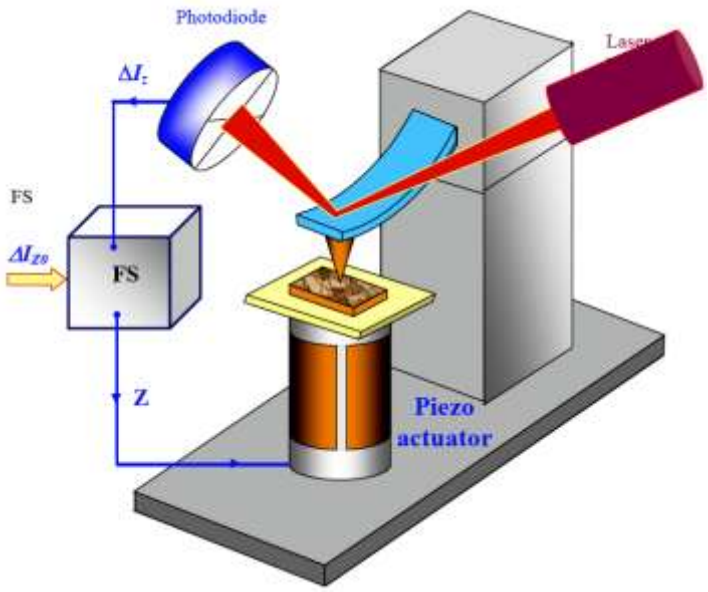

Image 2.8Simplified scheme of the feedback in optical lever detection AFM.

When scanning a sample in a $\Delta Z = const$ mode the tip moves along the surface, thus the voltage on the scanner $Z-electrode$ is recorded in the computer memory as a surface topography $Z = f(x,y)$. The AFM lateral resolution is defined by the radius of curvature of the tip and by the sensitivity of the system in detecting the cantilever deviations.

2.4.2 Resonance frequency and Quality factor

The first AFM was made by meticulously gluing a tiny shard of diamond onto one end of a tiny strip of gold foil. In the fall of 1985 G. Binnig and C. Gerber used the cantilever to examine insulating surfaces. A small hook at the end of the cantilever was pressed against the surface while the sample was scanned beneath the tip. The force between tip and sample was measured by tracking the deflection of the cantilever. They could delineate lateral features as small as 300 Å. The force microscope emerged in this way. In fact, without the breakthrough in tip manufacture, the AFM probably would have remained a curiosity in many research groups. It was Albrecht, a fresh graduate student, who fabricated the first silicon micro-cantilever and measured the atomic structure of boron nitride. Today the tip-cantilever assembly typically is micro-fabricated from Si or Si_3N_4. The era of AFM came finally when the Zurich group released the image of a silicon (111) 7x7 pattern. The world of surface science knew that a new tool for surface microscope was at hand. The

interaction force F of a tip with the surface can be estimated from the Hooke law:

$$F = k \cdot \Delta Z, \qquad \textit{Eq. 2.11}$$

where k is the cantilever elastic constant; $\Delta Z$is the tip displacement corresponding to the bending produced by the interaction with the surface. The k values vary in the range $10^{-3} \div 10 N/m$ depending on the cantilever material and geometry. The cantilever resonant frequency is important during AFM operation in oscillating modes. Self-frequencies of cantilever oscillations are determined by the following formula (see, for example, [11]):

$$\omega_{ri} = \frac{\lambda_i}{l^2}\sqrt{\frac{EJ}{\rho S}}, \qquad \textit{Eq.2.12}$$

where $l$is the cantilever length; $E$the Young's modulus; J the inertia moment of the cantilever cross-section; ρ the material density; $S$the cross section; λa numerical coefficient (in the range $1 \div 100$), depending on the oscillations mode.

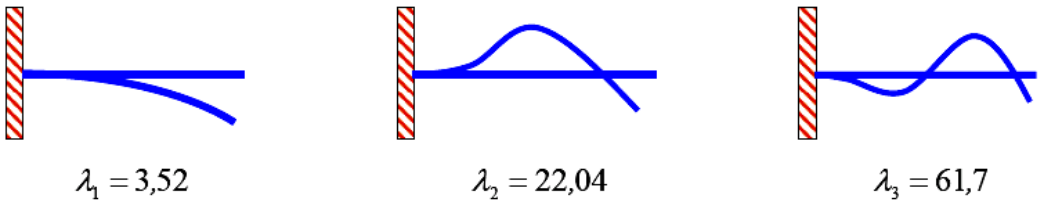

Image 2.9Main cantilever oscillations modes.

Frequencies of the main modes are usually in the $10 \div 1000\,kHz$ range. The quality factor Q of cantilevers mainly depends on the media in which they operate.

Typical Q values are represented in Table 2.1.

	In Vacuum	In Air	In Liquid
Q	$10^3 - 10^4$	$300-500$	$10-100$

Table 2.1 Q values achieved with the beam bounce method in three medias.

The exact description of the AFM cantilever oscillations is a complex mathematical task. However, the basic features of the processes occurring during interaction of an oscillating cantilever with a surface can be understood on the basis of elementary models, in particular, using the approximation of a localized mass model [12]. Let us approximate the cantilever as an elastic mass less beam (with

elastic constant k), fixed at one end on the piezo-vibrator PV, plus a mass m localized on the other end (Image 2.10).

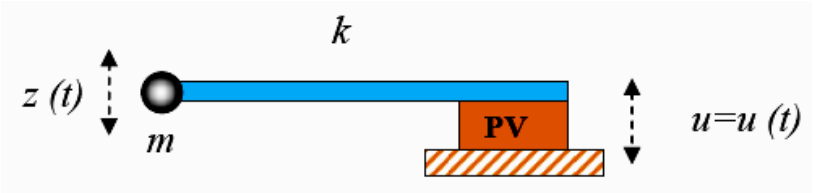

Image 2.10Probe model as an elastic cantilever with a mass at one end.

Let the piezo-vibrator oscillate with frequency ω:

$$u = u_0 \cos(\omega t), \qquad \text{Eq.2.13}$$

Then the motion equation of the system is,

$$m\ddot{z} = -k(z-u) - \gamma\dot{z} + F_0, \qquad \text{Eq.2.14}$$

where the term $\gamma\dot{z}$, proportional to the first derivative, takes into account the viscous force in air, and F_0 takes into account the gravity force and other possible constant forces. A constant force only displaces the equilibrium position of the system and does not influence the frequency, the amplitude and the phase of the oscillation. Therefore, with the variable substitution:

$$z = z_1 + \frac{F_0}{k}, \qquad \text{Eq.2.15}$$

the motion equation for the displacement z_1 from the equilibrium position takes the form:

$$m\ddot{z}_1 + \gamma\dot{z}_1 + kz_1 = ku_0 \cos(\omega t), \qquad \text{Eq.2.16}$$

Defining ω_0 as, $\omega_0 = \sqrt{\frac{k}{m}}$, and introducing the quality factor of the system $Q = \frac{\omega_0 m}{\gamma}$, we obtain:

$$\ddot{z}_1 + \frac{\omega_0}{Q}\dot{z}_1 + \omega_0^2 z_1 = \omega_0^2 u_0 \cos(\omega t), \text{Eq.2.17}$$

Finding first the solution to Equation 2.17 in the domain of the complex numbers and later substituting Equation 2.17 in Equation 2.16 we obtain for the complex amplitude a:

$$a = \frac{\omega_0^2 u_0}{\omega_0^2 - \omega^2 - i\frac{\omega\omega_0}{Q}}, \qquad \text{Eq.2.18}$$

The module of a is the forced oscillations amplitude $A(\omega)$:

$$A(\omega) = \frac{u_0 \omega_0^2}{\sqrt{(\omega_0^2 - \omega^2)^2 + \frac{\omega^2 \omega_0^2}{Q^2}}}, \quad \textit{Eq.2.19}$$

The phase of the complex amplitude a is the phase difference $\varphi(\omega)$ between the system oscillation and the forcing term $u = u_0 \cos(\omega t)$:

$$\varphi(\omega) = arctg\left[\frac{\omega \omega_0}{Q(\omega_0^2 + \omega^2)}\right], \quad \textit{Eq.2.20}$$

From equation 2.19 it follows, that the tip oscillation amplitude $A(\omega_0) = Qu_0$, at the frequency ω_0, is proportional to the quality factor. Besides that, the presence of dissipation ($\gamma \neq 0$, i.e. $Q \neq \infty$) in the system results in a decrease of the resonant frequency of the cantilever oscillations. Indeed, differentiating the radicand with respect to ω^2 in equation 2.19 and equating the derivative to zero, we obtain for the resonant frequency ω_{rd}:

$$\omega_{rd}^2 = \omega_0^2\left(1 - \frac{1}{2Q^2}\right), \quad \textit{Eq.2.21}$$

Equation 2.21 shows the real dependency of the resonant frequency from the Quality factor, where high Q values imply $\omega_{rd} \approx \omega_0$. In this way there are needed smaller forces for achieving resonant frequencies. As several works show [13], [14], is important of increase system's quality factor as it avoids sample deterioration. In future works there are a lot of groups which intent to increase the quality factor by hardware (by using two or more Lock-in amplifiers, MAC mode of Agilent Technologies [15]) for augmenting Q.

2.4.3 Acquisition and image processing

Scanning a surface with *AFM* is like moving an electronic beam on the screen in the cathode ray tube of a TV. The tip goes along a (row) first in forward, and then in the reverse direction (horizontal scanning), then passes to the next line (frame scanning). Tip movement is done in small steps by the scanner that is driven by a saw tooth voltage produced by digital-to-analog converters. The surface topographic information can be stored during forward/backward pass. (Image 2.11)

The information collected by the scanning probe microscope, is stored as a two-dimensional file of

integer numbers a_{ij} (matrix).

The physical meaning of these numbers is determined by the kind of interaction, which was measured during scanning. In $AFM$is stored piezo (z direction) displacement, indicating the relative height of the actual sample point.

To each value of ij pair of indexes corresponds a certain point of a surface within the scanning area. Coordinates of points of the sampled area are calculated (see Equation 2.22) simply multiplying the corresponding index by the value of the distance between points:

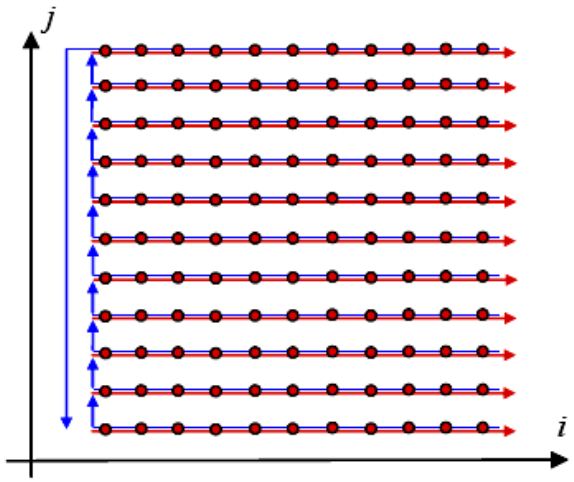

Image 2.11Schematic illustration of the scanning process. Red arrows indicate the direction of the forward motion of the scanner. Dark blue arrows indicate reverse motion of the scanner. Registration of the information is made in points on direct pass.

$$x_i = x_0 \cdot i, \qquad y_j = y_0 \cdot j. \qquad Eq.2.22$$

Here x_0 and $y_0$are the distances between adjacent points, along X and Y-axes, where the information was recorded. As a rule, the AFM frames are square matrixes (whose size is commonly 256×256 or 512×512 elements). Visualization of the AFM frame is done by computer graphics, basically, as three-dimensional $(3D)$or two-dimensional brightness $(2D)$images. At $(3D)$ visualization the image of a surface $Z = f(x,y)$, is plotted in an axonometric view by pixels.

In addition to this, various ways of pixels brightening corresponding to various height of the surface topography are used. The most effective way of $(3D)$images coloring is obtained simulating the surface illumination by a point source located in some point of space above the surface (Image2.12).

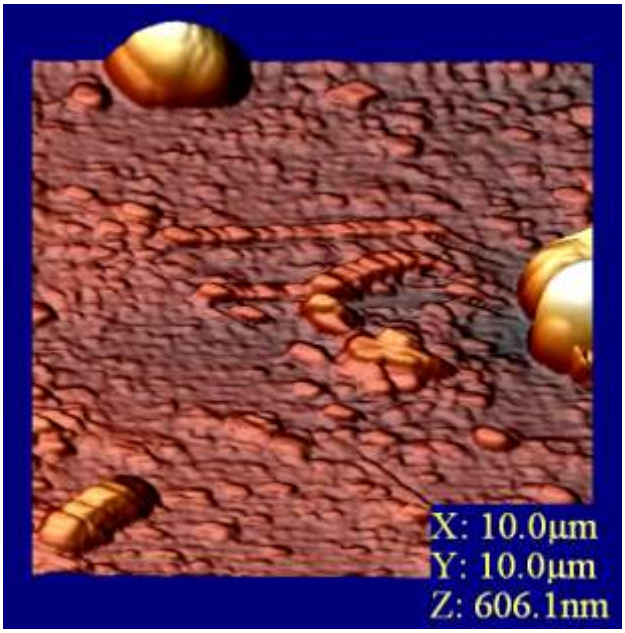

Image 2.12 3D rendering with surface illumination by a special point source.

Thus it is possible to emphasize small-scale topography inequalities. Even more, WSxM (Software controlling Cervantes Nanotec AFM), can create scaling and rotation of acquired AFM images. In $(2D)$ visualization (also named "Top View" image) to each point of the surface $Z = f(x,y)$ is assigned a color (or a brightness) that corresponds to its z-value according to a given color-scale (or gray-scale). As an example, the $(2D)$ image of a surface area is presented on Image 2.13.

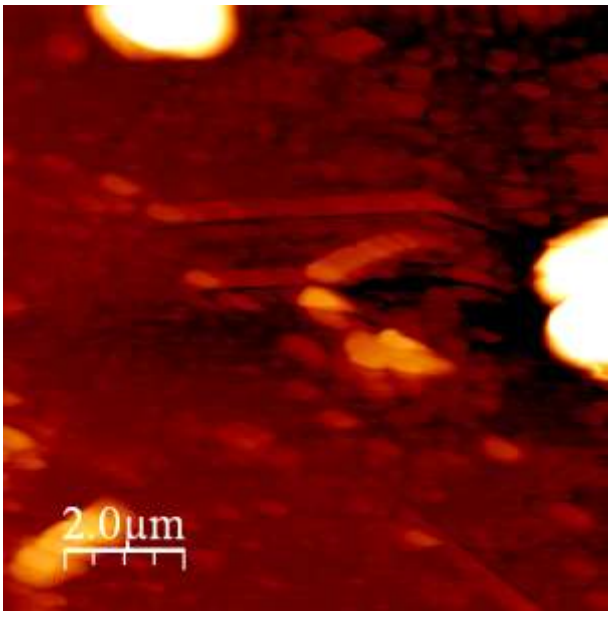

Image 2.13 2D brightness image of surface topography of image 2.12.

In general, the physical meaning of the SPM images depend on the parameter that is used in the feedback loop. For example, the values stored in the $Z = f(x,y)$ matrix may depend on:

- The electric current value flowing through the tip-surface contact with constant applied voltage (STM).
- The main tip-surface interactive force in case is electric than is EFM, and in case is magnetic is called MFM.

Besides these "maps" of the tip-sample interaction over the scanned area, a different type of information may be retrieved using SPM. For example, on a single point of the sample surface we may collect the dependence of the tunneling current on the applied voltage, the dependence of the interactive force on the tip-sample distance, etc.

This information is stored as vector files or as matrixes of $2 \times N$ dimension, that may be displayed or printed using a set of standard tools for graphic presentation provided by the generic AFM/SPM software that we are using. SPM images, alongside with the helpful information, contain also a lot of secondary information affecting the data and appearing as image distortions. Possible distortions in SPM images caused by imperfection of the equipment and by external parasitic influences can be eliminated by some general treatments like: subtraction of a constant component or constant inclination, elimination of the distortions due to scanner imperfection, median filtering, line averaging and Fourier filtration of the SPM images, surface restoration using a known tip shape, etc.

Chapter 3: State of Art **pp.26**

Chapter Index

Is normal that during your training period, there is need for participating in meetings, workshops, congresses etc. Because in this ambient you find people working in the same field as you. People with more o less the same interests as you but the most important thing is that there will be always a researcher who has been in the same difficulties as you.
So, what a perfect moment for exchanging ideas and frustrations! But, despite jokes, these meetings are really important and can give a solution or redirect your research line in the proper direction, as happened to me.

The International SPMuser meeting organized by *Scientec* (Agilent Technologies) [16] gave me the possibility to meet different firms producing near field microscopes like: *Nanonics* [17], *Agilent Technologies* [18] and *NanoSurf* [19].Leaders in :optical, near field, and SPM.

3.1 Nanotec Cervantes AFM equipment

3.1.1 Mechanics

Nanotec AFM mechanical system can be divided into two main parts: chassis and head. Image 3.1 (gentle courtesy of *Nanotec Electronica*[20]) represents the AFM chassis, a general view of the different elements that integrate the mechanics, pointing out their different components:

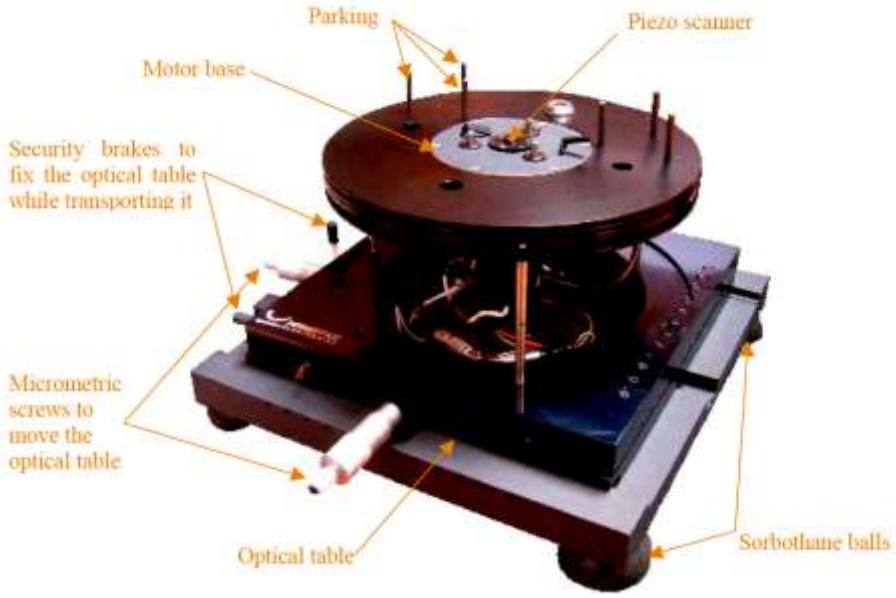

Image 3.1 Chassis

Let's explain shortly each part's function:

- Beneath the *motor base* stands the micrometric motor, which rotates the micrometric screws for approaching and withdrawing the AFM head from the sample. In this way the cantilever holder, held in the AFM head, approaches the sample carried on the top of piezo scanner.
- *Piezo scanner* is the place where is situated the piezoresistive part of scanner. Is a cylindrical space where is introduced the piezo as shown in Image 3.5.
- The *micrometric screws* are used to move the whole chassis with micrometric precision during the optical phase. Depending on the optical microscope sometimes isn't possible to move it laterally with micrometric precision. In this way the chassis design permits us to go through optical microscope limitations for a better optical visualization of the tip/sample.

Image 3.2 is an upper vision of the chassis, and it's interconnections with *Dulcinea* electronics.

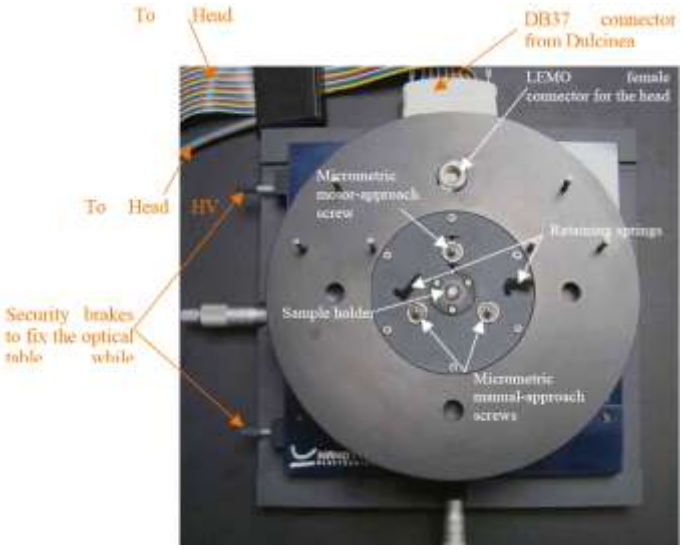

Image 3.2 AFM Chassis.

Meanwhile the other important part of AFM mechanics is illustrated in Image 3.3. AFM head hold the cantilever and is situated over three micrometric screws. Two of them are in a frontal position and ensures the planar holder collocation respect to the sample. The third one is controlled by software and is moved from the motor.

With arrows are represented the main important parts of the head:

- The laser is situated in vertical direction injecting its beam directly to a couple of mirrors redirecting it over the cantilevers holder (See Image 3.4).
- There are *micrometric screws* for laser alignment on the cantilever. Useful for detecting the

real position of laser beam. In this way we can displace the beam along cantilever's length or in lateral directions.

- Following beam direction, after reflection over cantilever is situated the photodiode, which detect the real laser intensity reflected over cantilever's surface.
- In this way there are some screws for coarse adjustment of photo diode. These screws permits photo detector alignment with laser beam.
- The previous screws make rude alignment between photodiode and laser beam reflected over the cantilever. Due to small intensities detected, there is need for further micrometric alignment. Now is time for moving photodiode's micrometric screws for fine adjustments. Adjustments that can be noted only by software a Photodiode section over data acquisition frame.

Image 3.3 AFM head.

Here bellow in Image 3.4 is shown a 3D reconstruction of the head indicating lasers path through first mirrors, cantilever and finally over the photodiode.

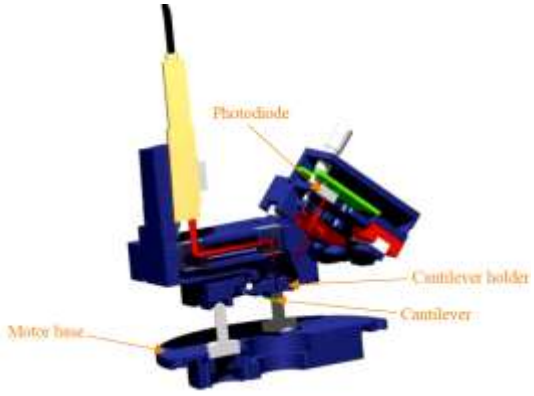

Image 3.4Detail of the AFM head showing laser's path through optical system (in red).

The piezo scanners are responsible for movement of the sample in x, y and z directions.

Image 3.5 Piezo scanners (long and short).

Image 3.6 is a photo of a generic *Cervantes Nanotec*holder. In the central channel is situated cantilevers deposit. In this demo is collocated a cantilever for demonstrating it's correct placement (Orange circle).

Image 3.6 Cantilever holder.

With the system is also provided a glass cover, which allows covering all the system to protect from acoustic and environmental noises, as well as to perform atmosphere control as: humidity, temperature, gas concentrations etc.

Image 3.7 AFM head glass cover and cantilever exchange bay.

In Image 3.8 is shown the metallic base and fork for an easy cantilever placing or removal when using the elastic stripes to fix it to the cantilever holder.

Once correctly placed the microchip over the holder, it's time to situate holder in the AFM head. In Image 3.8 is a photo of the AFM head with holder correctly placed. Is easy to detect if is correctly

placed because of magnetic contacts. While on the right shows how to correctly handle AFM head before placing it over the chassis.

Image 3.8 (Left) Cantilever holder in the head.(Right) Handling the AFM head.

3.1.2 Dulcinea electronics

Dulcinea electronics is designed to drive SPM equipments. While its more immediate application is for controlling *Nanotec Electronica* SPM systems, it is designed in an open and modular way in order to facilitate the interfacing with any other $AFM/SNOM/STM$ system.

In the following pictures are shown the front/back views of *Dulcinea's* electronics, with detailed explanation of use for each visible part of it.

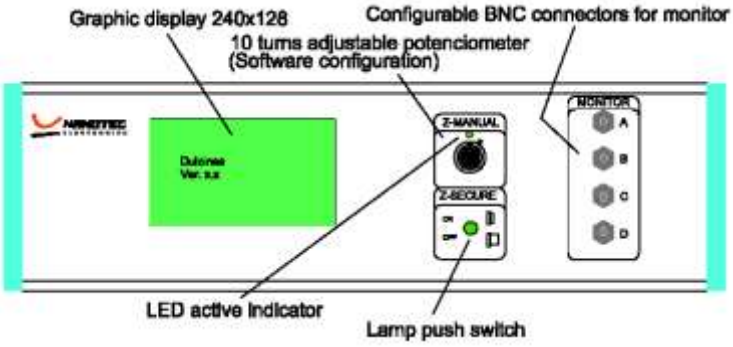

Image 3.9 Dulcinea's front view.

- *Graphic display:*It is used for notifying the user about events like the start/end of the communication with the computer and the gains changes.
- *Z Secure lamp push switch:*At any moment is possible to press this button for generating an offset voltage of +150V to the Z piezo voltage. This allows fast withdrawal of the tip from the sample without using the software. Useful when software hangs on.
- *BNC connectors for signals monitoring (A, B, C, D):*Software configurable BNC monitors.

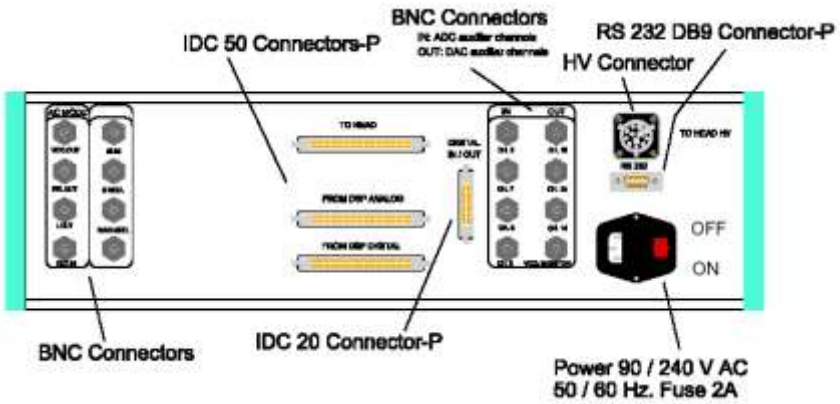

Image 3.10 Dulcinea's back view.

- *BNC connectors:*target specific BNC monitors and BNCs for external inputs:
- *VCO Out:*Driving signal for cantilever oscillation (+/-10V).
- *I. Out:*Driving signal for magnetic cantilever oscillation. It is an AC current source with the same frequency as the VCO Out (selected in the WSxM tapping menu).
- *Ext. In: [Input signal].*Allows introducing an external signal as the dynamic mode reference signal (+/- 10V).

3.1.3 Optical microscope

In the AFMequipment is included an optical microscope (Image 3.11) for several purposes; laser alignment over the cantilever, probe positioning, recognizing ROI's in over the sample surface. Etc.

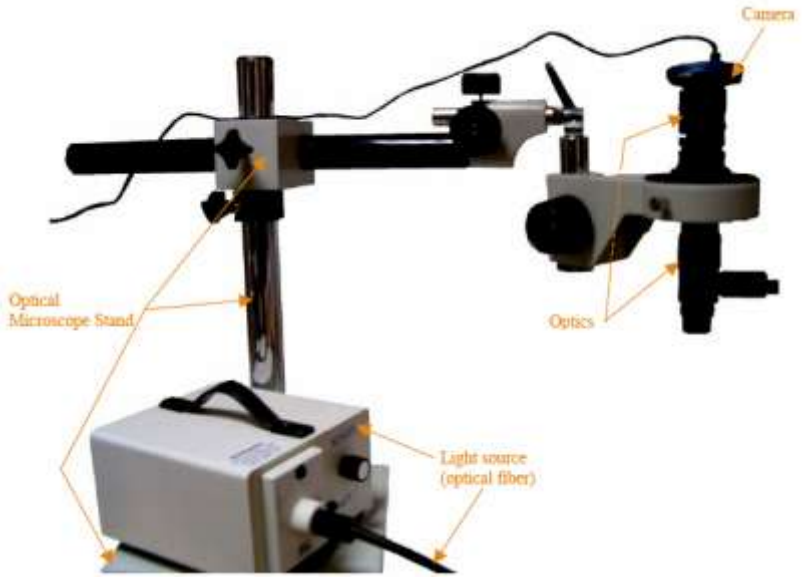

Image 3.11 AFM optical microscope.

3.2 Nanonics $NSOM/AFM$ equipment

Nanonics equipment integrates $AFM/SNOM$ microscopes. There is the intent to include more than one microscopy technologies in one compound microscope, the so-called Multiple Probe $SNOM/SPM$ systems. They have achieved several good results and we are going to list some of them:

- No need for a laser beam monitoring cantilevers deflection (tuning fork principle).
- *3D Flat Scanning ™ Technology.*
- Ability to integrate up to four probes in one microscope.
- Their huge flexibility in different types of probes.
- Complete integration of SEM/SPM.
- Simultaneous On-Line AFM and Confocal microscopy.
- The first to integrate $AFM/Raman$ microscopy (patented).
- Possibility to follow optically above and bellow the sample.

In the following paragraphs we will illustrate the solutions adopted from *Nanonics* (All the images of $MultiVew4000$ are a gentle courtesy of Dr. David Lewis, *Nanonics* vice-president).

3.2.1 3D Flat Scanning ™ Technology

While building an AFM, the fundamental problem is the piezo scanner. Its position normally prohibits introducing more than one probe simultaneously due to dimensions. In Image 3.12 we illustrate the general positioning of the piezo actuator.

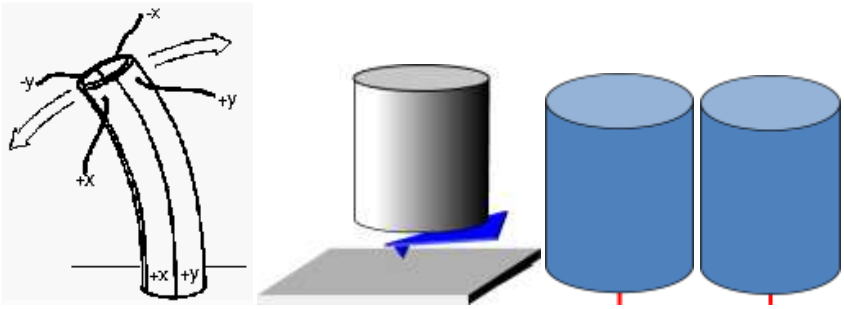

Image 3.12 Piezo collocation with one (left) and two probes (right).

In this way we can see that it isn't possible to approach by nanometers two or more probes, because the minimal distance between them depends on piezo dimensions.

For these reasons that was introduced ***3D Flat Scanning ™ Technology.***

*Nanonics*solution was, developing a scanner with a geometry that allow great flexibility in multi-probe design, while providing optically and electron/ion optically friendly systems that can fit any optically based technique such as Raman [21] or electron optically based techniques such as a SEM [22] or ion optical technique such as an FIB [23] or for that matter even in SEM/FIB systems.
This technology provides:

- A novel planar, folded-piezo, flexible scan design with their advantages.
- Allows large simultaneous lateral and axial sample scanning.
- Ultrathin scanner can be incorporated into systems where conventional scan stages are too bulky and geometrically limiting
- The minimal stage height of 7 mm allows for easy access with high-powered microscope objectives from either above or below the scanning stages.
- The large vertical (axial) displacement of up to 100 microns allows for multiple probes and allows for tracking of structures with very large topographical features.

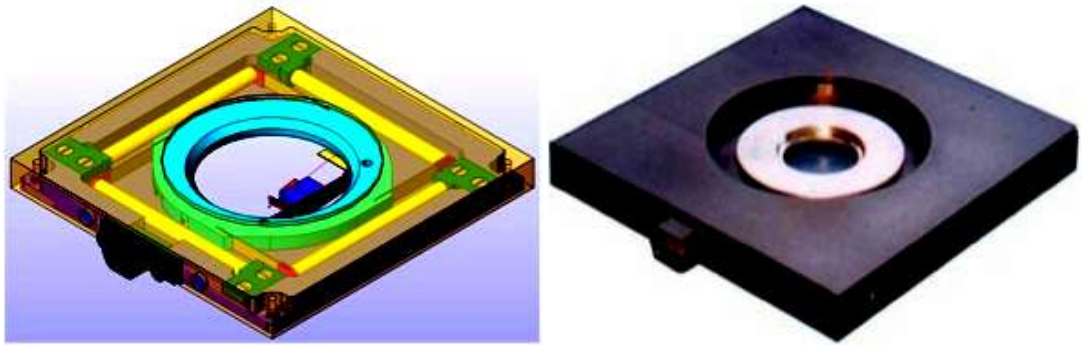

Image 3.13 3D FlatScan™ technology.

Its main features are:

- >20 mm clear axis.
- 7 mm thin scanners.
- 100 micron 3D fine scanning in X, Y and Z directions.

3.2.2 Multiple probing

In Image 3.14 is shown $MultiVew4000$ with one, two and four probes installed. It has a geometry directed toward an open architecture, and for scattering $NSOM$experiments with piezo control of the tip while the tip is scanning for ultra-accurate positioning of the tip in a laser beam and in addition sample scanning.

As we mentioned above, it has a completely free optical axis from above and below and with open

access from the side for additional high numerical aperture lens access at 90 degrees to the opticalaxis or for that matter at any other angle of choice. Individual probes can be brought into intimate contact with each other with individual AFM control or can be separated with nanometric control.

Image 3.13 The $MultiVew4000$ *in it's configurations with one, two and four probes.*

3.2.3 New probe design

The second problem faced is trying to get probes closer to each other. Their own geometry doesn't permit to approach them closer than is shown in Image 3.15. Even if the microscope control system gave such opportunity to avoid crashing it's not possible that probes scan the same line.

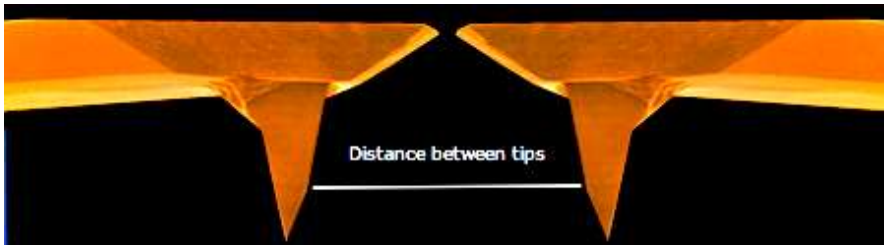

Image 3.14 Distance between tips approaching each other.

Nanonics has developed spatially and optically friendly glass based probes that allow a close approach of the probe tips, crucial for multi-probe imaging systems. Also these probes offer good imaging not only in AFM modes but as will be indicated further, specialized glass probes also allow; singular electrical imaging, thermal imaging and chemical writing. The probes have unparalleled aspect ratios and allow for deep trench imaging and even sidewall imaging. Tip geometry and parameters are illustrated in Image 3.16.

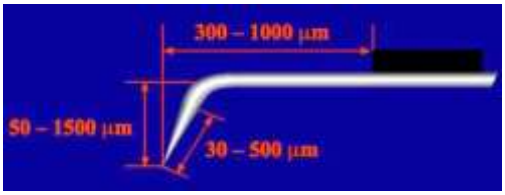

Image 3.15 Glass tip dimensions.

But this firm has been producing too, other types of probes like: thermal conductivity probes; wired electrical probes, glass probes, tuning fork probes etc.

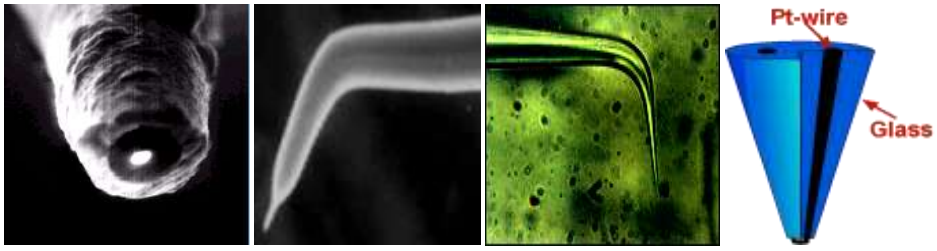

Image 3.16 NSOM, wired, glass and thermal conductivity probes.

In the following, (Image 3.18) are two images presenting simultaneous imaging of carbon nanotubes with two probes. On the left there is an image taken from the first probe and on the right the image taken from the second probe.

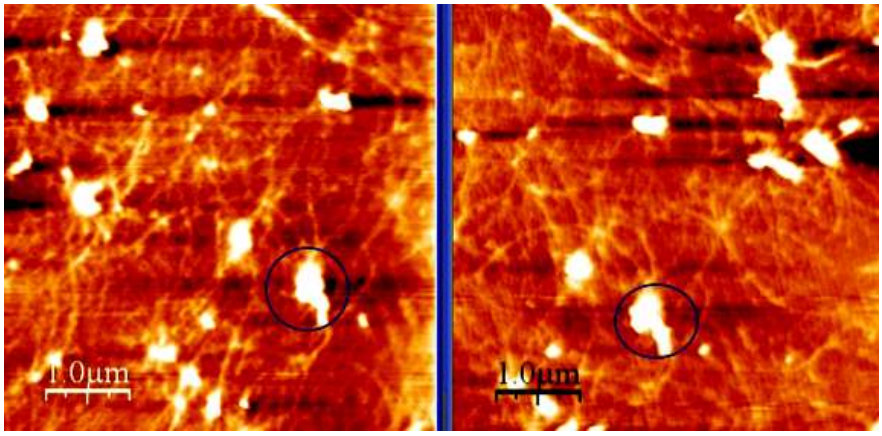

Image 3.17 (Left) First probe. (Right) Second probe.

The circles show the same nanotube associations, but the coordinates in the image (showing distance between tips) are:

	X Position	Y Position
First Probe	4,6 μm	2,9 μm
Second Probe	1,3 μm	1,0 μm
Probes Offset	1,9 μm	300 nm

Table 3.1 Probe coordinates x, y, and offsets. MultiProbe4000 achieves 300nm offset in y positioning.

3.2.4 Tuning Fork

Commercially available atomic force microscopes AFM presently employ a diode laser whose beam is reflected from the back of a micro machined Si cantilever to monitor the tip–sample interaction (Usually known as the beam bounce method, see paragraph 2.4.1) Laser diode in AFM introduces several problems:

- For many types of measurement, illumination from the diode laser is a deteriorating factor.
- The diode laser introduces driftinto the measurement from sources such as *thermal mode hopping* [24] and can cause an apparent noise of several nm in AFM images.
- Due to the low spring constant of Si cantilevers, AC-AFM-related techniques require large oscillation amplitude, typically tens to hundreds of nm, which can cause damage in biological samples.

Researchers in the $NSOM$field have been exploring non-optical means of sensing the tip–sample interaction.In recent studies [25], the probe tip oscillates parallel to the sample surface; in a shearing motion byattaching the probe to a quartz tuning fork in which tines are oriented perpendicular to sample surface. High spring constant of tuning-fork tines allow use of small oscillation amplitudes as small as 0.1 nm, offering potentially improved spatial resolution for AC-

AFM-related techniques.In AFM, the great advantage of using such smaller oscillating amplitudes is when imaging biological samples. Small excitation amplitudes imply less force applied to the sample. In this way is possible to measure the real dimensions or at the worst case to avoid destroying soft samples as: proteins, DNA etc.

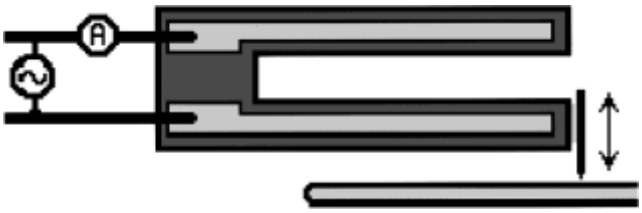

Image 3.18 Principle of tuning fork.

Nanonics has a patent for tuning fork probes but with the gentle permission of Dr. David Lewis we represent it in Image 3.21 how is build the system.

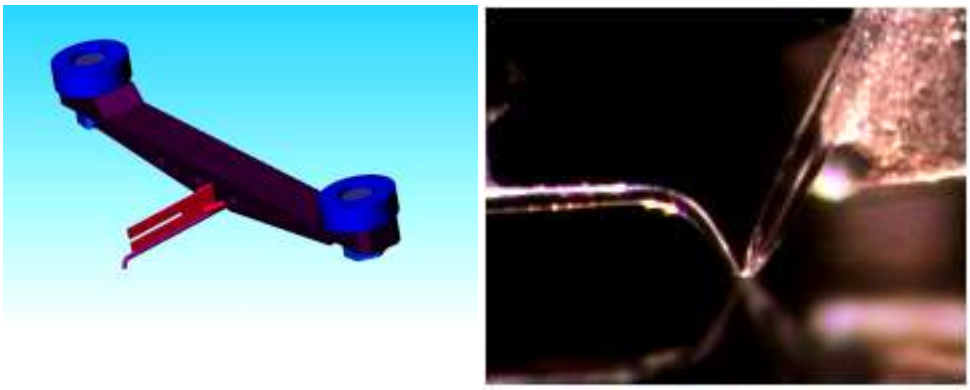

Image 3.19 (Left) Model of tuning fork (approx). (Right) On the left there is a tuning fork probe.

3.2.5 Probe holders

There is needed a normal holder while making liquid imaging or normal force imaging in the normal configuration. Even if recent studies [35], [36] have demonstrated that the quality factor Q increases dramatically when using tuning fork probes [26]. While M. Koopman [27] [34] reveals achieving quality factors in liquid of about 1020, when in air they achieved Q of 1460. We would like to stress over the normal Q values for the traditional beam bounce method (see Table 2.1). This because the beam bounce method implies laser passing through aqueous media, reducing even more the intensity received by the laser photodiode. The configuration of the microscope changes as follows.

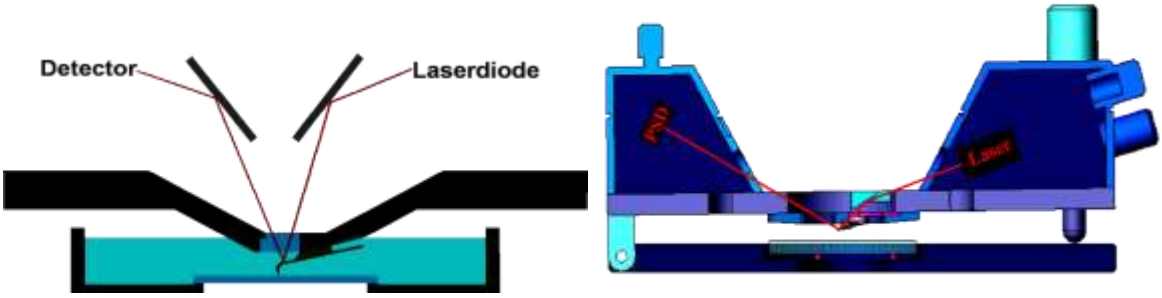

Image 3.20 Schematic view of the laser path for the feedback in liquid and in normal force imaging. (Left) Liquid imaging. (Right) Normal force.

In a close up view of a mounted *Nanonics* probe we can see that the cantilevered nature of the probe allows for not only the geometry and the topography of the device to be measured with nanometric accuracy using atomic force microscopybut alsoallows for on-line feedback with 0.02 dB stability, repeatability and reconfigurability of the probe on the device under test (DUT).

Image 3.21 (Left) Liquid holder. (Right) Liquid bath.

Other AFM producers:

Agilent Technologies[28]	AIST-NT[29]	Asylum Research [30]	JPK Instruments [33]
Angstrom Advanced Inc [32]	NanoSurf	Nanotec	Park Systems [40]
Pacific Nanotechnology [39]	NT-MDT [37]	Surface Imag. Sys[42]	
Veeco-Digital Instrument.[31]	Omicron [38]	RHK Technology [41]	

Table 3.2 AFM main producers.

4.1 Brief tutorial over WSxM

In the following paragraphs it will be described, as a compound number of steps, how to start an imaging section. We refer to WSxM ver.12.1 (September 2008).

4.1.1 Getting started

The following steps illustrate how to get started using the WSxM software.

- Turn on the Computer for data acquisition.
- Turn on the Dulcinea Control unit. (Turn on the red switch at rear part)
- Start control-program WSxM.

The first screen shows whether all parts of the system are properly connected and ready to work. The program can also be started in simulation mode without AFM and control unit.

Image 4.1 First frame of WSxM.

Click onto the symbol “DA” – Data acquisition and afterwards the button “Go” in the upper control bar. The acquisition process is started now. The following window (or similar) should be displayed:

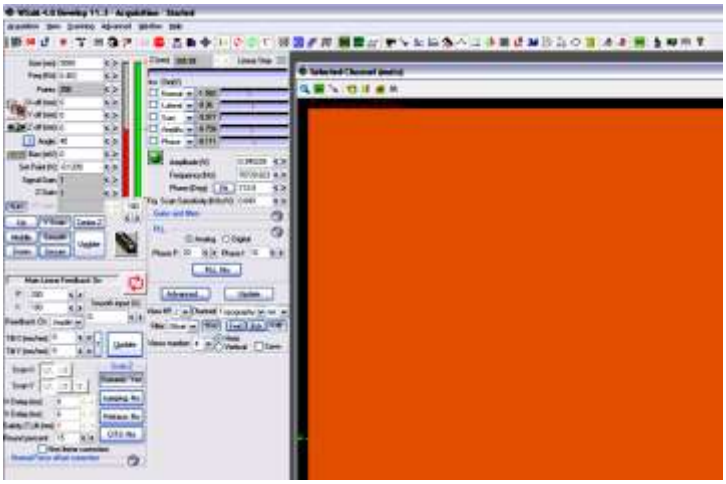

Image 4.2 Screening of the Acquisition mode of WSxM.

On the left side we see a control panel that shows the parameters of the scanning process. Let’s have a closer look onto this panel and see what the meaning of these parameters is.

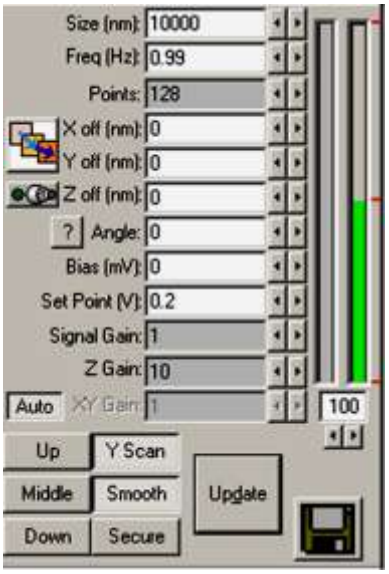

Size: in nm of the squared zone that is scanned.

Freq: number of lines that is scanned per second in x direction.

Points: number of lines that contain the square

X/Y/Z off: offset

Angle: in x-y plane the scan is performed, in order to get a good scan, angle should be modified so that each scan line is in a plane.

Bias: Voltage applied between tip an sample.

Set Point: feedback is performed to adjust the feedback parameter to this value.

Z Gain: defines the margin in which the z-piezo can extend.

Image 4.3 Main Control Panel.

4.1.2 Laser and photodiode calibration

During this phase the user have to center the laser beam in the extreme part of the cantilever and in the centre of the photodiode, for alignment (See Image 2.6). First starts with laser spot recognition over the extreme part of cantilever, and later continues with positioning of the photo detector for maximal intensity detection.

Laser calibration: Tune the laser beam in order to focus in the cantilever. Click on the button as indicated by the arrow in Image 4.4. At "Photodiode", switch on the laser and later click on "Tune Photodiode". After this phase the laser beam in the AFM head is turned on.

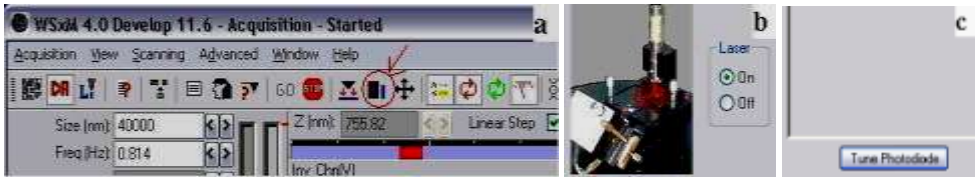

Image 4.4 Sequence of laser activation. A) Photodiode activation button. B) Laser activation. C) Photodiode tuning frame.

Later, take off the measuring head and point with the laser-spot onto a white sheet of paper. (This is going to serve us for laser spot recognition). Is a simple but effective method for lasers tuning. We should recognize in the paper the shape indicated in Image 4.5.

Image 4.5 Laser spot reflection over the cantilever.

After this, turn the calibration-screws (see paragraph 3.1.1) of the laser diode in order to position the laser onto the very end of the cantilever. The whole process can be done by the aim of the optical microscope. In Image 4.6, there are two probes (left an Arrow-NC-10, right *Nanonics* multi-probe) with the laser spot placed in the correct distance from cantilevers base. Laser spotlight surrounding cantilever shape, is the one projected over the white sheet paper. This is another way to calibrate the laser, using an optical microscope (Image 3.13).

Image 4.6 Optical microscope image of laser spot over a probe chip.

Photodiode calibration: After passing through cantilever, the laser beam is reflected overt photodiode (see Image 3.4). So there is needed a further alignment process, the one that centers laser spot in photodiode.

Calibrate the position of the laser diode with the screws centering the spot exactly in the middle of the four quadrants. The first phase uses screws for coarse AFM head alignment. Due to the small intensities measured this task normally (if user isn't customized) is a little bit tedious to center the laser spot in the center. Green bars should approach the red ones, while the laser intensity reflected on the photodiodes should be high. (Blue bar on the right of the window).

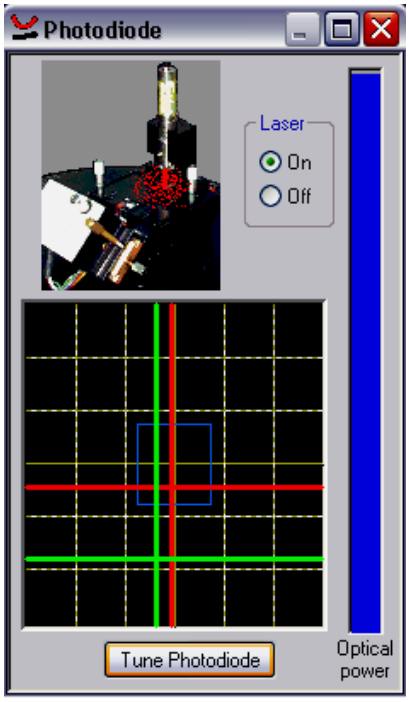

Image 4.7 Photodiode tuning frame. On the right there is the intensity bar, showing the actual laser intensity acquired (sum of the four photodiode components). In the center there are the two crosses that gives feedback

over the coarse movements induced to photodiode. In this way, when both red crosses are inside square, appear green crosses. They help for fine adjustments and should overlap the red ones.

This is as a result of the following configuration a disposition of the photodiode.

As the photodiode is compound of four pieces (lets call them 1,2,3 and 4), the resulting intensity of the laser beam is a composition of the four intensities of each piece. In Image 4.8, is shown how is calculated the resulting intensity. While linear combinations of them gives more information regarding Normal and Lateral forces.

Hint: The total intensity received at the photodiode (blue bar), depends on different factors such as geography of cantilever, dimensions of cantilever etc… As a consequence, not always will be possible to have maximum height of the bar. Is considered god one, which is higher than 2/3 of maximum height.

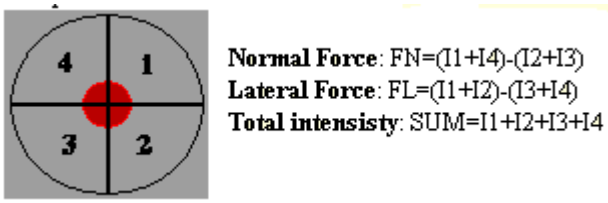

Image 4.8 Calculation of Normal and lateral force from laser photodiode sections.

4.1.3 Contact Mode

In contact mode the feedback is performed on the normal force that is the vertical deflection of the laser spot in the photodiode. When the tip gets into contact with the surface, the cantilever will bend and deflect the laser beam into this direction.

Approach: Click onto the button “Approach” and open the approach-menu. Choose a *Set Point* slightly higher (10-20 %) than the actual normal-force value.

The value for “Force difference to range” should be: 0.1V (harder tips), 0.3V (softer ones).

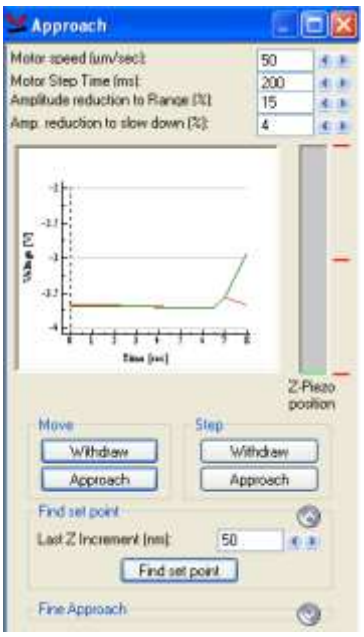

Motor speed: Detemines the rotation speed for the micrometric screw (μm/sec).

Amplitude reduction to range (%): how should be the amplitude reduction for reducing the motor speed.

Amplitude reduction to slow down (%): Percentage of amplitude reduction to slow down the motor. Approach sensibility.

Hint: Scan Size has to be set to 0 for avoiding tip damage. Instead the Z-Gain in has to be set to 15, equivalent to maximum range for getting higher sensibility at approach.

Image 4.9 Approach panel. Used both for AC, DC and JM.

Now approach by clicking the button “Approach” on the left (“Move”). Suddenly you can hear the motor rotating with its characteristic noise. While at the window we can see how it changes in time the graph of approach. When the amplitude changes in the ranges imposed, the motor speed slows down, for higher sensibility in detecting engages. Be careful in avoiding false engages (See 4.1.6).

When the approach is successful (sudden change in normal force) select an appropriate *Set Point* by withdrawing the z-piezo (*Set Point* to -9). The cantilever is not bended anymore and a correct value for the *Set Point* may be chosen. (The system itself proposes a *Set Point* at the end of the approach procedure, but it is more secure to choose it by your own.)

*Image of a calibration sample:*In order to calibrate the system a sample with a well-known structure is needed (e.g. SiO_2- grid). The calibration sample is mounted onto the sample-piezo. A cantilever-chip has to be mounted in the measuring head. As follows, here we show the SiO_2-grid.

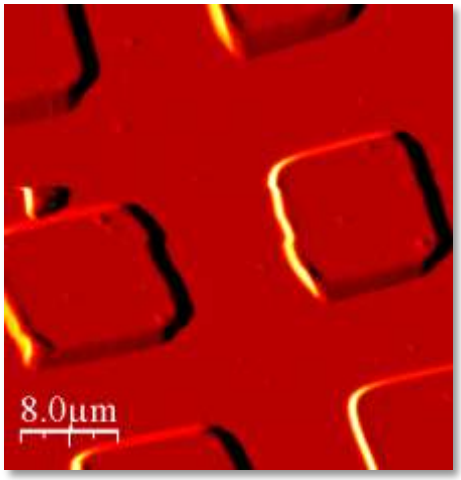

Image 4.10 Calibration grid.

An image of a calibration sample (e.g. grid) can be scanned now increasing the scan size first to a small size (1-5 μm) and than to a bigger size (10 μm). The measured dimensions can be compared with the dimensions indicated on the calibration-grid, as the grid manufacturer gives the dimensions of the cyclic structures.

The piezos can be calibrated now clicking on the button "Select head" and changing the values in X cal, Y cal and Z cal.

*Scan Options:*Is important that in the scan options the Dynamic button should be deactivated in order to stay in contact mode. While this dialog permits to change some parameters like Scan directions, delays, applying non linear corrections etc:

- *Scan X:* Allows to effectuate scans in both directions of only in one, more in concrete permits to effectuate scans in Forward and Backward directions. In this way we impose to the microscope to measure and collect points in both directions. This option at the beginning is important because gives the possibility to compare forward and backward images. And to detect if are real images of there are present artifacts in the scan.
- *Scan Y:* This button permits to scan continuously up down the ROI. Useful when piezo presents a lot of non-linearity and derives.
- *Jumping:* Activates the Jumping mode, only present in Cervantes Nanotec.

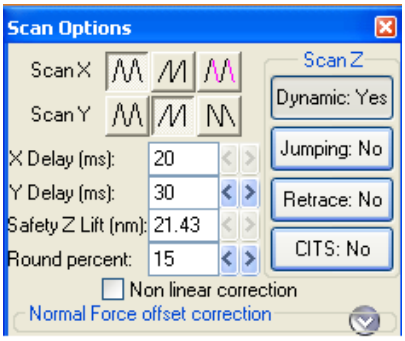

Image 4.11Scan Options dialog menu.

Channels: In this dialog are presented the channels that are relevant for the actual scan mode in use. In contact mode the feedback is done over the normal force channel. In this way the set point in use should be a little bit bigger that the value read in the channel. This implies that we impose to the feedback system to maintain the distance *SetPoint*from sample surface. Normal values of this channel are round (0.1-03V).

Amplitude channel is the channel where is done the feedback in AC. Here we see that when SetPoint is set to -9, the current value on this channel shows the free amplitude oscillation of cantilever without presence of other forces (Van der Waals, electrostatic etc.)

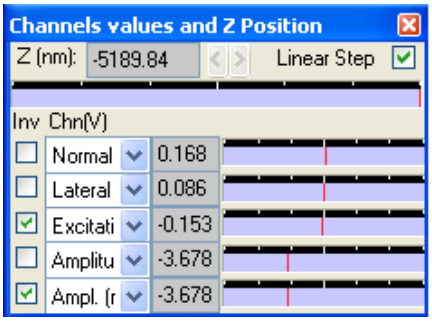

Image 4.12 Channels Values and Z position offsets.

Saving Options: This dialog permits to determine the channels to be saved. Also it can be determined if we like to apply filters, the directions Forward/backward…etc.

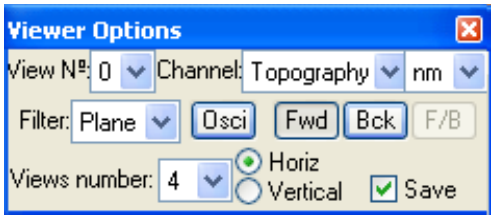

Image 4.13 Saving options dialog menu.

*Positioning Window:*Gives the area of actual scanning. With a square is shown the actual scan size, and its relative positioning in comparison with the whole scan size.

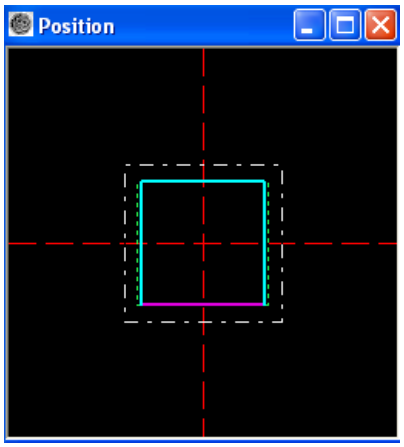

Image 4.14 Positioning window, gives the actual scan positioning in comparison with whole scan range.

4.1.4 Dynamic Mode AC

In tapping mode the cantilever is excited to oscillate by a piezo under the chip-holder. The amplitude of these forced flexural vibrations is related to forces between tip and sample. So in this mode the feedback is performed on the amplitude of the oscillation. To find the optimal excitation frequency we have to find the resonance frequency of the cantilever (adding the damping frequency of the surrounding system). For this we have to activate the corresponding dialog (Image 4.2).

This Dialog is more or less as the one shown in Image 4.15. The main characteristics are the minimal and maximal frequencies, which determine the search ranges for the resonant frequency and the cantilever excitation amplitude. Is important the excitation amplitude imposed because can happen that the maximal intensity detected in the photodiode (Gaussian curve in green) presents a kind of local minimum due to higher oscillation amplitudes (normally more than 4V) not detected from the photodiode. It can be easily resolved by imposing smaller excitation amplitudes.

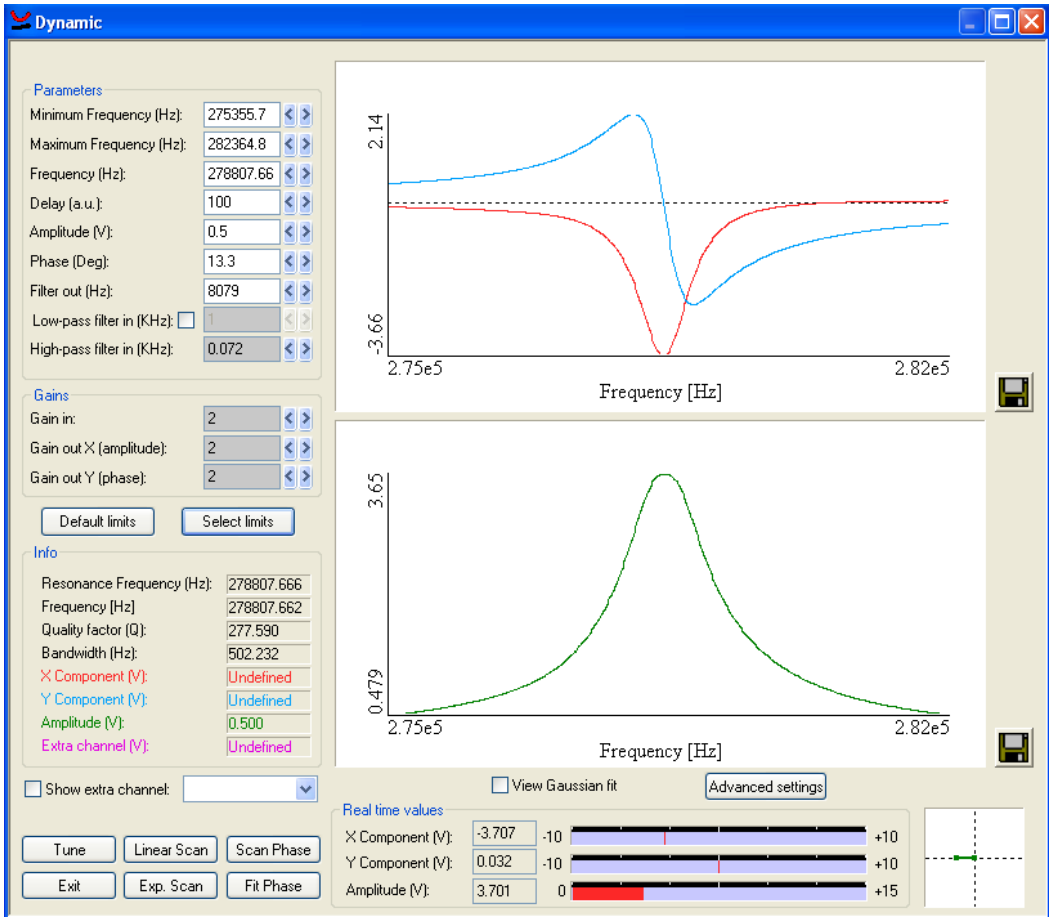

Image 4.15 Resonance frequency search window.

By clicking on the button "Init dynamic" there is an algorithm compound of several phases from which we can distinguish two basic ones:

- Exponential: searches the resonant frequency by oscillating the cantilever on determined frequencies separated from exponential search. In this way there is a first approximated search. If we pass this search in the logarithmic base, it's linear and in time base is really fast.
- Linear: after the exponential phase, we have determined the decades where is collocated the resonant frequency. In this way it can be done a linear search over this decade for finding the real resonant frequency, the excitation amplitude, the phase shift and the Quality factor.

Is normal that it can be faster if it is imposed the frequency segment where to search the resonant frequency, based on the cantilever manufacturer specifications. Choose a minimum- and maximum frequency (the manufacture indicate a typical resonance- frequency of the cantilever chips) wide around the supposed frequency and start a linear scan to see whether there is a maximum of the first mode oscillation. The search-interval may be narrowed now and by clicking on "Tune" the

resonance-frequency will be determined automatically and applied on the system for measurements. Close the window by pressing “Exit”.

Hint: Is good practice to control the phase shifts; if too big, press “Fit phase” for getting round zero the phase shift.

Add the panel “Dynamic Settings” to the control panel. The excitation amplitude (V) has to be chosen in a way that the cantilever swing just with an amplitude of some nanometers (5-10nm). The system gets more sensitive the lower the amplitude of the oscillation is. When approaching the sample surface the interactions between tip and sample lead to decreasing amplitude. So when there is already small amplitude the detection of small force changes is easier. (To find out about the oscillation amplitude see “force curves”.)

Since the amplitude is always displayed as a negative value the *SetPoint* in this mode has to be set always to a negative value. High values (close to zero) mean a lot of applied force on the sample; low values (e.g. -9) make the piezo to withdraw. It is dangerous to set a positive *setpoint* as the system will probably damage the cantilever trying to get to this *setpoint*.

The feedback: - values in this mode are usually higher than in contact mode. The P.I corrections are linear corrections and are implemented by the Lock-In amplifier present in the *Dulcinea Electronics*. The correct values are relative depending on a lot of factors like: higher scan sizes (decreases P.I), number of points per line (decreases P.I), Sample surface (the more rougher is the sample the less adaptable to the changes is the system). It can bee changed the channel where is done the feedback for different types of AFM (Contact, non contact, lateral force).

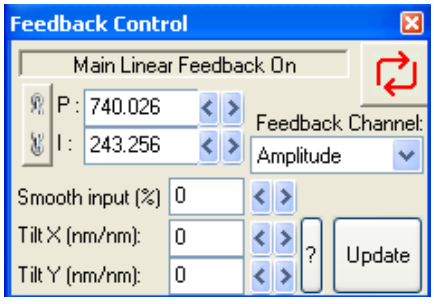

Image 4.16 Feedback control wondow.

*Dynamic settings:*In this dialog is possible to change the dynamic values like: Ampliude of oscillation, frequency of oscillation activating PLL…etc.

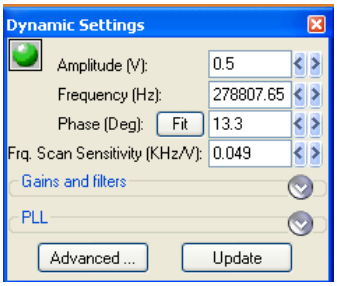

Image 4.17 Dynamic settings dialog.

Force curves

Force curves may deliver some important information about the sample, the current operation mode and the chosen parameters. In order to find the best operating parameters the different scanning modes it may be suggestive to do a force curve on a sample point.

In our equipment it was possible to make Force Vs. Displacement curves only in the middle of the actual scan line. This means that it's not possible to determine the exact point where to make FZ. This is one of the topics studied in chapter 6 where we, by means of Lithography section scripting, determine the exact point where to make FZ curves.

First should be activated the "FZ"- dialog. In the force curve the deflection of the cantilever is recorded in function of distance between sample and tip (z-position). In the picture such a force curve for an approach and withdraw of the tip of 200nm is shown.

The FZ dialog has a lot of menus for higher performances, but we would like to emphasis over the most used like: First Forward/Backward selection (Selects the direction of the FZ curve, if it withdraws first the tip of approaches), Initial Z; explains the distance in nanometers of the first step, and Oscillation Off; quits oscillation during FZ curves (results in the curves may vary the slope in the linear stage).

While it can be modified the quantity of FZ curves done at once, and at the final result can be an averaging of the N FZ curves done.

After "Do FZ", in the Viewer, is shown the channels selected like; normal Vs. displacement, lateral Vs. displacement, … etc. The channels can be selected from a pop up menu.

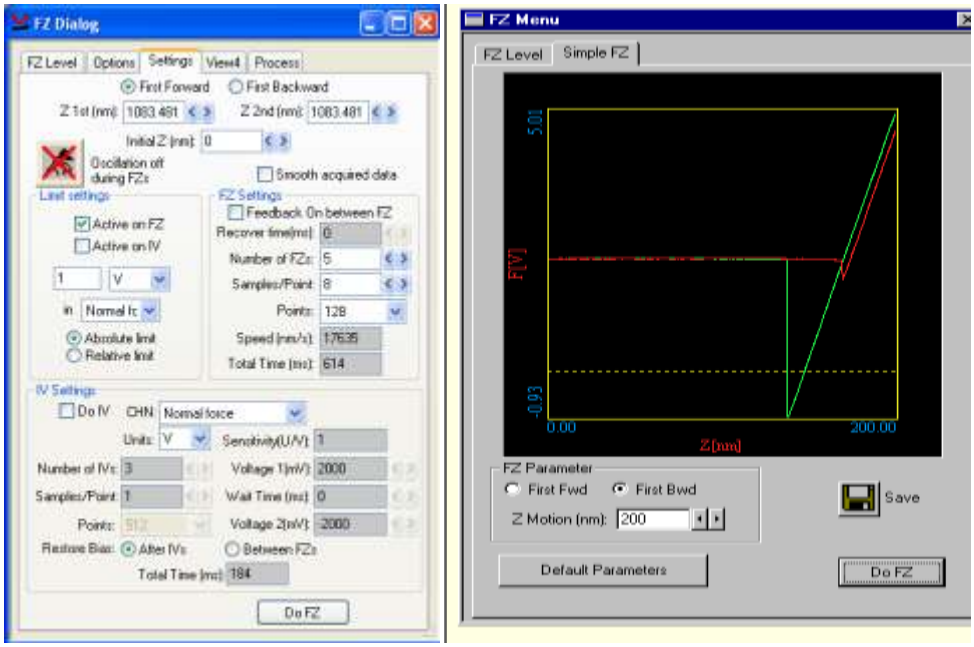

Image 4.18 FZ curve panel.

In Contact mode: when a force curve measurement is started in contact (First backward) the tip is withdrawn from the surface (green line from the right to the left) jumping suddenly from contact into non-contact. Approaching afterwards generates a similar pattern with a much smaller jump onto the surface. The jump into contact distance is related to the adhesion of the sample (e.g. in air promoted by capillary forces). The slope of the increasing part is related to the stiffness of the sample. In order not to harm the sample and to get better resolution, measurements in contact should be performed applying very low forces.

4.1.5 Jumping Mode

In jumping mode the cantilever performs Fz-curve for every image-point. First the feedback loop is closed to measure the topography of the sample and then opened to evaluate the tip sample interaction by moving the tip away and towards the sample. So apart from the topographic information, also information from each force curve about the stiffness and the adhesion of the sample is extracted. The parameters for this mode can be controlled in the jumping-menu shown above but the most important are: Jump Off (jump in nanometers from sample surface), Control cycles (Each N cycles makes an adjustment of the set point). The most important is the type of *Offset* correction is applied. The correction can be switched off, switched on in slow mode (correction is performed after every point) and in fast mode (correction after every line). In case that the correction is switched on, a good value in this mode will be 0.1V.

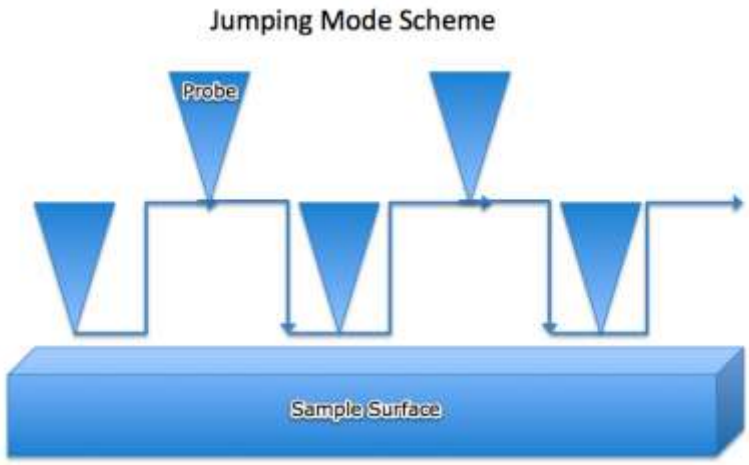

Image 4. 19 Jumping mode scheme.

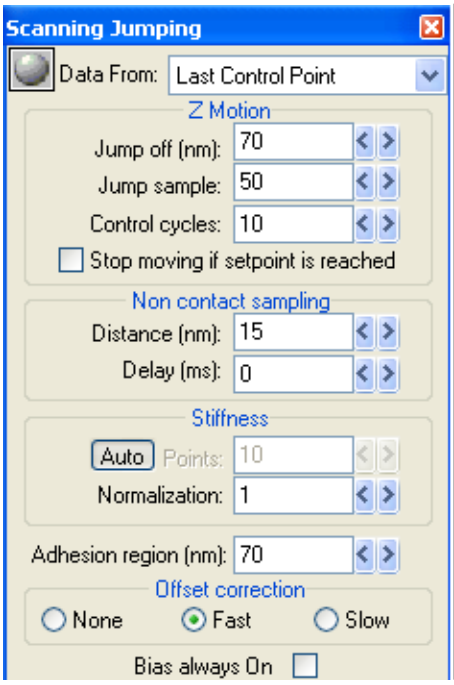

Jump off: Maximum distance between the tip and the point on every jump.

Jump sample: Set here the number of steps taken for every jump. This number is inversely proportional to the scanning speed, since each step takes a DSP defined unit of time. (In air 2/3 of *Jump Off* or less, in water 2 times *Jump Off*)

Control cycles: Set here the time the tip spends with the feedback closed after every jump. It is also inversely proportional to the scanning speed.

Offset Correction: Is the type of set point correction. Good practice is to use the Fast one. These recalibrations are needed due to the continuous jumps and contacts with sample surface that changes *SetPoint* values.

Image 4.20 Jumping parameters.

Apart from the information about stiffness and adhesion of the sample, the mode offers also the advantage to recalibrate the *SetPoint* in case that the normal force tends to change systematically during the measurement.

In order to perform very sensitive and faster measurements the jumpoff and the setpoint should be chosen as small as possible observing still the typical shape of the Fz-curve in the oscilloscope.

4.1.6 Artifacts

False engages: Among the most common artifacts during imaging with afm are false engages. We can easily detect and avoid them in the approach phase. When we approach, the final part is when near to range, the motor stops. Then later comes a phase of *SetPoint*best value search, while the scan size is set to zero, the best indicator of engage is the topography channel (In oscilloscope mode). Here the forward and backward lines (red/blue) make a cross (adjusting in the proper way the channel range values).

*Double tip:*During scan, the lifetime of probes (if going carefully) is round 2-3 days of scans. But if probes aren't especially rigid, they can breake their final part of the tip, the sharpest part. In this way we still continue to make images but the images aren't real. The following image explains a little bit the situation that occurs.

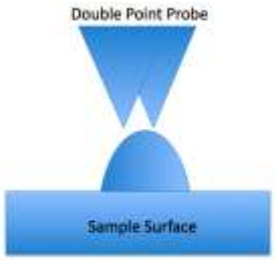

Image 4.21 Convolution of sample surface with double tip probe.

In this particular situation the image taken is the convolution of the sample surface (In that particular scan line) with the double tip probe. The effect is as we are imaging with two probes really closer to each other. And the final result is like overlapping the same image to it's self but shifted of the distance between two tips.

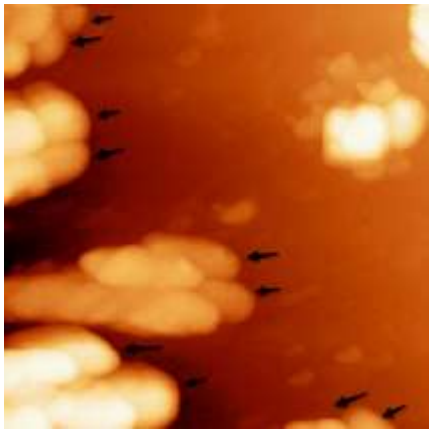

Image 4.22 Double tip effect. Let's note the symetric structures in between

Deep trench: As we previously said, the resulting image is a convolution of two planes (plane because we scan in lines); the profile of the tip and sample surface profile. In reality the situation is more complex because there are more than one plane that influence, with different weight, the resulting image or height lecture form the photodiode.

In this way, when the tip is bigger than the substrate aperture, is presented the following situation:

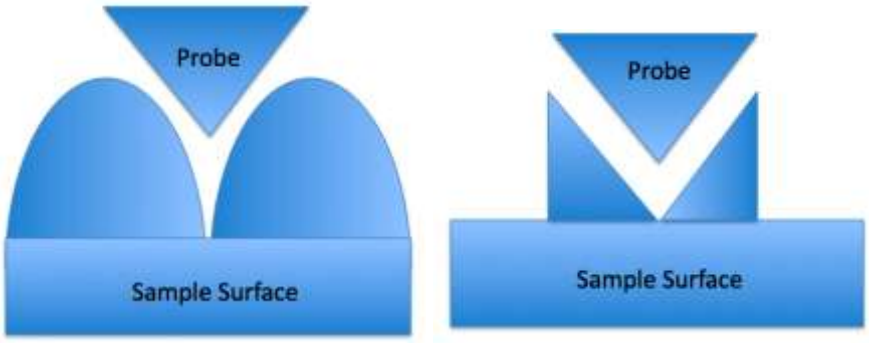

Image 4.23 Probe convoltion with sample surface.(Left)The real situation. (Right) How is transmitted o us the surface topography that follows the surface contours of tip.

Tip radius enlargement: During scans there is a lot of micro-dust that for different forces like electrostatic forces can engage to the tip. Resulting in an enlargement of the tip. This situation is similar to the previous one described, because the tip is once again bigger than the surface apertures. This effect is resulting in augmenting the effective dimensions of the substrate measured. A way to go through is to scan with a grid with known geometry and dimensions.

Bluried image due to ionic presence: When working in liquids with charged surfaces, we should keep in account the fact that it could be some repulsive forces due to ionic charges in the surface (While making liquid measurement the effect is more visible).

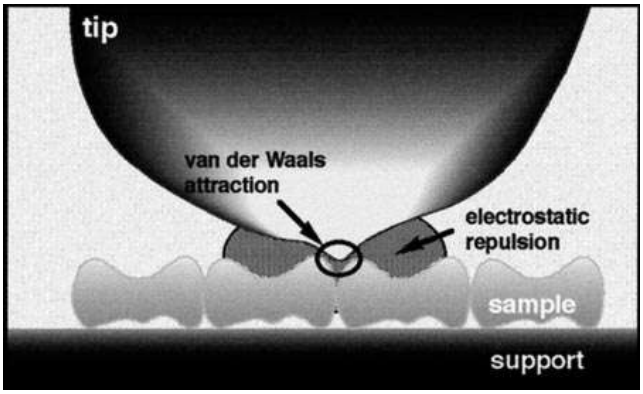

Image 4.24 Electrostatic repulsion due to ionic superficial charges, Muller et al 1999.

Trouble Shooting:

- *Low resolution. Everything seems to be quite blurred.*

In this case, both in contact DC and jumping JM is better to increase the *SetPoint* in order to apply more force between tip and sample, for gaining the repulsive forces. Be careful whether piezo is still moving when varying the *SetPoint*.And as usual is good to make an Fz-curve. In tapping mode increasing the excitation amplitude might help to get into contact with the sample. Once a stable image is achieved the amplitude may be reduced again.

- *Water measurements:* Apart from the advantage to do an image in a biological friendly environment doing AFM-measurements in water (buffers) may also increase the resolution of the images, as the influence of surface charges is reduced.

Mounting the tip holder for liquid measurements

A different tip holder has to be used for measurements in water. The disadvantages of this holder are that vibrations performed by the small piezo in the holder for tapping-mode are noisier and in general alignment of the laser-spot onto the tip is more complicated.

1. First, the tip should be cleaned the holder and putting a drop of vacuum fat onto the holder.
2. Take a new cantilever chip and “glue” it now onto the sample holder. The adhesion will be strong enough to perform measurements.

The tip holder may be mounted onto the measuring-head and a rough alignment of the laser can be done. The readily prepared sample has to be put onto the sample-holder. Wet the sample with a (big) drop of buffer. Wet the tip-holder carefully from above to get a drop of buffer surrounding the cantilever and protecting when approaching later to the sample. Mount the tip holder.
Approach the sample and tip manually (micrometer screws) until both drops (from tip and sample) band together. The vertical alignment of the laser has changed now. So the laser has to be recalibrated looking at the tip itself (throw the crystal-window in the tipholder) and the reflection from the tip (typical refraction pattern when calibrated). Fine adjustment is done as usual with intensity-meter of the photodiode in the software.

- In general in water the whole measuring-setup has to equilibrate much more time than in air. But with increasing time the risk of “tip-contamination” is also increasing, what will lead to lower resolution. So in contrast to measurements in air there is a smaller time frame to perform qualitatively high measurements.

- Beginning measurements with a freshly mounted sample it maybe favorable to start in *jumping mode,* as the automatic recalibration (*SetPoint*-correction) tends to be less harmless for the sample.
- For measurements in water the *jump off* may get as low as 20 nm. The value for the *sample rate* should be twice the one of the *jump off* to stabilize the system.
- In stable conditions measurements in contact mode may deliver the highest resolutions. It is important to apply the lowest amount of force possible (also choosing the right tip).

4.2 GxSM

The GXSM is the Gnome X Scanning Microscopy project [43], [44] is SPM control and data analysis software. It provides a solution for all homemade SPM; especially new prototypes intended to invent new modes of operation, where the development of a complete new software system from scratch would be too expensive and time consuming. Since GXSM is licensed under the GNU general public license the full source code is published and everyone is allowed to use and modify the software package for his own needs. The GXSM project has been developed under the GNU/Linux operating system to a full-featured SPM software. The user interface is based on the modern Gnome/Gtk1 library

4.2.1 DSP Controller

Using the PCI32 data acquisition board with the TMS320C32 [45] floating point DSP running at 60 MHz specialized DSP software is used to operate STM, AFM, and similar instruments. The design of the DSP program is similar to a state machine and able to do quasimultitasking. All time dependent tasks such as the feedback loop and certain signal generations are performed via hardware timer driven interrupt subroutines to ensure proper timings.

Due to slightly different needs (e.g., logarithmic or linear feedback signals for STM or AFM, respectively) optimized DSP codes are available for each supported instrument type. The DSP source code (written almost completely in the ANSI C programming language) and precompiled DSP binaries for several hardware configurations (ready to launch) are freely available.

4.2.2 Installation of Signal Ranger Board & GxSM (ver. 1.9)

- Is important to have an updated linux kernel.

  At the moment is used version (2.6.20).

  For knowing your kernel version, you may prompt in a terminal the following command:

root@ijoni-desktop:/SRanger# **uname -r** {the following line is the message text, given...}
2.6.20-16-generic
In case the kernel version is rather old (previous than 2.4), is needed a kernel update.

- Than later if it is needed, there should be an update of the following packages by using the command: *apt-get install <package_name> (allways as root, :# sudo su -> pass -> :/#)*
  ex: **apt-get install cvs** {is installing the cvs package}
  During our instalation we used the following packages:

  cvs, libtool, libgtkglext-dev, autoconf, automake1.9, libglib2.0-dev, libglib2.0-data, intltool, libgtk2.0-dev, libgnomeui, dev, libgtkglext, gnome-common, g++, libnetcdf3, netcdfg-dev, freeglut3-dev, fftw3-dev, libquicktime-dev, libncurses5-dev, linux-headers-generic
  You might also want to install these ones:
  kate, anjuta, crossvc, doxygen-gui, ddd, devhelp

- As follows, the gtkdatabox pakage has to be downloaded and compiled.
  1. Download the *.tar.gz file form: *http://www.eudoxos.net/gtk/gtkdatabox/download/gtkdatabox-0.2.4.7.tar.gz*The version of the *gtkdatabox* is important because is related with kernel version.
  2. For unpacking: tar zxvf gtkdatabox-0.2.4.7.tar.gz
  3. Enter at the directory: cd gtkdatabox-0.2.4.7
  4. Execute the configure program: ./configure –prefix=/usr
  5. Executing make: make
  6. And **make install**. Will create the Makefiles.m
- Next step is downloading the programs Gxsm & SRanger.

There are two ways of downloading it:

1.by coneccting to the server in an anonimuos way, with the following command:/home/ijoni# cvs -z3 -d:pserver:anonymous@gxsm.cvs.sourceforge.net:/cvsroot/gxsm login
after this, we have the following notification:
Logging in to :pserver:anonymous@gxsm.cvs.sourceforge.net:2401/cvsroot/gxsm
CVS password: (*Simply press Enter*)

Later with the following, is possible to download the source code: **cvs -z3 -d:pserver:anonymous@gxsm.cvs.sourceforge.net:/cvsroot/gxsm co Gxsm-2.0** wich will be saved in the directory of work.*(Identical for downloading SRanger)*

2.The simplest way is downloading directly from the web page of SourceForge.net. at this link: *http://sourceforge.net/projects/gxsm*

- Then we will need to compile the programs, *(Compiling)*
  1.Change into the Gxsm-2.0 directory and type (if you have the "stow" utility installed and liketo sort your local soft enter the optional prefix like below in brackets):
  $ ./autogen.sh [––prefix=/usr/local/stow/gxsm2]
  This should finally create all Makefiles in several sub-directories.
  2.Type make in the Gxsm-2.0 directory:
  $ make
  This command will compile everything, if you want to compile it step by step, you can run this command in the src sub-directory first separately to see if all works OK. But later you want to compile all plug-ins and tools as well – if it works in src it is most likely works for the rest, so try **make** in the Gxsm-2.0 dir again.
  Hint: To speed the make process up on multi core systems, use $ make -j2, $ make -j4... for spawning multiple compile jobs.
  3.Simetrical situation for SRanger, while the list of commands is as follows:
    a) **$ ./autogen**
    b) change into directory Sranger/modules and run**$ ./make**
    c) To create the dev/sranger0 **$./make install**

Later there is needed to load the firmware, by loading the *firmawareloader*.

Installation Manual of nvidiaglx

During the installation of Gxsm2 we encountered serious problems concerning the video CardNVIDIA GeForce 6600.This was because GxSM installation (in a step) consists on rewriting thekernel modules, as consequence, probably rewrites something concerning the video card.As a result, the system wasn't able to start in normal mode, because the graphical environmentXwindow gave few errors.

Solution: By making a refresh of the packages, with **apt- get -f install** there is an update of thepackages. The package name is nvidiaglx(is easier to make the upgrade by apt-get install tool,because solves the problem of package dependencies).

During the installation there is needed further installations of the plug-ins of control.

Modifying the file spm_autoconf.py found in the following path: /SRanger/TiCC-project-files/FB_spmcontrol/. This file has to be modified in order to correctly use the control plug-ins. By modifying the source codeas follows:

```
sranger_file_location = "/dev/sranger0"
offset_file_location = "/home/jordi/offset"
loadusb_folder_location = "/home/jordi/SRanger/loadusb"
dspcode_file_location = "/home/jordi/SRanger/TiCC-project-
files/FB_spmcontrol/Debug/FB_spmcontrol.out"
```

and in this way, by executing at the command prompt:

```
/SRanger/TiCC-project-files/FB_spmcontrol# ./spm_autoconf.py
```

4.2.3 Brief tutorial of GxSM

After startup, the main window appears. The actual user interface provided by the main window depends on the configuration. GXSM can be configured for use with SPM techniques, which is the default, or SPA-LEED.

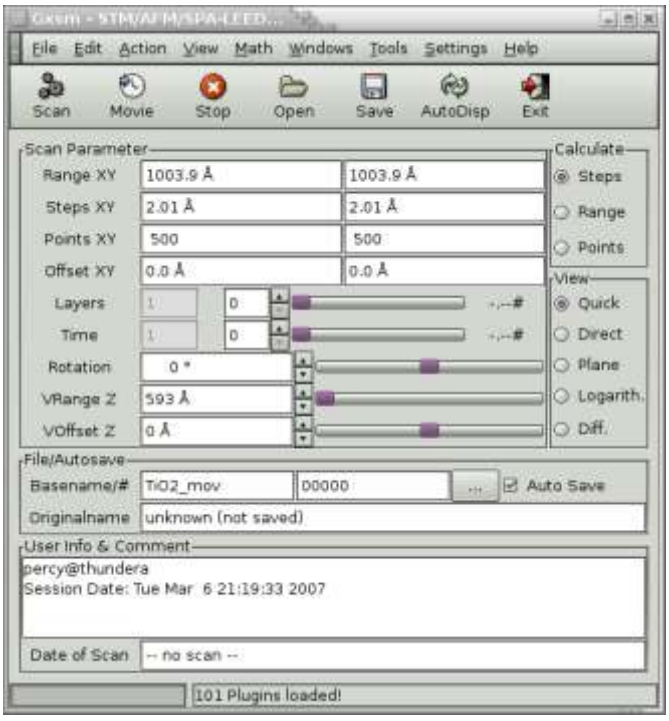

Image 4.25 GxSM main window.

The main window provides two different functions: Firstly, it has a menu bar with pulldown menus. These menus provide the user with the usual File and Help menus that can be found in practically every mouse-driven software piece. Some of these pull-down menus interact with (Math) or start-up (Windows) other windows. Secondly, the main menu contains a large number of control fields, which can be used, e.g., to control an instrument, or just display certain parameters. These control fields are described in the following two sections.

The main window contains from top to bottom the menubar, a taskbar, the scan parameter, view mode, file, and info/comment sections, and a status and progress bar. The scan parameter and info sections of the main window are used both for entering parameters during data taking and displaying them after loading data.

Scan parameters: Each scan or image is characterized by its size and resolution. The size, or Range XY, gives the scale of the image like the scale of a city map and denotes the height and width of the scanned area. The resolution is determined by either the distance between the single scan points/pixels given by Steps XY or the number of points in X and Y direction given by Points XY. Given two of these parameters, the third one can be computed. The check box Calculate determines, which of them is calculated by GXSM. For instance, if Steps is checked, a change of Range XY results automatically in a new value for Steps XY.

The parameter Offset XY determines the distance of the zero-point of the image coordinates from the center of the physical scanrange. The actual location of the zero-point within the scan depends on the source of the data. If the data was acquired using GXSM, the zero-point is the middle of the topmost line. Using Rotation, the imaged area can be rotated. Both inputs using numeric values and the scrollbar are possible.

GXSM can be used to do spatially resolved spectroscopy (“probing”) measurements. Channels containing probing data are essentially three-dimensional (3D) datasets. In these 3D datasets the X and Y coordinates correspond to the 2D position like in conventional SPM images. The third dimension, V, can contain spectroscopic information, such as I/V curves for scanning tunneling spectroscopy. GXSM displays only one slice corresponding to one V value at a time. A layer denotes the number of points in the V direction. Using Select, one of these slices corresponding to one V value can be selected for visualization. VRange Z and VOffset Z are used for the visualization of the scan data. They do not influence the data itself.

Problems faced with: During these months passed in installing the program, there have been spent a lot a time in understanding the structure and hierarchy of the program. The impossibility to spend more time in understanding it, have made us renounce.

In this chapter, I represent that part of work dedicated to scanning different biological samples over different substrates. During these months there have been scanned three sets of samples, as are presented in the index. They were gently prepared from Dr. Rosa Carmen Baños(Post doctoral researcher at Institut de Bioenginyeria de Catalunya, IBEC). Bacteria like *Escherichia Coli* (E. Coli see Appendix C) and *Pseudomonas aeruginosa* (Pseudomonas au. see Appendix C) were selected in base of: their widespread in daily life (relevance as a pathogen), recognized as emerging opportunistic pathogens of clinical relevance due to their increasing resistance to antibiotics (in isolated cases) as recent studies [46] have noted persistence of E. Coli and Pseudomonas au. biofilms. (More over biofilms, see Appendix A)

At first there is an optical phase, which helps to give an idea of bacterial aggregations and later follows AFM mechanical and topographical characterization.

In this work is important to note that the whole is concluded with two main and satisfactory results:

1. Mechanical and topographical characterization of E. Coli and Pseudomonas au. biofilms, especially of the links found between them.
2. Topographical characterization of biofilms in liquid environment.

The first one is of mayor importance as for our group and the one that we collaborate (Prof. Dr. Antonio Juárez, *Group Leader Biotecnologia microbiana i interacció hoste-patògen.* IBEC) are the first experiments making possible biofim characterization with AFM.

The second one is a big achievement for our group as the first time to characterize bacterial samples in liquid environment. And more, we found once again links between bacteria, showing that liquid imaging gives similar results to air imaging and establishes the basis for further dynamic studies of bacteria's in their habitat. Studies that give more realistic results, in comparison to the ones shown here, as bacteria are fixed in the substrate.

Fixing bacteria implies, loosing information regarding bacteria-substrate surface adhesion forces. In the sixth chapter we establish the basis for calculating these forces.

5.1 First set of Experiments: Nanobiocharacterization of Pseudomonas and Escherichia Coli over different substrates

5.1.1 Pseudomonas au.

There have been cultured Pseudomonas over: glass, plastic, mica, silicon and gold.

5.1.1.1 Characterization by Gram's staining method

Referring to the Gram's staining (see Appendix A) we can see that plastic and glass are the substrates where bacteria grew the most. Followed by mica, on which they grew in an average way, and finally over gold they grew less. Glass and plastic substrates are ruled out because of the impossibility of characterization with AFM.

5.1.1.2 Characterization by optical microscopy

The equipment utilized is an optical microscope Carl Zeiss that was working on reflection mode on air. The objectives used were: 20x, 50x and 100x coupled with a CCD camera of 640x400 pixels resolution.

The total equipment was mounted over a table (anti-vibrating isolation, see HW chapter) and illuminated with white light (wide spectrum), where no filter was used.

General note: We should note that due to small dimensions of bacteria, there are some difficulties in interpreting the images obtained from optical microscopy. Probably this wouldn't happen with other types of bacteria's, such as E.Coli. As follows, are shown optical images of E.Coli and Pseudomonas au. in gold with 100x: (Optical microscopy courtesy, J. Otero)

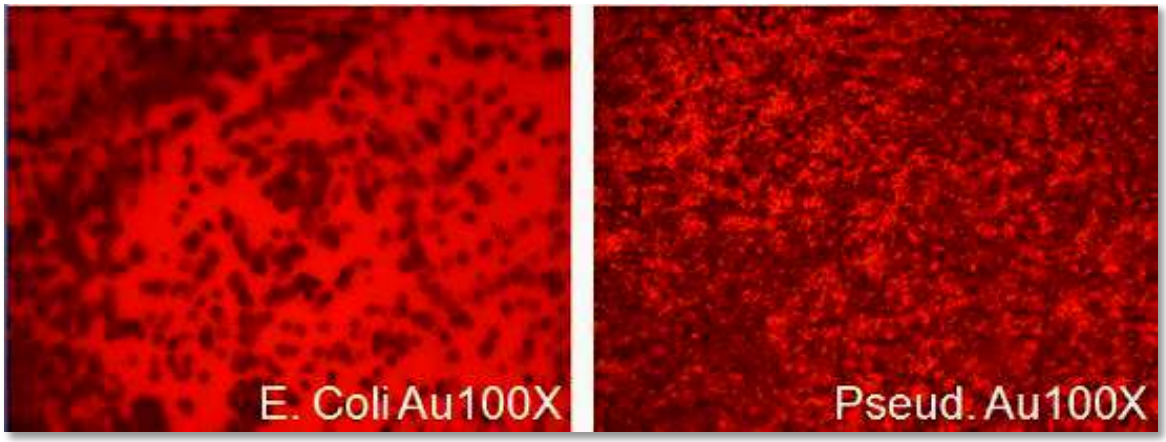

Image 5.1 E.Coli (left) and Pseudomonas au. (Right) over gold, optical microscopy 100x.

Mica: The image suggests absence of huge bacterial proliferation.

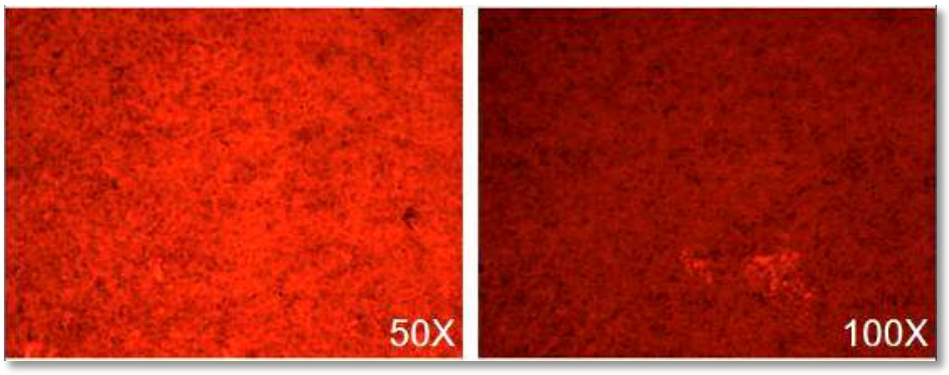

Image 5.2 E.Coli (Left) and Pseudomonas au. (Right) over mica, optical microscopy 50x.

Silicon: The surface looks more colonized than mica, and seems that bacteria are creating series of associations while leaving other places empty:

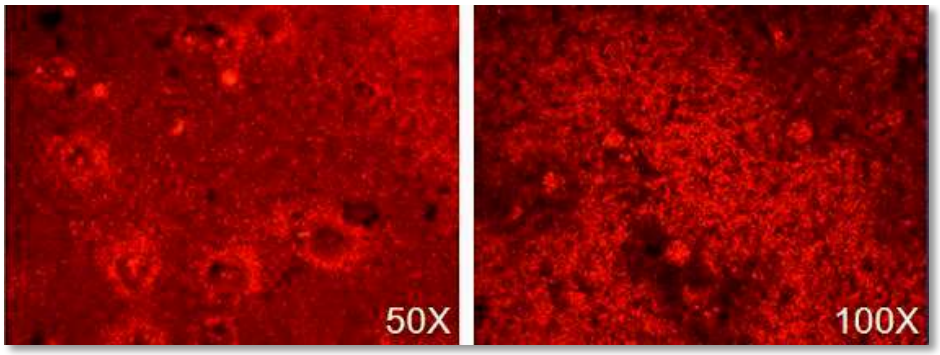

Image 5.3 E.Coli (Left) and Pseudomonas au. (Right) over silicon.

Gold: The images from optical microscopy (see Image 5.4) shows that gold is the surface wherebacteria have been creating bigger associations, covering for entire certain zones:

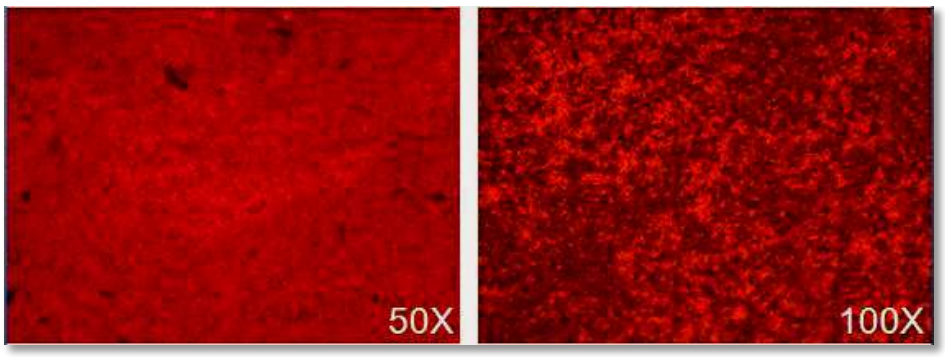

Image 5.4 E.Coli (Left) and Pseudomonas au. (Right) over gold.

5.1.1.3 Topographical characterization using AFM

The equipment used was a Cervantes Atomic Force Microscope of Nanotec Electronics, by using the dynamic mode (AC mode) on air. The AFM cantilever used is made of nitride silicon with a spring constant of 42N/m. With this kind of cantilever is relatively easy to image faster the sample (by applying faster scanning speed over lines), but at the moment of calculating forces (due to his stiffness) has small sensitivity. This means; that are needed higher forces for making small deflections of cantilever and vice versa. If we needed to make high resolution imaging it would have been better applying softer cantilevers, in this way, at the same time is easy to make Force Curves and calculate sample stiffness. After this we collocated the AFM head on an active anti-vibration table (25dB – 40dB of attenuation factor) inside an acoustic isolating bell. (Chapter 3.1.1)

Mica: While over mica there wasn't any kind of associations. We found only few bacteria that were jointed together, maybe due to the drying process. (See comments at end chapter). Here bellow in image 5.5 we show a typical view:

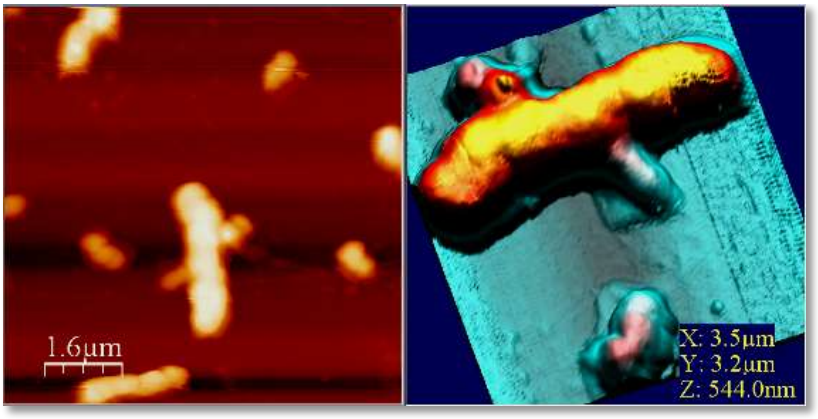

Image 5.5 AFM image of Pseudomonas au. over mica. (Right) 3D reconstruction.

Silicon: In silicon (Image 5.6), as suspected from the optical images, the bacteria are more associated and they occupy more sample surface. They don't look like overlapping with each other and looks like are organized in a monolayer. Whatever, there is no sign that indicates the existence of something different ex. links, channels etc. distinct from cellular membrane. While scanning different zones, the one, which was less crowded, is shown in image 5.6:

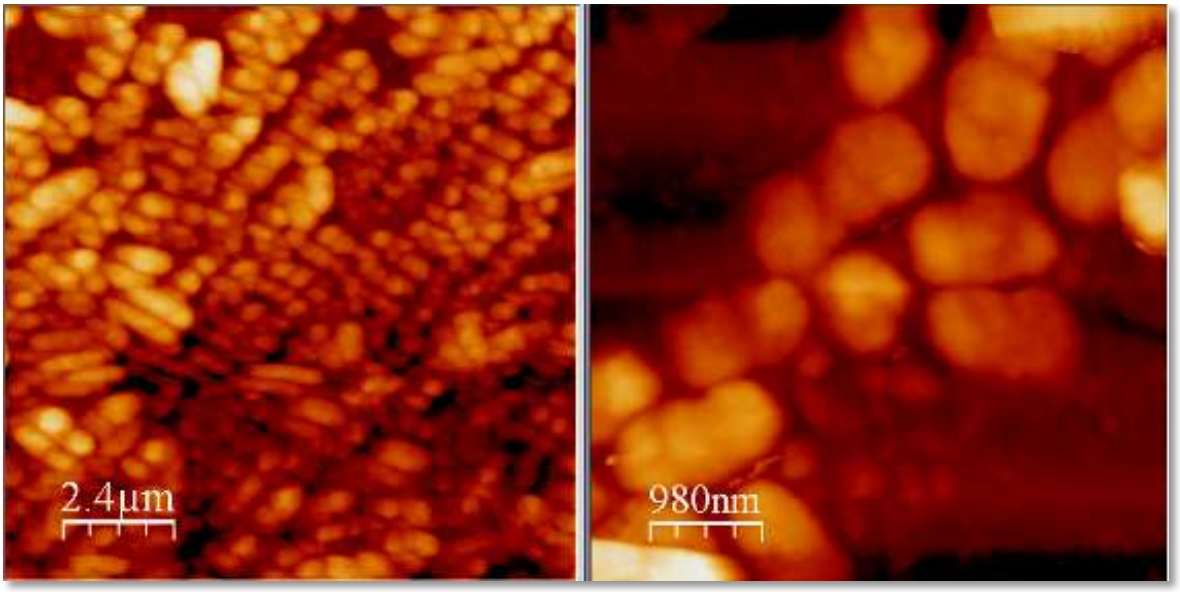

Image 5.6 AFM image of Pseudomonas au. over silicon.

For a better understanding of this region, we liked to make further zooms and a line of profile over few bacteria as is shown in Image 5.7:

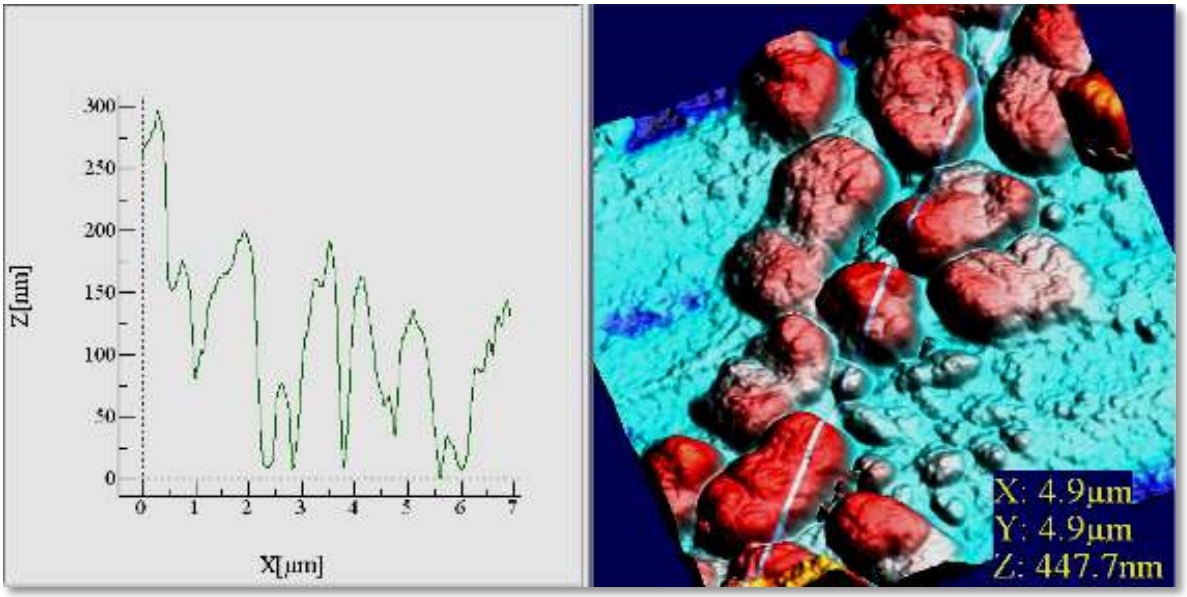

Image 5.7 3D profiling of a previous section of Pseudomonas. (Left) Profile of the line visible in 3D reconstruction.

Gold: The substrate, as we can see from the optical images in image 5.1, is covered with bacteria. We can definitely say that here bacteria form a monolayer, as in general they aren't deposed one upon the others forming higher aggregations.

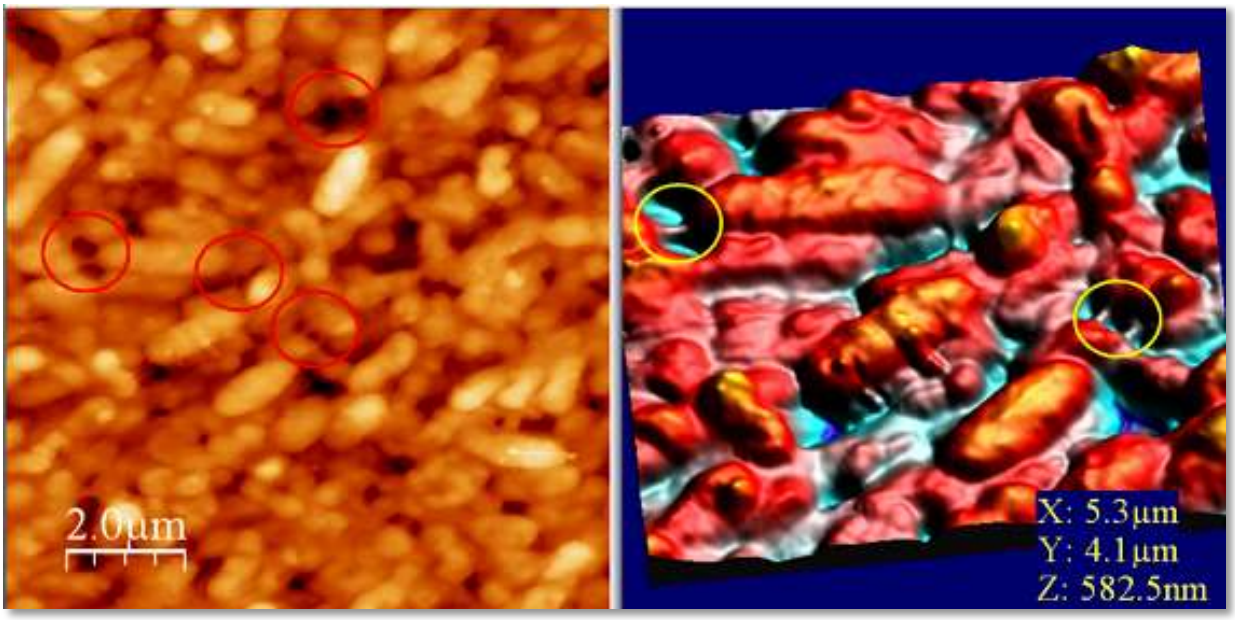

Image 5.8 Pseudomonas au. over gold. (Left) In circles are evidenced interconnections between bacteria. (Right) 3D reconstruction of zone of interest.

Remarkable is the appearance of interconnections (normally simples, and sometimes doubles) between bacteria (but not in general, only between few of them). Links with dimensions of about 100*nm* in height and 200*nm* in width:

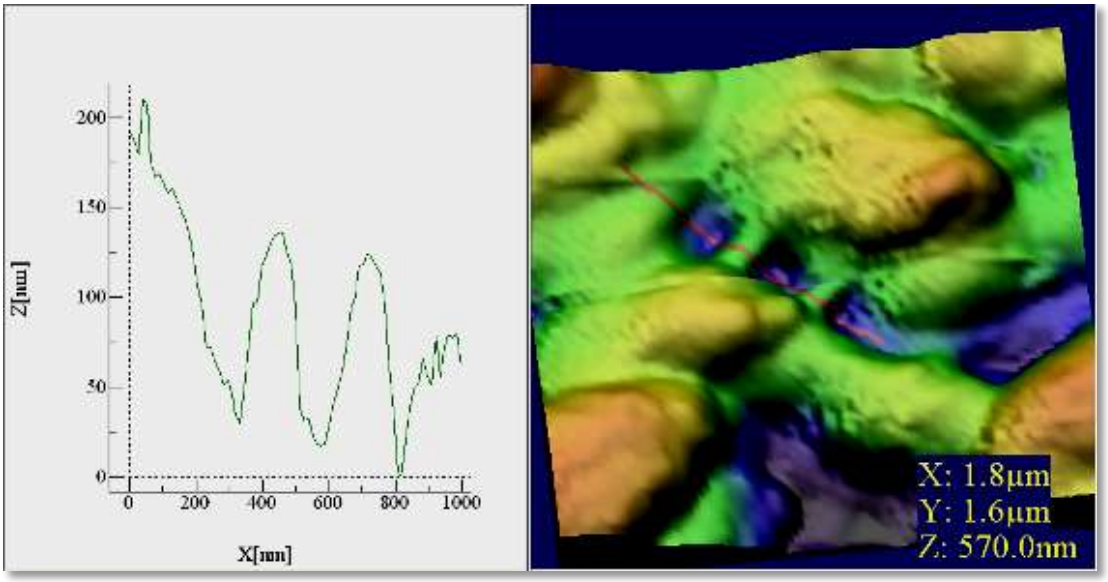

Image 5.9 Pseudomonas over gold. Zoom in over interconnections. (Left) Profiling of double interconnections between two Pseudomonas. (Right) 3D reconstruction.

5.1.1.4 Mechanical characterization with AFM

The links appeared in the images seems to be specific and different from the bacterial membrane. For demonstrating this, it's important to make some mechanical test over them (Force Vs Displacement curves) in order to compare with tests made over bacteria membranes.

We used the same AFM microscope as in the topographical characterization measurements, but with a cantilever that has higher resolution when making mechanical tests. This implies using a cantilever with smaller spring constant k (we used Olympus cantilevers)

More in detail, it was a cantilever made of silicon nitride with spring constant around 0.76 N/m. The images, previous to mechanical tests (essential for localizing the working points) were made in air using dynamical mode. This kind of cantilever isn't the proper one for these requirements, but working slowly (40min/image) and leaving the whole system stabilizing (round 1-2 days), is possible to get images of similar quality than the previous ones. And here bellow in Image 5.10 is shown the result of the choices made at the time when to image the sample:

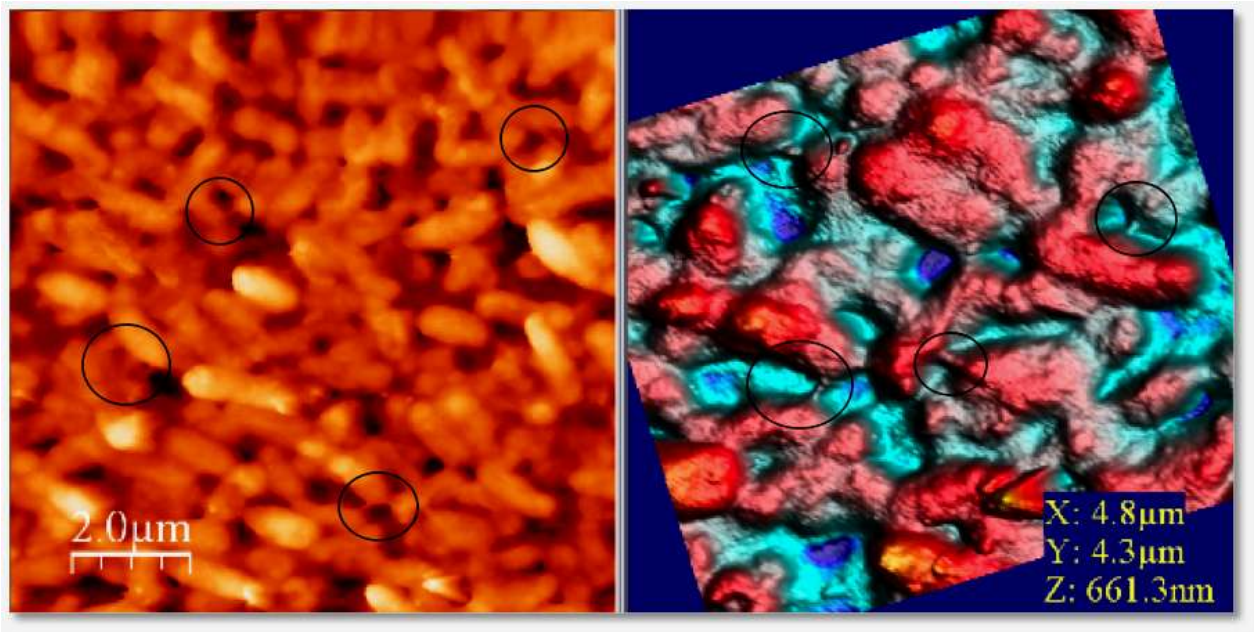

Image 5.10 Pseudomonas au. over gold.

Later there have been tests (force curves: force vs. displacement):

- 20 force curves over the "channel".
- 20 force curves over the central part of bacteria.

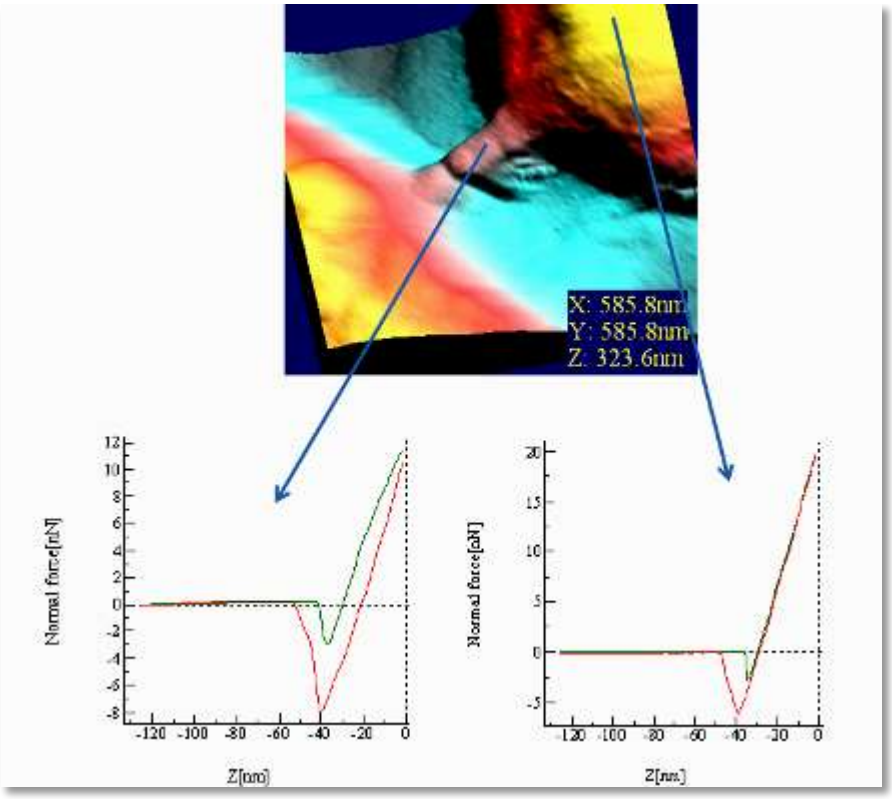

Image 5.11 Force curves over channel between two Pseudomonas and over membrane.

From the analysis of the average 20 curves (Image 5.11) there is a clear difference between channel composition and bacterial membrane composition. We can see more adhesion (need of 8nN force to unhook from the "channel" in comparison of the 6nN to uncouple from the membrane).

At the same time if we focus on the graph at bottom left in image 5.11, there are slope differences between forward (green) and backward (red) curves. In this way bridges presents' higher viscoelastic behaviour than membranes, which in turn presents more elastic behaviour.

For each displacement in one of the curves at the contact zone (slope part of FZ graph), let's say -20 nm, the applied force over the bacteria almost doubles the force over the channel. This shows that the channel is more easily deformable (for same Z movements, the channel sinks more, so the cantilever deflexion is smaller), having smaller elastic module (softer material).

We should note the necessity of a calibration process of the whole AFM, regarding the photodiode calibration, piezo calibration, and at the end comparison of these slopes with a slope over sample surface where aren't present membranes. This further step will permit us to compare different slopes between membrane and rigid surface.

5.1.2 Escherichia Coli

There have been cultured E. Coli over the following substrates: glass, plastic, mica, silicon and gold.

5.1.2.1 Characterization by Gram's staining method

Referring to the Gram's staining method (see Appendix A) we can see that plastic and glass are the substrates where bacteria grew the most. Followed by mica, on which they grew in an average way, and finally over gold they grew less. Glass and plastic substrates are ruled out because of the impossibility of characterisation with AFM.

5.1.2.2 Characterization by optical microscopy

The equipment utilized is an optical microscope Carl Zeiss that was working on reflection mode on air. The objectives used were: 20x, 50x and 100x coupled with a CCD camera of 640x400 pixels resolution (see Chapter 4).

The total equipment was mounted over a table (anti-vibrating isolation) and illuminated with white light (wide spectrum), where no filter was used. The illumination with white light is for default illumination mode by the microscope.

Mica: Images obtained with the OM show high differences between different zones of the substrate. We saw zones with high proliferation of bacteria and other ones where we found isolated bacteria (now, in comparison with size of E. Coli, we have enough optical resolution to distinguish single-cells). In image 5.12 we can see easily the E.Coli populations over mica, and by augmenting magnification, we can distinguish them even better.

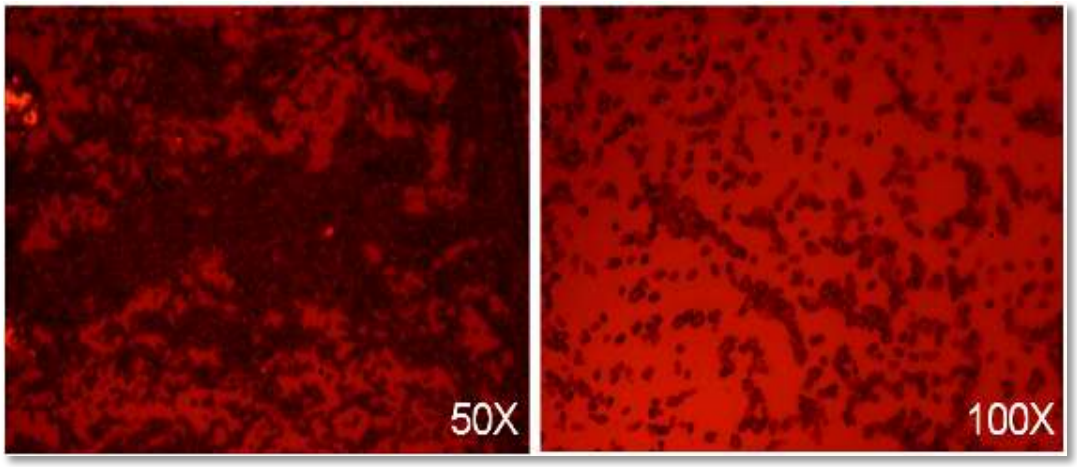

Image 5.12 E.Coli over mica with 50x and 100x zoom.

Silicon: is the substrate where E. Coli grew the most. Let's focus over Image 5.13; we see the whole substrate full of bacteria. Fortunately, there are several regions non-covered or where bacteria aren't filling the whole sample substrate, so we can make AFM experiments and evidence even more the differences and even links.

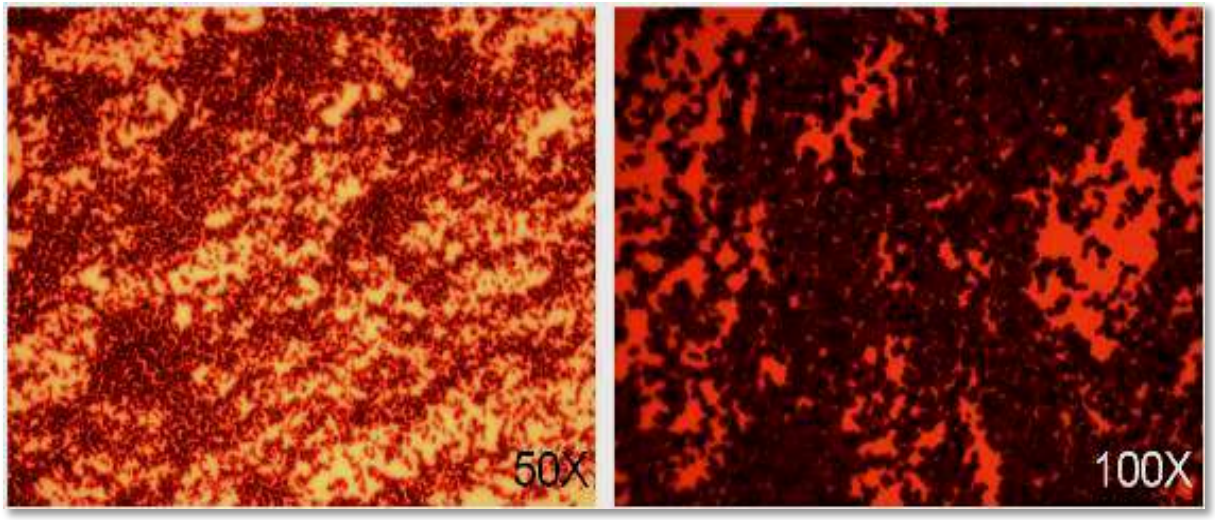

Image 5.13 E.Coli over silicon with 50x and 100x zoom.

Gold: Instead over gold substrate the situation was similar to mica, huge differences in population densities while switching from one zone to another:

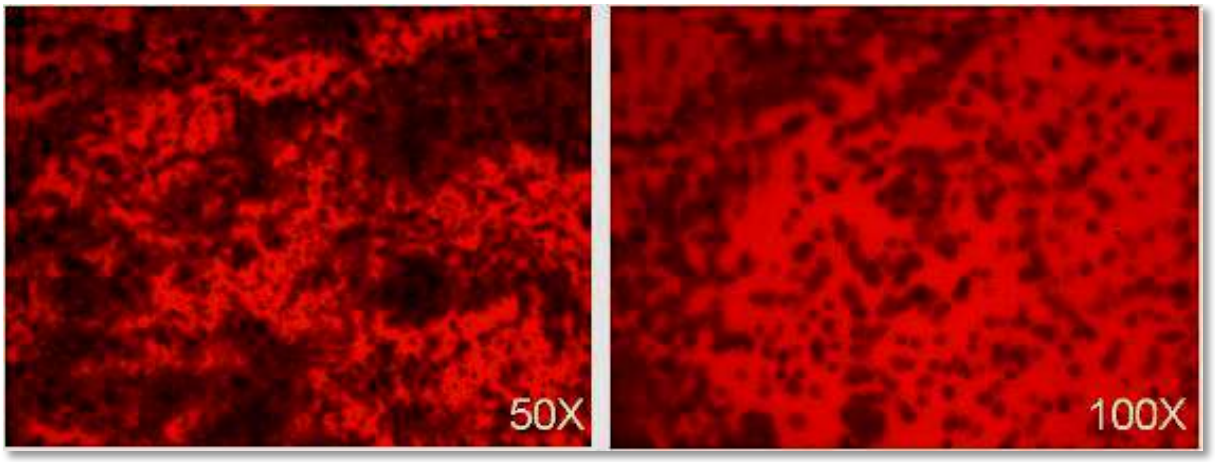

Image 5.14 E.Coli over gold with 50x and 100x zoom.

5.1.2.3 Topographic characterization by AFM

The equipment used was a Cervantes Atomic Force Microscope of Nanotec Electronics, by using the dynamic mode (AC mode) on air. The AFM cantilever used is made of silicon nitride with spring constant of 42N/m. All is mounted on an active anti-vibration table (25dB – 40dB of attenuation factor) inside an acoustical isolating bell.

Silicon: Is the substrate where it's easier to find bridges between E. Coli. During the scan, this particular region, showed more than one channel in between bacteria. Some of the bacteria are dried due to time passed since the sample was prepared, but some of them still present interconnections with their neighbours. In image 5.15 we can see in circles the links that we encountered. As we evidenced before, some bacteria are deteriorated. In image 5.15 right, is a 3D reconstruction showing some of them flatter and with smaller volume in comparison with the rest.

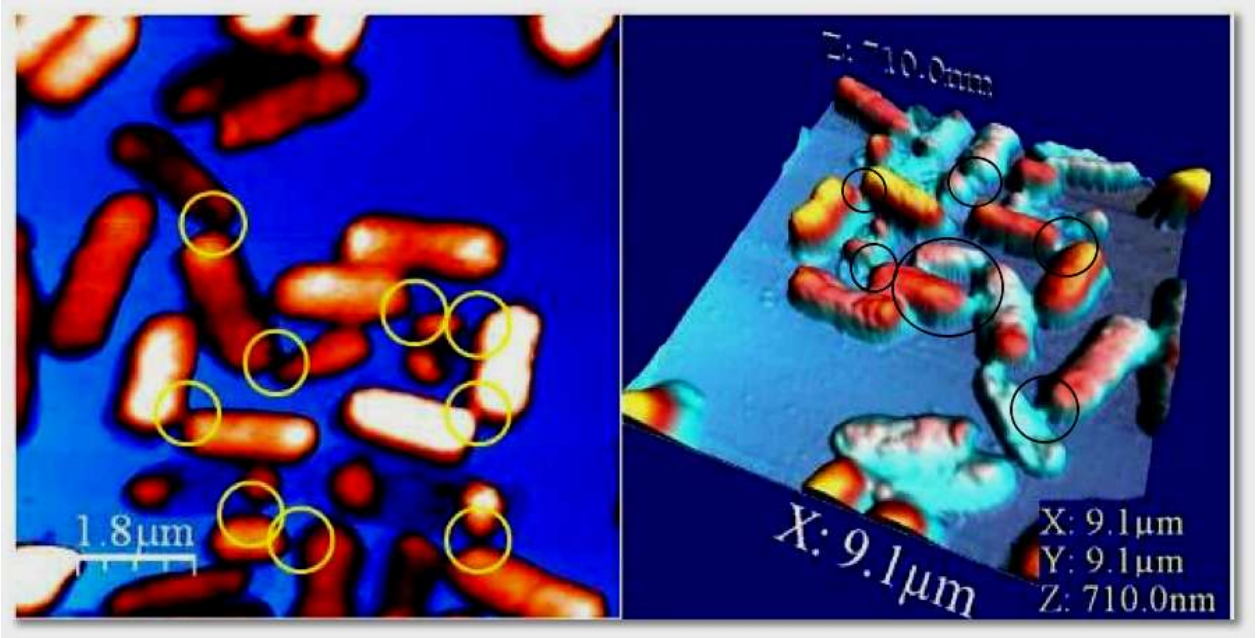

Image 5.15 E.Coli over silicon. (Left) Region with connections (see circles). (Right) 3D reconstruction.

As we have several "links" in the same image we can profile them. There is a huge dispersion in their size and width, but we still can classify them in two groups. One group let's call it "small links" and the other "big links". In the following picture we can see all the profiles studied:

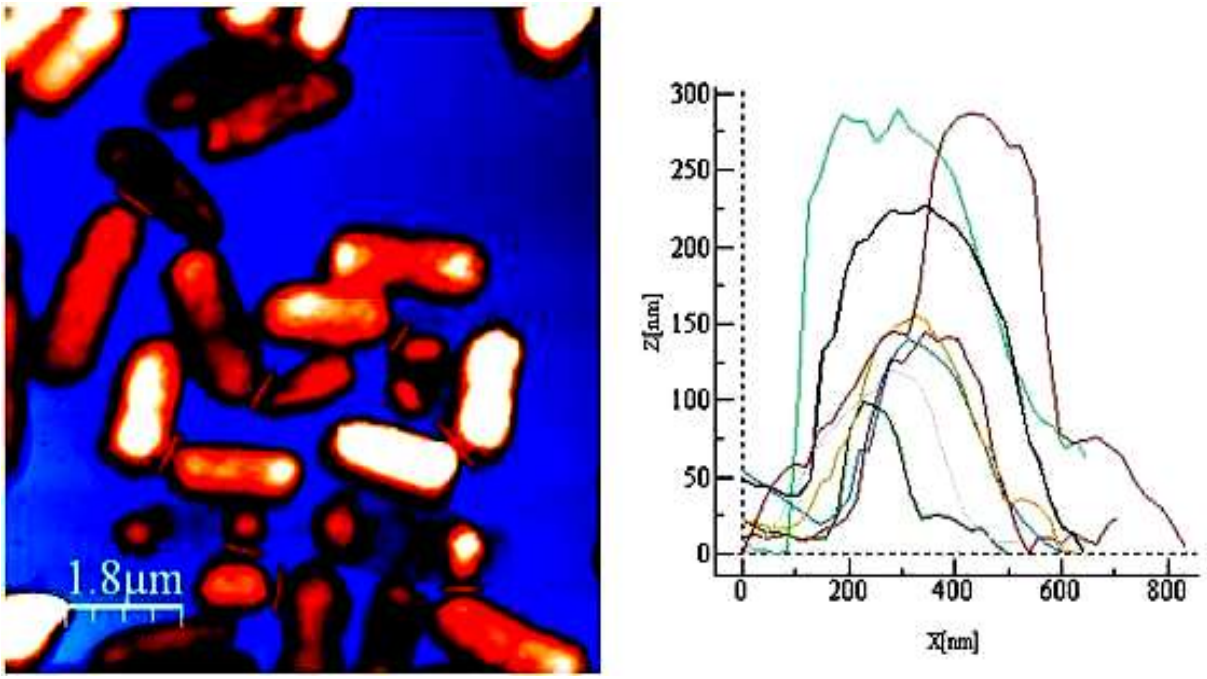

Image 5.16 E.Coli over silicon. (Right) Generic study over links dimensions.

The dispersion seems to be high, but we are still able to classify profiles in two groups. We can suppose they belong to different types of connections between bacteria. In image 5.17 there are two clearly defined groups, links of about 250*nm* x 150*nm* (left) and links of about 500*nm* x 300*nm* (right).

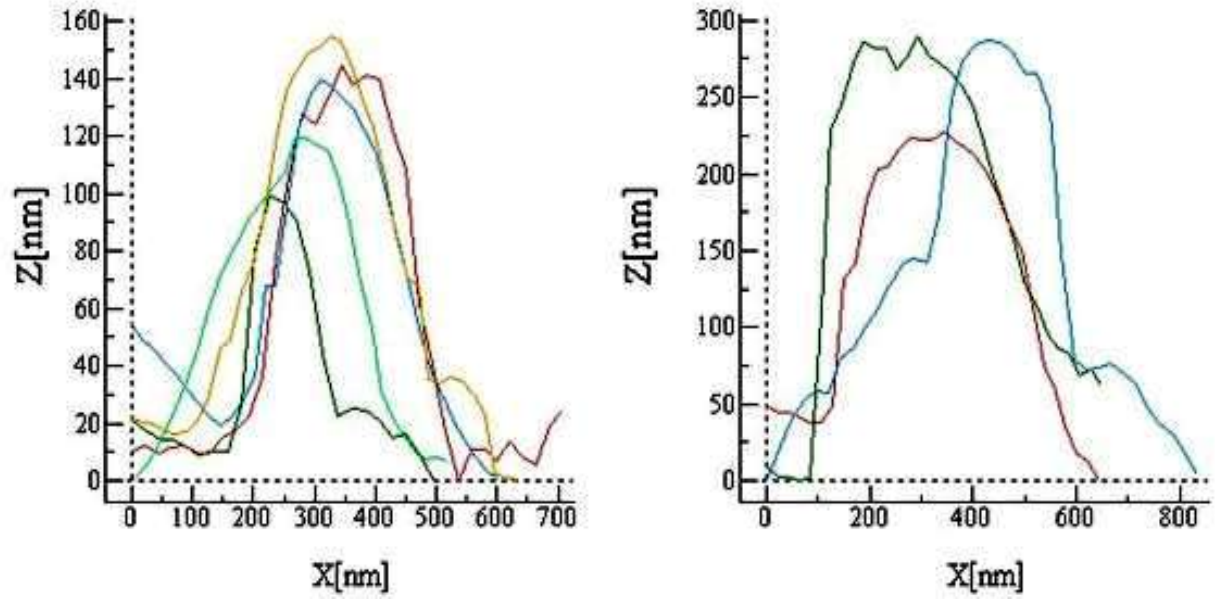

Image 5.17 The two groups of links. Left: 250nm x 150nm.Right: 500nm x 300nm.

It could be interesting to study if there are differences between the two groups by performing mechanical tests over them. But unfortunately we've seen this differences only when processing data acquired with AFM microscope. The experiment needs to be repeated in order to find the critical area and making force curves over different links ("big" ones and "small" ones). Maybe these tests could give us an idea about different mechanical behaviour.

We refer to critical area as that zone of substrate where we are interested in making mechanical tests. We need to specify an area instead of a point, because of piezoelectric drift; it's impossible to make mechanical tests in the desired point without errors. We reinforce that images were made without using 2nd Feedback correction in x and y scans directions.

We saw other interesting situations that are illustrated in the following images.

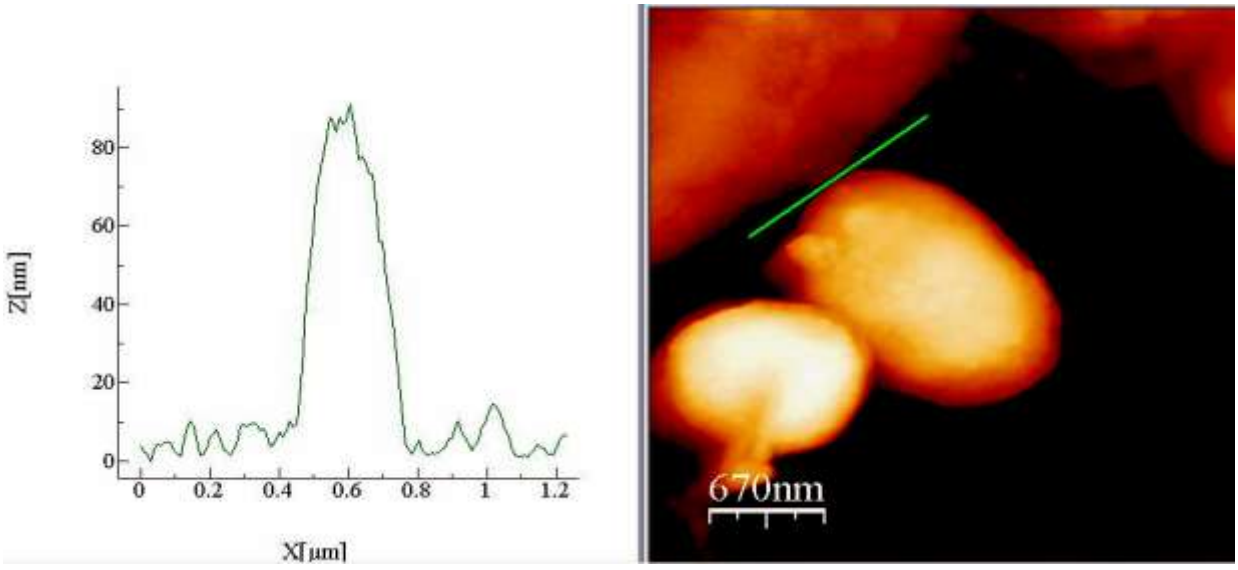

Image 5.18 Connection between two bacteria. (Left) It's profile.

Instead image 5.19 is a representative profile because has the average height and width, between all links saw:

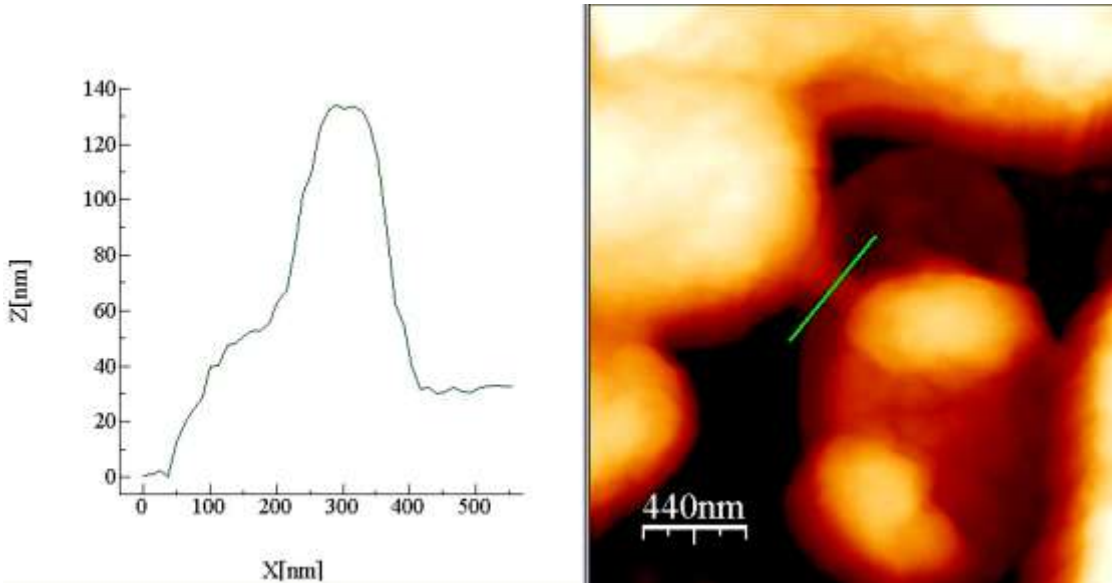

Image 5.19 Representative link. (Left) It's profile.

While in image 5.20 we had the border effects probably due to drift problems or because we didn't control in the right way set point, scan speed and feedback values.

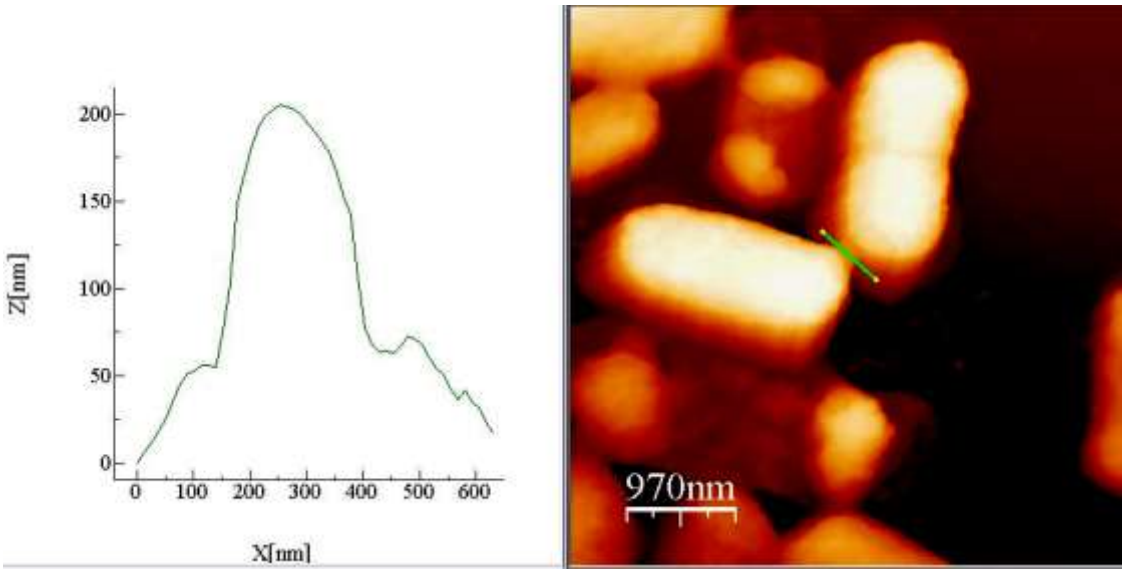

Image 5.20 Interesting link between two E.Coli. (Left) It's profile.

Further zoom in and 3D reconstruction of this link is shown in image 5.21.

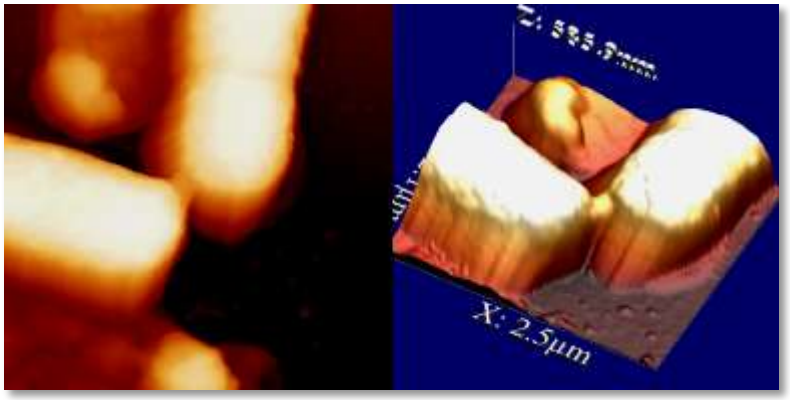

Image 5.21 (Left) further zoom in over ROI. (Right) 3D reconstruction of bridge.

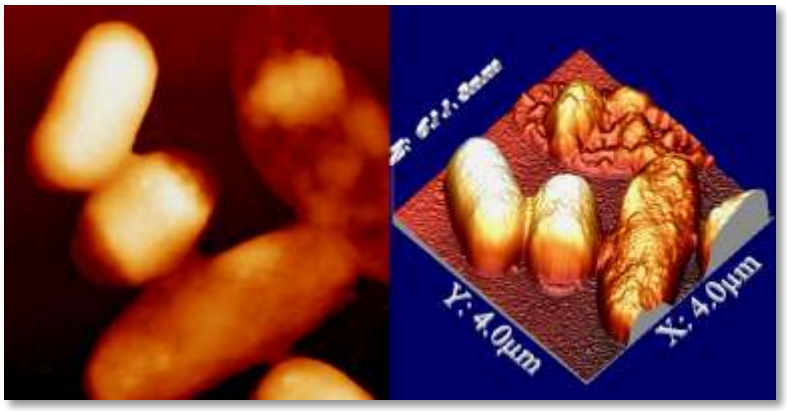

Image 5.22 Other interesting situation in between.

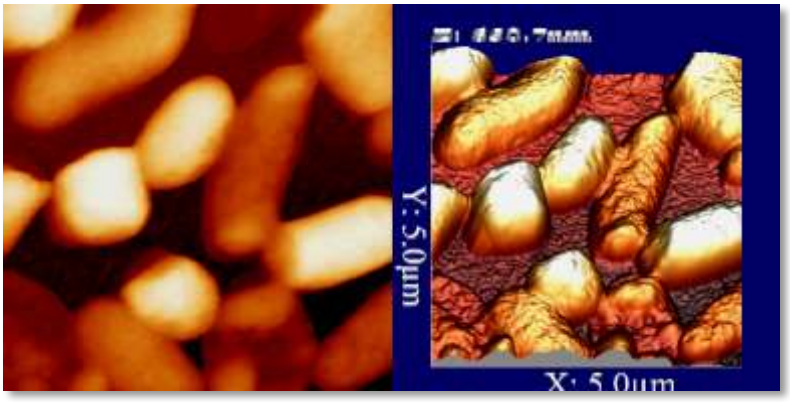

Image 5.23 Zone with connections and superposition of membranes.

Gold: In first approximation, we don't see a high population density or biofilm formation. While scanning the sample we didn't note evidences of links between bacteria:

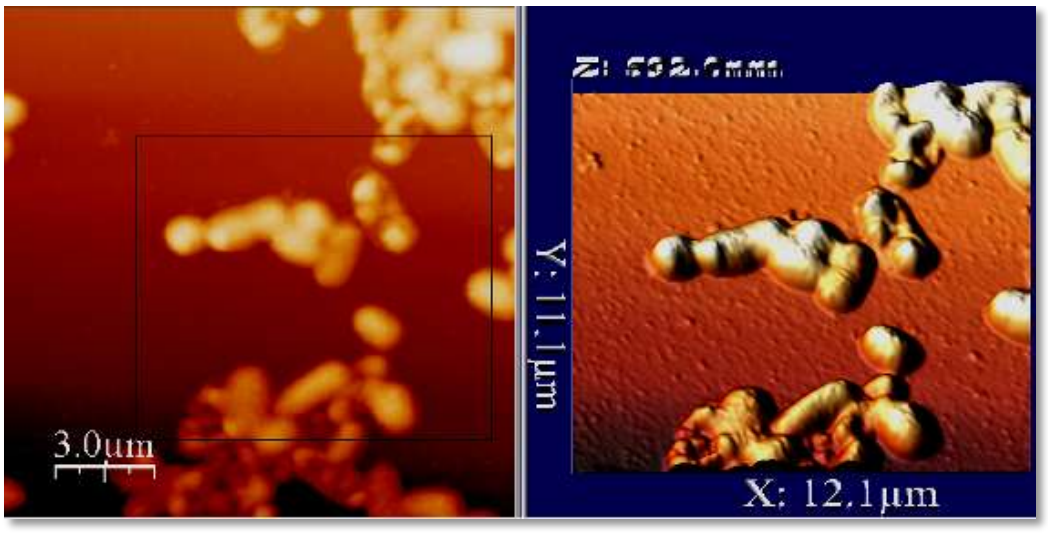

Image 5.24 E.Coli over gold.

It was only after processing images and applying the adequate palette that we could distinguish some bacteria who seems to be "linked" to the neighbour, as are illustrated in image 5.25.

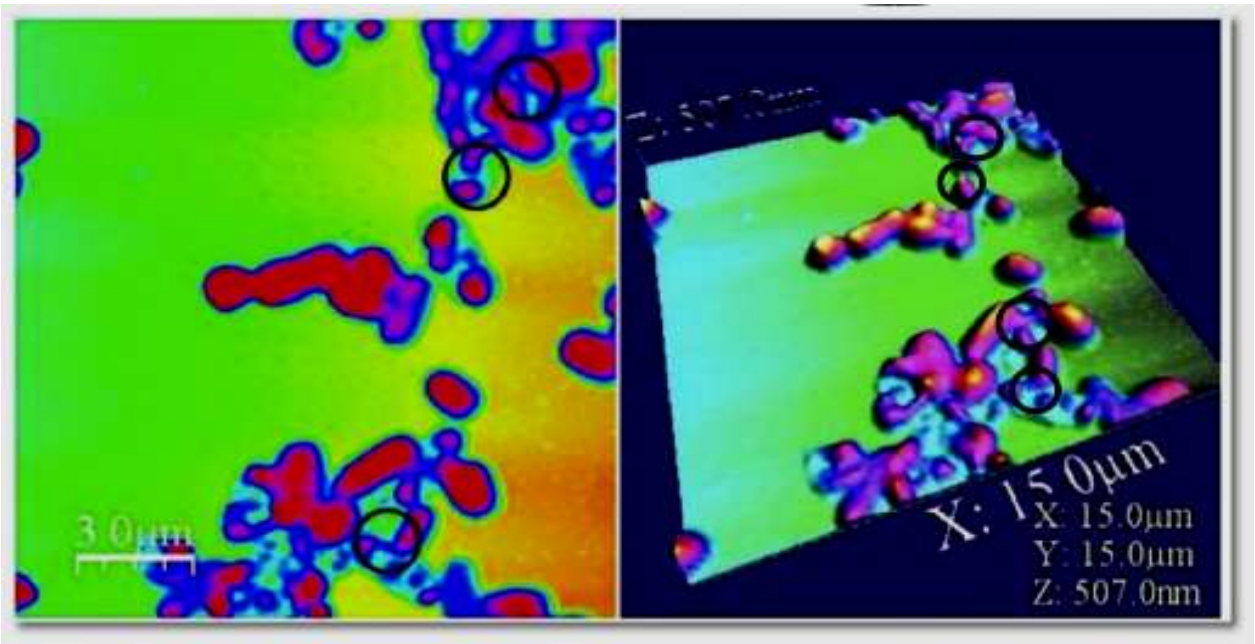

Image 5.25 E.Coli over gold. (Left) Identification of few links. (Right) 3D reconstruction.

While observing, we deduced that these links seem to be of similar dimensions as the ones seed over the other substrates. Image 5.26 shows a group of E.Coli which was applied a palette for evidencing the possible links and their profiles.

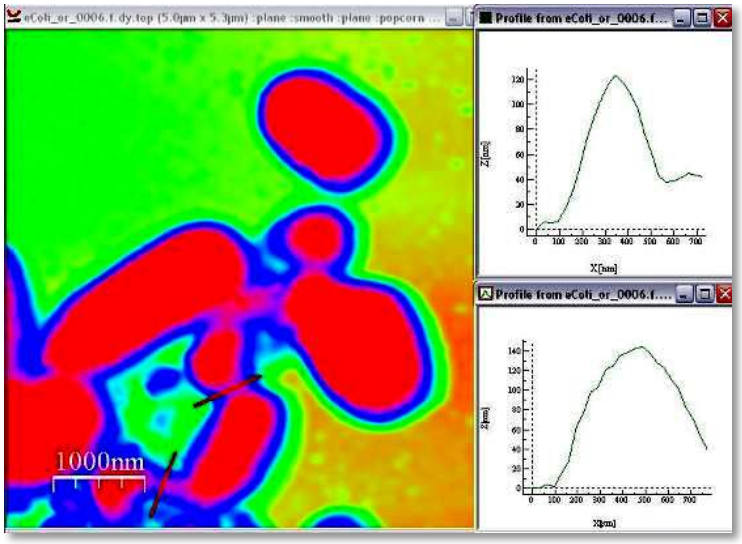

Image 5.26 E.Coli over gold. (Right) Profiling of selected links.

Mica: Here we found similar situation that over gold substrate. There aren't much links or bacterial structures that are different from simply two bacterial membranes attached together because of being closer to each other. In image 5.27 are shown some bacteria that possibly have created biofim.

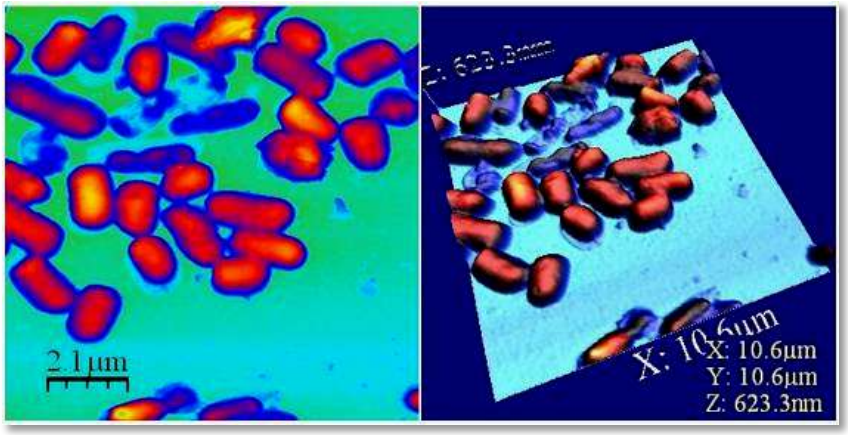

Image 5.27 E.Coli over mica. (Right) 3D reconstruction.

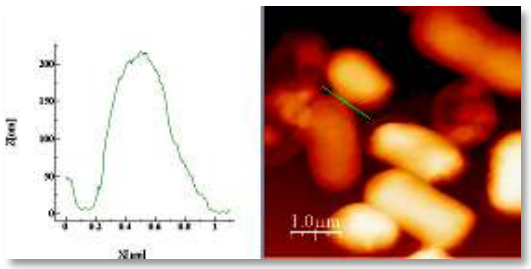

Image 5.28 Link of "big" dimensions.

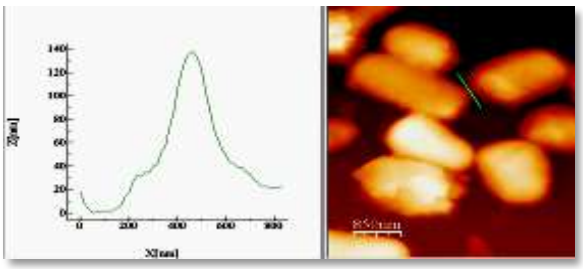

Image 5.29 Link of "small" dimensions.

5.1.2.4 Mechanical characterization with AFM

Due to few problems and mistakes in the procedure followed, the results of mechanical tests over E. Coli's links aren't valid. This because it was difficult to find these links between E. Coli when using a cantilever with enough sensitivity ("softer" cantilever) to perform these tests, we decide not to repeat them and leave this study for the near future.

A "softer" cantilever implies smaller *k* values (Olympus SiN, k=0.76 N/m); this means there are needed smaller force values to bend. Implying smaller forces exerted over substrate. But at the same time introduces more noise and is difficult to distinguish between real obstacles (bacterial membranes) and fictitious obstacles (noise). Typical artefacts when of using softer cantilevers are:

- False engages. At approach time, while getting closer to substrate with motors due to higer deflections of cantilever for small displacements; is easy to get a false engage. The "sensation" of overcoming the percentual cantilever deflection ranges that we consider approach (See for more in detail use of approach tool in chapter 4.1.3).
- Blurried images. Where from the topography backward and forward channels they seem like following each other, but the real situation is: cantilever floating over the surface. This is more evidences when makin FZ curves over the substrate; cantilever "feels" the surface much before we have real contact with surface. This efect is more evidenced when there is presence of ionic double layer (See chapter 4.1.6).

5.1.3 Preliminary conclusions of the first set of experiments

- Is possible that the results over mica could be erroneous because it seems there were few problems at the moment of separation from the culture due to exfoliation. In future studies of E.Coli's behaviour, it should be taken in consideration.
- The tests were made in the following order: mica, silicon and gold. Without previous experience in imaging pseudomonas with AFM, we consider that the ones taken in gold are the best. This because in gold we saw the connections perfectly this doesn't discard the possibility of other substrates.
- In case is needed more information over the material (Young module, etc.), experiments should be repeated in nitrogen ambient or liquid. Air results are important and can serve us in making compared analysis, "fast one", an can be the principle for detecting differences between those materials.
- We choose to follow with a second set of experiments only with pseudomonas over different substrates.

5.2 Second set of Experiments: Nanobiocharacterization of Pseudomonas over different substrates

5.2.1 Experiments

There have been cultured Pseudomonas over the following substrates: mica, silicon and gold.

5.2.1.1 Characterization by non-AFM methods

Referring to Gram's staining method we can see that in all three substrates bacteria have grown covering the whole substrate. Conscious of the results in previous characterizations with the optical microscope (OM), we didn't repeat the experiment because of less relevance due to small dimensions of these bacteria.

5.2.1.2 Topographical characterization using AFM

The equipment used was a Cervantes Atomic Force Microscope of Nanotec Electronics, by using the dynamic mode on air. The AFM cantilever used is made of silicon with a spring constant of 42N/m.

Gold: As evidenced by Gram's method, the whole substrate is covered with bacteria, but we cannot assure they form biofilm, so images reveal some kind of monolayer but with some bacteria over it. Note that the palette used shows in blue: the substrate, in red: the monolayer and in yellow: the zones of the monolayer with higher *z* values. Z is the piezo displacement in vertical direction. We evidence here that the yellow zone shows aggregations of bacteria which looks like overlapping. Image 5.30 shows all the particularities, and the convention applied for distinguishing the different zones.

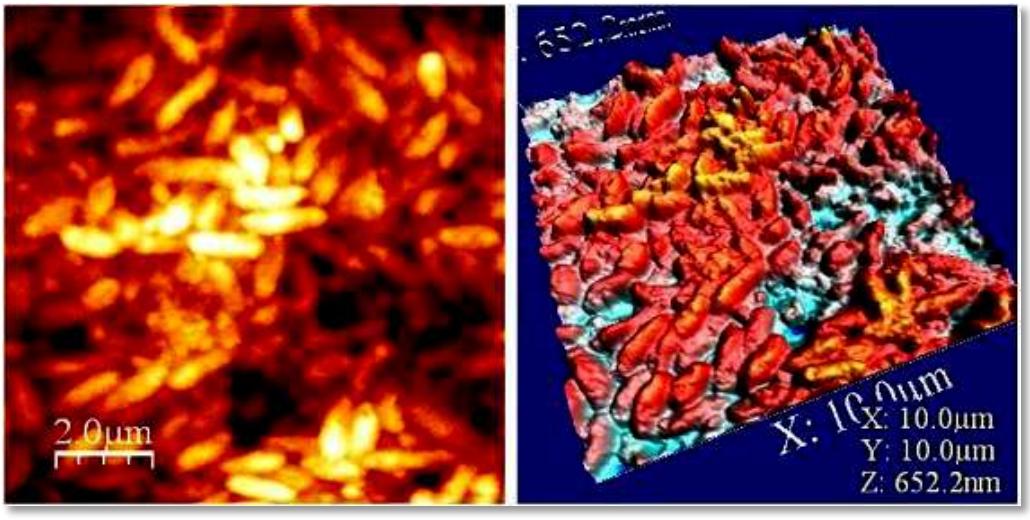

Image 5.30 E.Coli over gold. (Right) 3D reconstruction.

It's difficult to find links between bacteria because whole substrate is covered with, but there are a couple of bacteria that seems to be linked (but we can't asses it in the same way as we did with previous cultures). Image 5.31 shows their profiles (right), while the red lines shows direction where was done profiling.

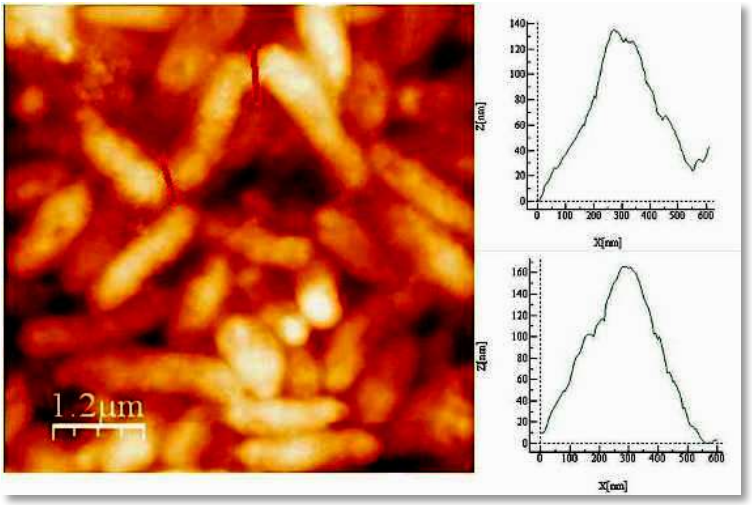

Image 5.31 E.Coli over gold. (Left) Possible links in between. (Right) their profiles.

Silicon: There is no evidence of links or biofilm formation over silicon substrate. While from the image we can say that substrate is covered with micro dust and is difficult to image it due to tip contamination. From the image artefacts we can say that image contamination could be because of substrate deterioration. This implies more small particles, membranes etc. spread in sample surface (see Chapter 4.1.6 where there are presented some AFM imaging artefact).

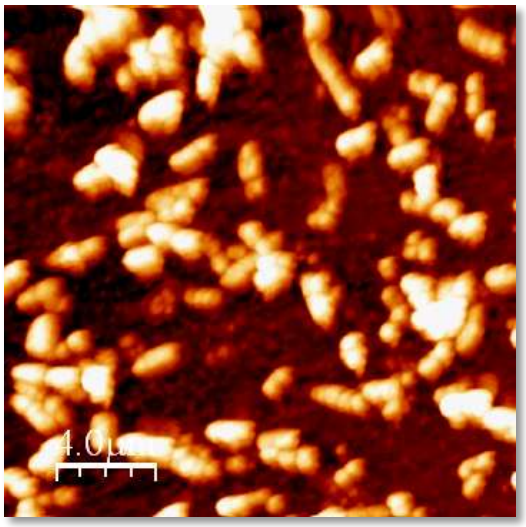

Image 5.32 E.Coli over silicon.

Mica: Bacteria seem to occupy whole mica substrate and they look like forming monolayer. But due to high population density of substrate, we're not able to find bridges between them. Is interesting to note that the relief is rougher and this is an index of les monolayer creation. More in specific, a monolayer looks like more planar and this one isn't so planar.

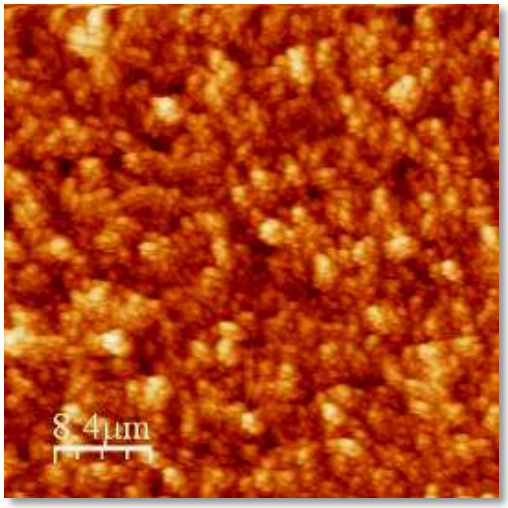

Image 5.33 E. Coli over mica.

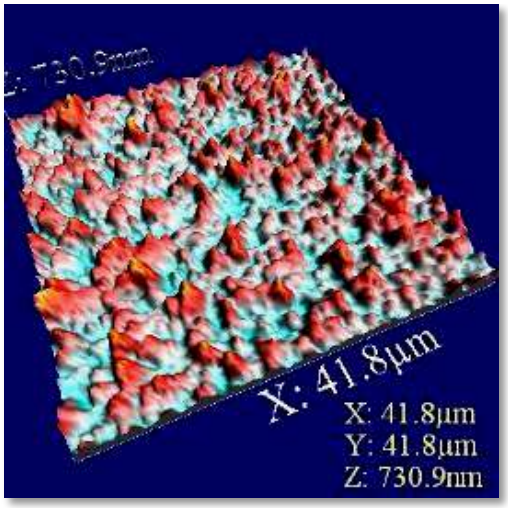

Image 5.34 Its 3D reconstruction.

5.2.2 Preliminary conclusions of second set of experiments

- Bacteria have occupied the whole substrate and it increases the difficulty of experiments.
- Samples seem to be quite different from the ones of the first set of experiments.
- This second set of experiments may confirm gold as the proper one for further experiments.

5.3 Third set of Experiments: Nanobiocharacterization of Pseudomonas over gold

In this third set of experiments we used the following samples:

- Pseudomonas over gold substrate forming biofilm. There have been prepared three sets of Petri dishes with cultivation time corresponding to: 20,24 and 28 hours.
- Inoculated bacteria of same cultures (in 20, 24 and 28h) dropped and dried over gold, without further treatments.

We didn't pass through Gram's method and optical characterization phase as we did in previous sections. The main reasons were: firstly, for getting fresh cultivations directly under observation. And secondly, because membrane properties and biofilm formation depends on time, we wanted to

save precious time. So we passed directly under topographical characterization, in this way we ensure that the results obtained are valid.

5.3.1 Preliminary results: Biofilm with cultivation time 20 hours

There is no sign of biofilm creation under this cultivation. As follows we illustrate the images taken in this sample.

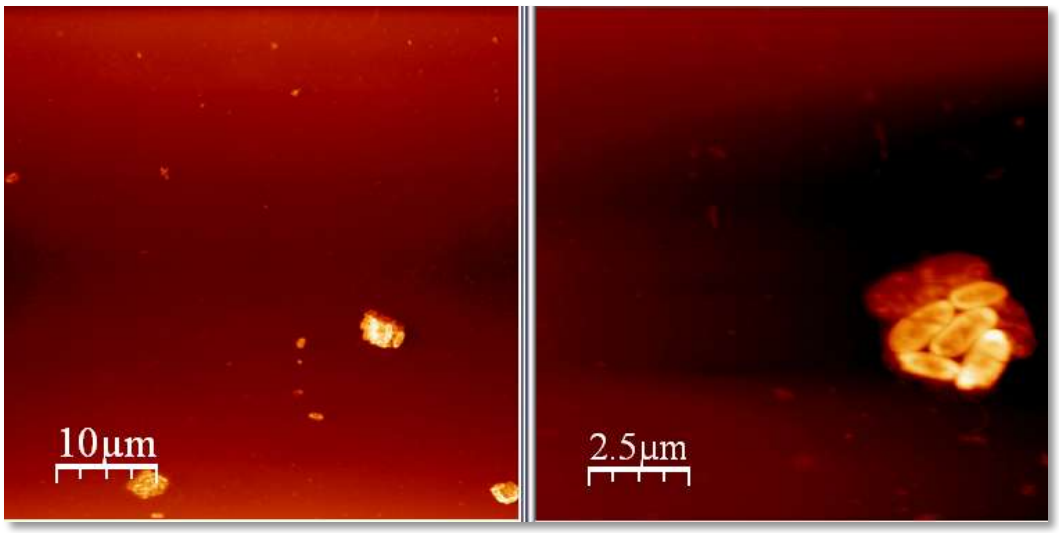

Image 5.35 Pseudomonas over gold. (Left) Biofilm creation at 20h hours from seeding. (Right) Zoom in over a possible bacterial aggregation.

As a matter of fact, almost 95 % of sample surface was void. In this way we had to search a little bit with the optical microscope for a region where it seemed like there were present aggregations of bacteria. Is remarkable the presence of flagella (Image 5.36), indicating possible biofilm formation.

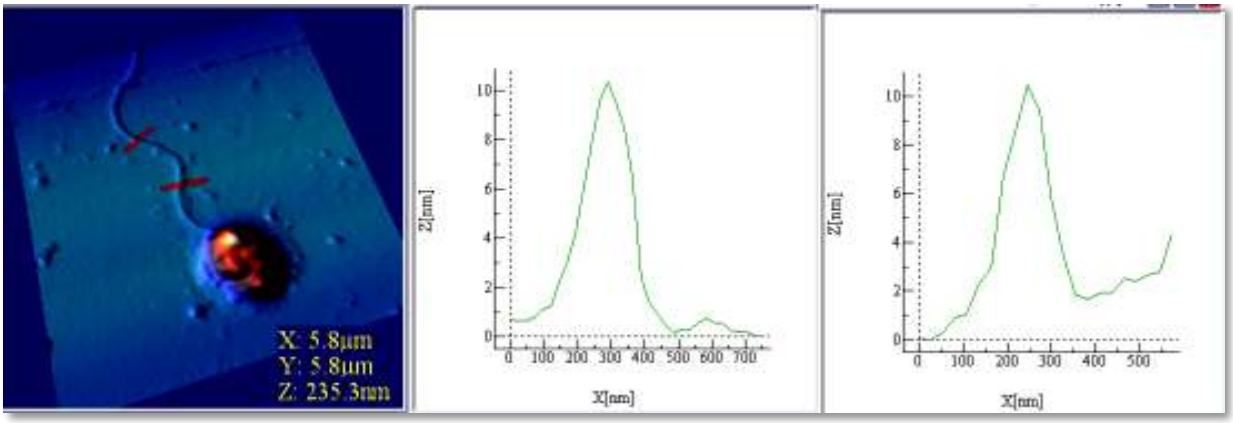

Image 5.36 Pseudomonas with flagella. (Right) Dimension of flagella.

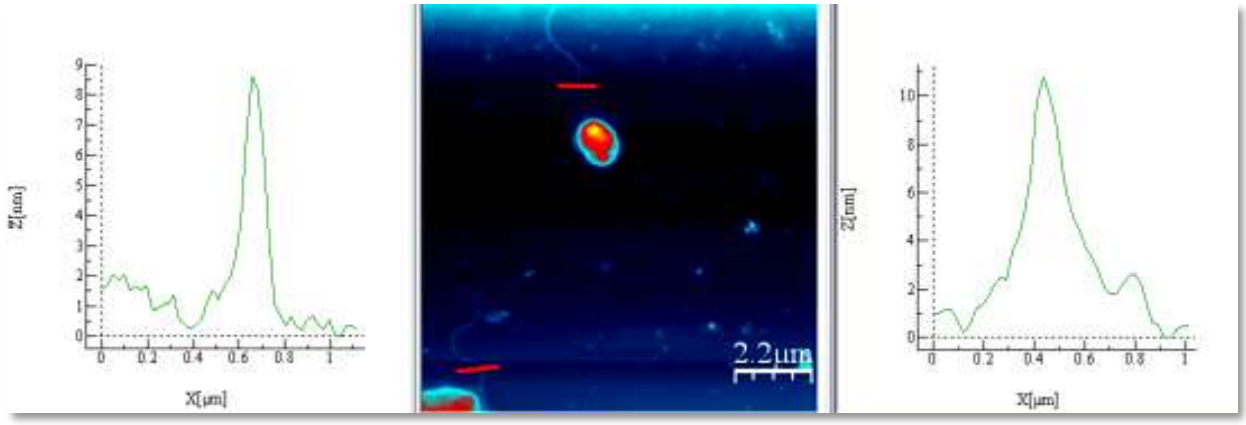

Image 5.37 Pseudomonas au. with flagella. (Sides) Profiles of flagella.

5.3.2 Preliminary results: Biofilm with cultivation time 24 hours

After 24 hours the situation is still the same. As previously done, we had to search with optical microscope and the only sign of possible biofilm creation was flagella presence in the substrate.

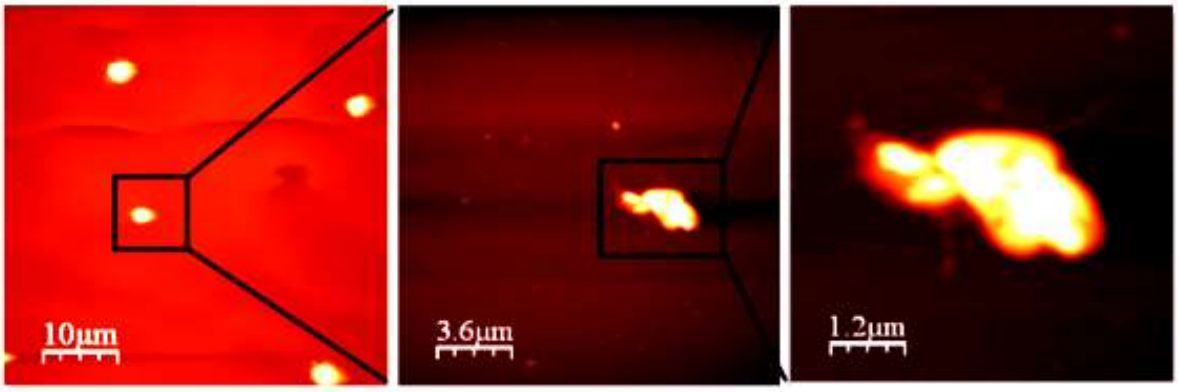

Image 5.38 Pseudomonas au. biofilm study after 24h of seed. Sequence of further zooms.

5.3.3 Preliminary results: Biofilm with cultivation time 28 hours

Here sample substrate is plenty of bacteria, so even moving to other places (which look less crowded from the optical microscope), the situation is similar to the one shown in image 5.39.

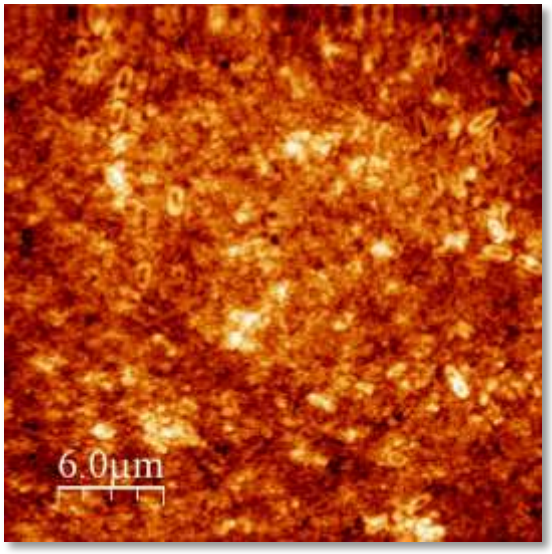

Image 5.39 Pseudomonas in biofilm study after 28h of seed.

Whole sample is full of bacteria. We scanned different zones and they confirm that it seems to be two different types of bacteria in the same sample distinguished by the relative difference in size. In image 5.40 there are zooms over ROI (Region of Interest), which are getting closer to the "two" different types of bacteria.

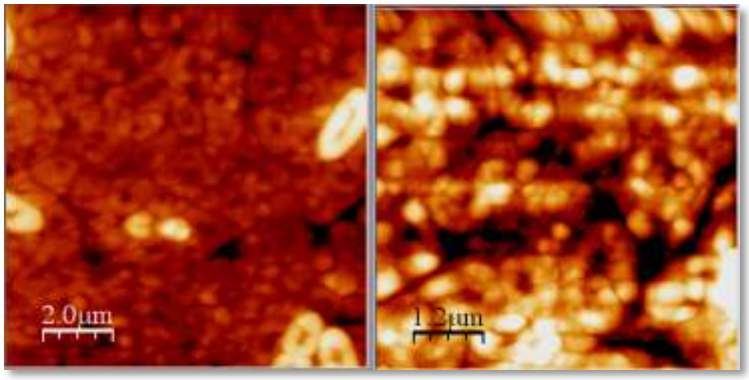

Image 5.40 Zoom in. Pseudomonas au. biofilm study after 28h. (Left) Two "different" bacteria sizes.

5.3.4 Preliminary results: Inoculated with cultivation time 28 hours.

We didn't image inoculated samples with cultivation time 20 and 24 hours because there is no biofilm (with these cultivation times) to compare with.

We suspect that it was difficult to find the right place where were concentrated inoculated bacteria due to the absence of dye in the sample. We stress the fact that samples at the third set of experiments, wasn't treated with dye.

5.4 First experiments in liquid environment

The purpose of these experiments is to acquire experience working in liquid environment, in order to have in the near future the ability to image and nanocharacterize the biofilms in their native ambient. First experiments are performed to tune the microscope (and ourselves) in imaging in liquids, and second ones are the first images of bacteria in liquid media we've obtained in our laboratory.

The high resolution and the possibility to study biological systems in their native environment have created an enormous expectation on AFM as an ideal tool for molecular biology [47]. In fact, AFM has been used not only to image a variety of biological samples [48], but also to perform experiments on single molecules [49].

An arsenal of working modes, which explore the different interaction regimes, is available for AFM imaging. In UHV (Ultra High Vacuum) and in ambient air, the dynamic mode (DM-AFM), sometimes also termed the ''tapping mode'', is the method of choice for imaging surfaces. In this AFM imaging mode, the tip is oscillated near its resonance frequency and either the reduction of the oscillation amplitude or the shift in the resonance frequency is kept constant as an image is acquired.

In the contact mode AFM (CM-AFM), the deflection of the cantilever, resulting from the mechanical contact between tip and sample, is kept constant. This imaging mode is not as flexible as the DM-AFM due to the irreversible damage produced in soft samples by the friction force between tip and sample. Applying low forces could minimize this, but the continuous drift in the zero force level makes it extremely difficult to keep constant the total force during the scan.

The jumping mode AFM (JM-AFM) combines features of CM-AFM and DM-AFM.

In UHV, the strong adhesion force derived from the Van der Waals forces and the capillary forces present in ambient air (even stronger than the Van der Waals forces) make it difficult to obtain reproducible images of biomolecules using JM-AFM. In liquids, the situation is not so clear.

- Van der Waals forces are very weak.
- The resonance frequency of the cantilever drops as a consequence of the large effective mass of a cantilever.
- The high damping strongly reduces the Q factor of the system that results in a reduction of the sensitivity of the technique.

Therefore, noncontact operation in liquids is very difficult, or in most cases impossible. DM-AFM becomes an intermittent contact mode similar to JM-AFM [50].

In liquids, the most appropriate imaging mode depends on the sample characteristics and preparation methods [51]. Contact or dynamic modes are the best choices for imaging molecular assemblies arranged as crystals such as the purple membrane. In this case, the advantage of image acquisition speed predominates over the disadvantage of high lateral or normal force. For imaging individual macromolecules, which are weakly bonded to the substrate, lateral and normal forces are the relevant factors, and hence the jumping mode, an imaging mode that minimizes lateral and normal forces, is preferable to other imaging modes.

5.4.1 Setting up the equipment

5.4.1.1 Imaging modes

There are three different imaging modes in which AFM can work in liquid environment: dynamic (AC mode, oscillating the cantilever), contact (DC mode, constant force over the sample) and jumping (JM mode, approaching and withdrawing the tip from the sample in different points and calculating the contact point). We use a grid (PMMA) of known geometry to set up the system, and after obtaining optimal parameters for the imaging settings we obtain images in the three modes:

Image 5.41 Grid scanned from left to right in: Contact, Dynamic and Jumping.

5.4.1.2 Force curves

The experiments in liquid require controlling the pH. Due to ionic double layer forces the tip "feels" surface at long distances. While hydrophobic forces attract water molecules to the tip increasing it's effective radius (and consequently the convolution surface) increases, decreasing resolution. Image 5.41 represents generic force curves when working in distilled water. Let's note that we start feeling substrate since $1\mu m$ far from surface. This is visible in the graph because the forces are different from zero. We would like to add that normal ranges of contact distance in AC mode are definitely smaller than this one.

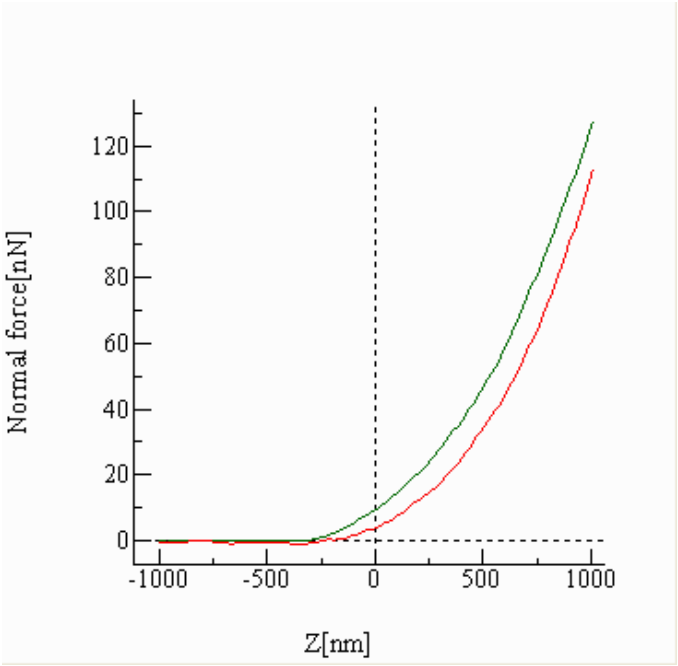

Image 5.42 Force Vs. Displacement curve in distilled water.

When changing ionic concentration using a buffer (PBS, pH 7.4) we found out that our imaging resolution increased so we obtained force curves similar to the ones obtained in air or in dry (nitrogen) ambient. Image 5.42 shows the generic FZ curves obtained after modifying the pH of the liquid environment. Similar results [50] are obtained while working with purple membranes.

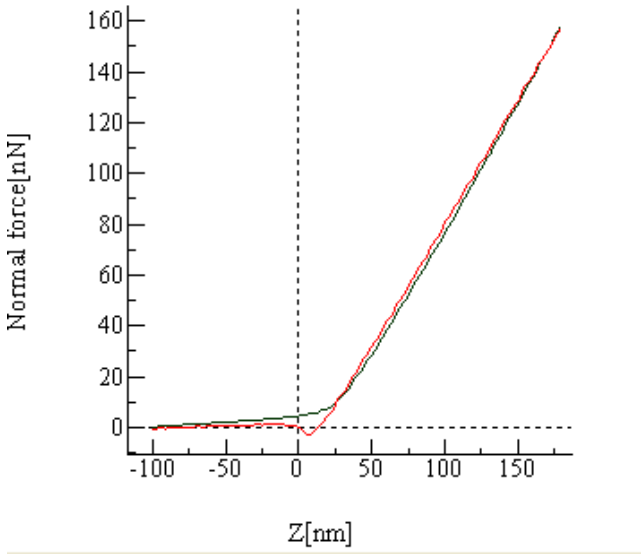

Image 5.43 Force Vs Displacement curves with PBS (pH 7.4)

5.4.2 Experiments with biological samples

As results from previous experiments suggests, we image pseudomonas over gold substrate using contact and dynamic mode. Olympus cantilevers with K=0.76 N/m seems to be the proper ones, which are some kind of standard while working in liquids, as reported in several works in the literature [50].

We start in contact mode (DC) but we can observe in the following image that tip grasps surface and we have very low resolution working in this mode. Even in this image is possible to identify a link (see black circle in Image 5.43), and few others that we aren't sure if they really are links of artifacts during imaging.

Let's focus on the borders of the image. We note these side effects due to scanning and as Moreno - Herrero [51] note, the deteriorating effect of this method. While at the same time they depreciate the effect of lateral forces while using purple membranes with thickness of round 5 nm. Instead in samples of bigger dimensions isn't depreciable sample deterioration, from this the horizontal stripes that follow the scan direction.

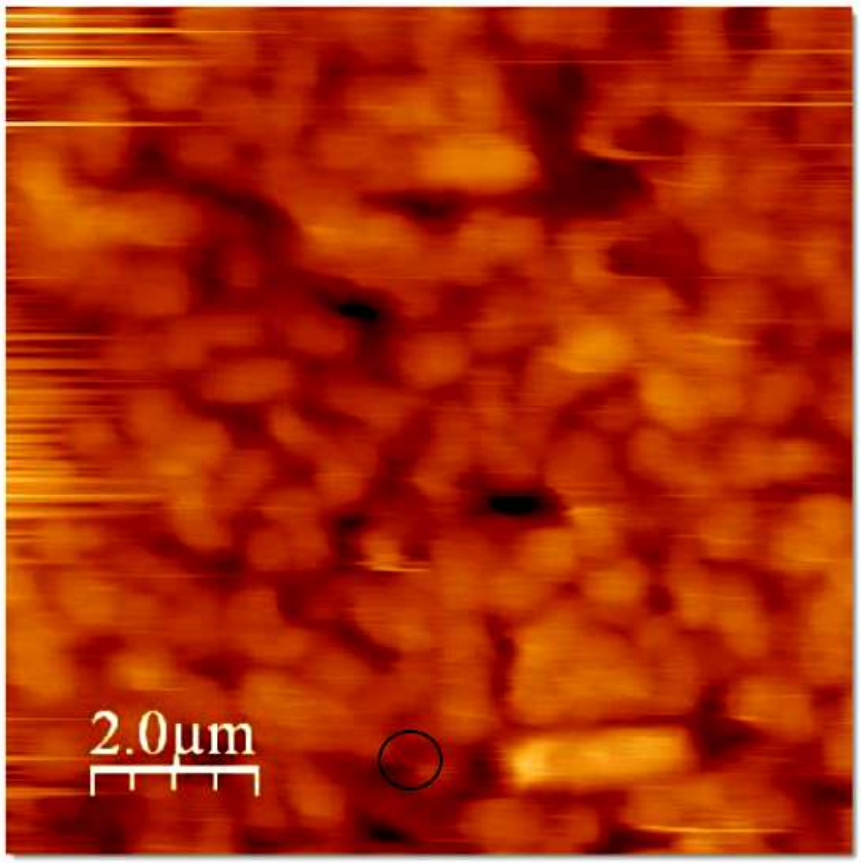

Image 5.44 Pseudomonas over gold, in liquid environment DC contact mode imaging. (PBS, pH 7.4)

In a second intent, we tried to image the sample in AC mode (Tapping) and achieved getting higher resolution in comparison with DC mode. Bellow we show the results obtained (see black circles in Image 5.45). While scanning sample we had to apply slower scan speed (time for scanning one single line). Then we change to dynamic mode and we can see more clearly the sample, and even distinguish some (Image 5.44) links between bacteria:

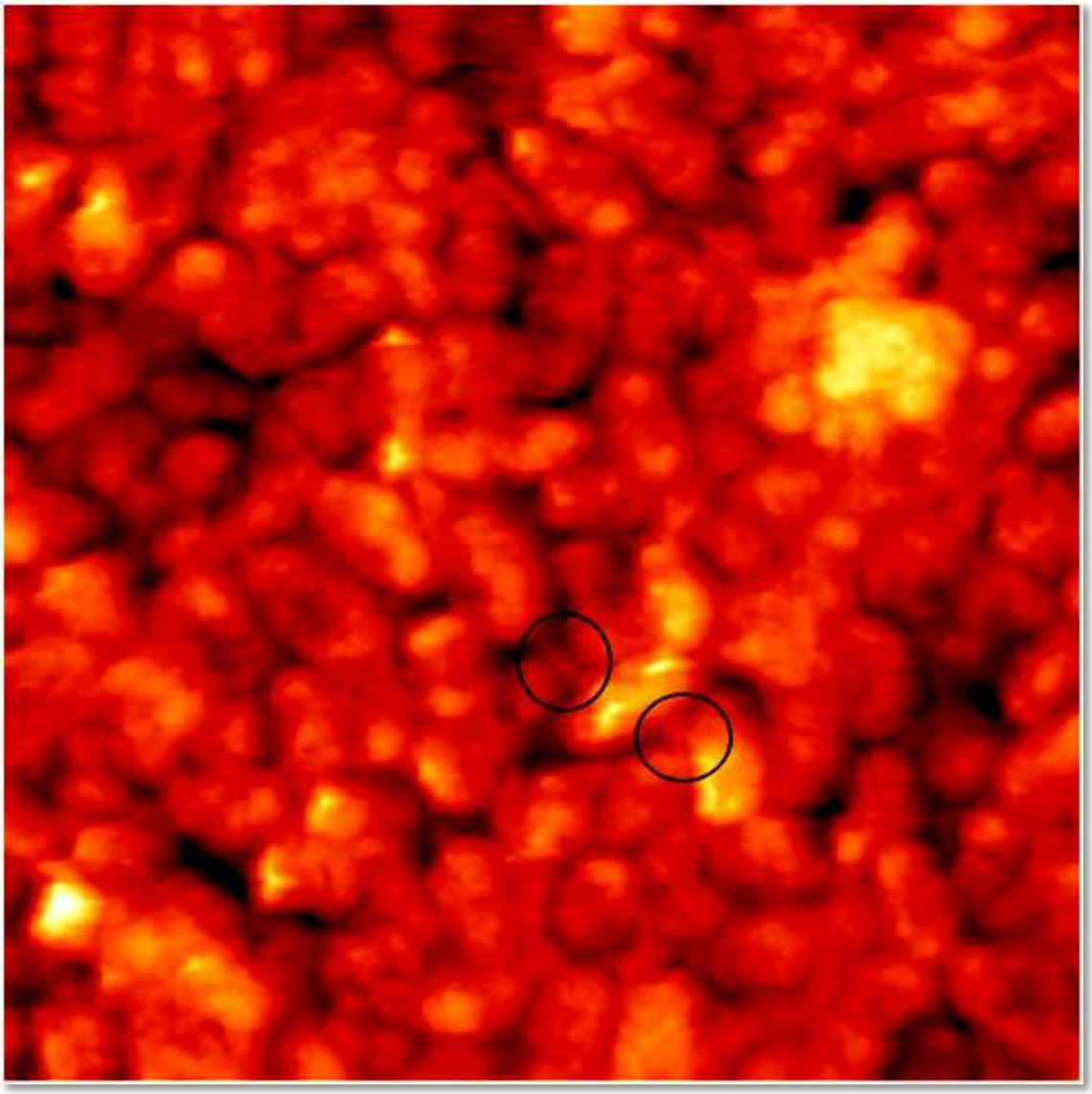

Image 5.45 Pseudomonas au. over gold. AC mode, in circles are evidenced the links found in the sample.

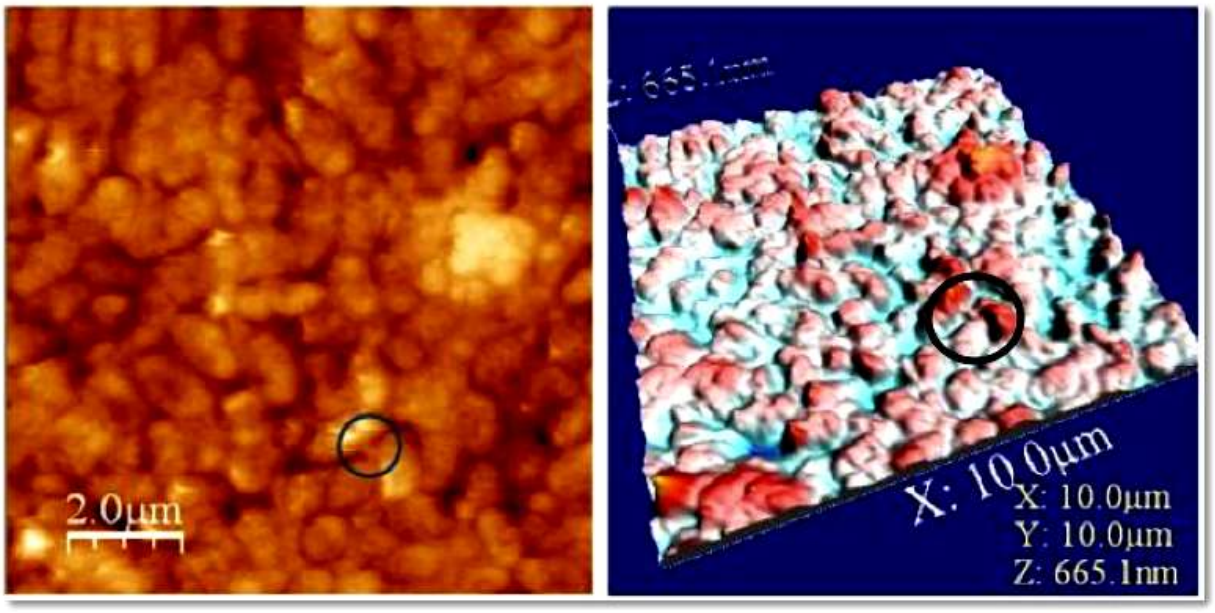

Image 5.46 Pseudomonas over gold in tapping mode. Evidence of links (circle left). 3D reconstruction (right).

While zooming and profiling, effectively it looks similar to the ones found in air:

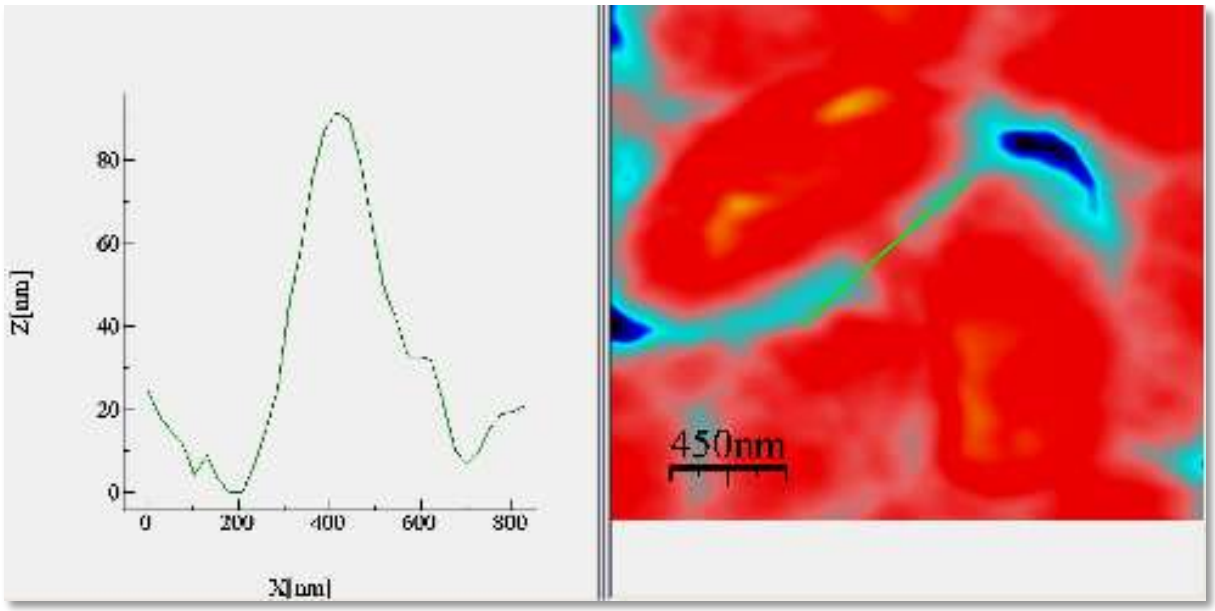

Image 5.47 Zone of interest. (Left) Link profile. (Right) Link.

5.4.3 Preliminary conclusions of first set of experiments in liquid

- Biofilm imaging in liquid with the AFM is possible, so we're working in the proper direction towards "living cells studies".
- Experimental results give us a starting point to continue:
    - Using a pH 7.4 with normal PBS
    - Softer cantilevers k=0.7 N/m or less
    - Over gold substrate
    - Better with pseudomonas
- Due to the time spent for imaging only one substrate (several days for one sample), we focused more over gold especially with one sample/cultivation. The sample choice is of high importance in the near future.
- More tests are required, for a better performance in imaging procedure and in sample "construction".

During previous chapters we have seen AFM as a microscope, a really good instrument for making good imaging, but the reality is that that's not enough. While thinking over the microscope construction, is easy to think that the tip can be used booth for imaging and even as a nanomanipulating tool.

In this way the same tip does imaging and manipulation sections. And one of these processes is the automation of tip movement.

By tip movement automations we mean the joint of different small built-in movements for achieving a bigger and more complex tip movement. These built-ins are defined by microscope constructors and we can se them as the universe of discussion, as the whole "AFM dictionary", and by these "words" that we can build more complex and meaningful "sentences".

This metaphor explains and describes a little bit the limitations in movement and automation complexity imposed by these built-ins, because there is always dependence by the given dictionary. And in the following paragraphs will be showed how we achieved solving these limitations.

6.1 Short Introduction in Lithography

Lithography is a part of the WSxM program. In this frame is possible to draw on a sample, define the tip motion and write on a sample (More exhaustive in Appendix B)

WSxM Lithography section allows moving the tip over the sample performing different actions. We can think in the tip as a pen, and the sample as a paper. If we can somehow define what does "draw" mean, we can "draw" with our tip over the sample, as it was a pen.

And vice versa, if the pen point is far away from the paper surface, it will draw nothing. In a symmetric way it can be done with WSxM Lithography if is defined previously what "do not draw" means in our tip-sample system.

In this way there is the possibility to decide what "draw" stands for and what "do not draw" stands for.But we still need another concept; move. So we can make a workflow describing how it works lithography.

Here "draw" can be at the same time a single one instruction or a set of instructions that compose the complex concept of draw.To explain it better we can illustrate some examples of what a draw instruction can be.

- *Oxidation process*

  In our equipment is possible to apply a voltage between tip and sample without contact between them. These voltage differences induce surface oxidation, a process that deposit a layer of samples oxide due to electron exchanges occurring bellow the tip.

  Nanotec Electrónica S.L developers have made oxidation experiments.

  In the Image 6.1 was induced a bias voltage between tip and silicon surface following a pattern. These images are 3D reconstructions of the topographical images. The relief is obtained by SiO_2 deposition over Si substrate. Here the tip moves with voltage applied over the surface following patterns already established in the lithography section.

  So, the "Draw process" here is: Set Bias voltages between tip and sample. In this way the previous flow diagram can be specified like this:

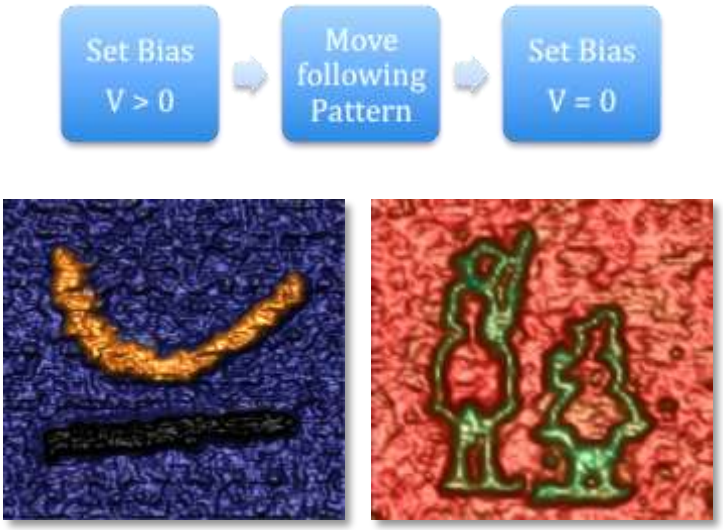

Image 6.1 (Left) Logo Nanotec 1um x 1um. (Right) Don Quijote and Sancho 1.3um x 1.3um.

- *Surface modification process.*

  Surface modifications can be obtained as a collection of more than one "Draw Instructions" like: Zmove, Line, DoRamp…etc. These kind of manipulations will be the aim of my work in the following chapter, and will be explained more carefully.

If we take a closer look to WSxM diagram, it could be represented with the diagram of Image 6.2.

There are three main sub-trees:

- Data acquisition.
- Lithography.
- Data processing.

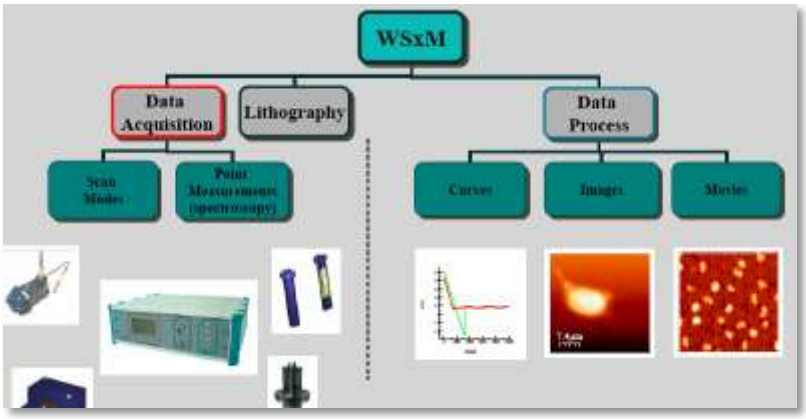

Image 6.2 Diagram of WSxM.

Lithography and Data acquisition sessions are closely related when we are making real lithography. When there is need for making nanomanipulations over the sample acquired in the Data acquisition, we need to switch between the two modules. This switching is facilitated from the software by activating the main lithography frame in the data acquisition main frame.

Performing a real lithography session can be illustrated in the following flow diagram. First, there is need for sample scanning to individualize the ROI (Region of Interest). Second, for making real modifications we need to pass at the lithography session to make the modifications to the sample. Third, there is need for a further scan to se if it was effective the nanomanipulation.

So in the diagram of above, it can happen the following:

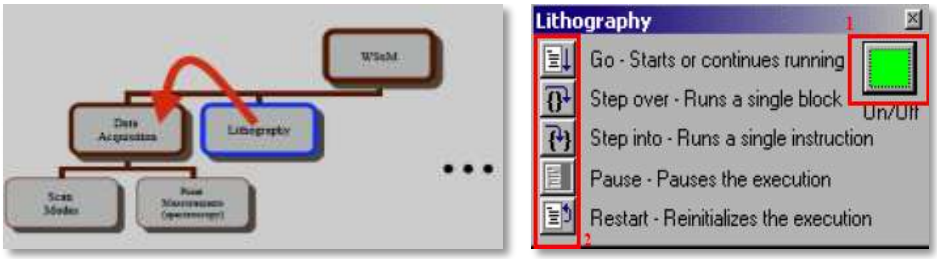

Image 6.3 (Left) Flow diagram passing from Lithography to DA and vice-versa. (Right) Main Lithography frame.

There are two constrains for activation: a) if there is a lithography pattern in the main lithography frame, b) the scan size is different from 0.

6.2 Lithography language

Lithography is a language defined from the constructors of WSxM. As a consequence, there is lack of a lot of constructs found in normal high-level languages like C/C++, Java, FORTRAN etc.

The constructors have defined on their own way the basics constructs, like *variable declaration*, flow control instructions *(do, for, while if).*

- Variable declaration.
  - Format:
    1. ***Float*** *identifier*
    2. ***Integer*** *identifier*
    3. ***Boolean*** *identifier*
    4. ***Numeric*** *identifier*
  - This will declare a variable, of the specified type, while variables must be declared before using them. Is possible to declare variables only in the main block and before any otherinstruction.
  - Integer variables can hold integers in the range –2147483648 to 2147483647
  - Boolean variables can hold the logical values *true* and *false*.
  - Optionally, it can be declared a constant variable, by writing the ***const*** keyword before its name. In such case, it must be provided its constant value in an assignment expression.
- Assignment instruction.

  The generic assignment instruction is done as in all other programming languages, following the same pattern:

  ```
  variable-ident = math-expression ;
  ```

  We should stress the fact that is possible to declare variables only at the beginning of the main block.

  Later they should be followed by an assignment instruction. For example:

  ```
  begin
  // Main block
  Float x
  Boolean flag
  // Assignment
  flag = true;
  ```

```
x = 0;      // Initial value of x.
y = 0;
(other inner blocks)
end
```

- Math functions.

  Here bellow is shown a table with *all* math functions admitted:

Function	Description
ABS	The absolute value of the given numeric expression.
ACOS	The angle, in radians, whose cosine is the given numeric expression.
ASIN	The angle, in radians, whose sine is the given numeric expression.
ATAN	The angle, in radians, whose tangent is the given numeric expression.
CEIL	The smallest integer that is greater or equal to the given.
COS	The cosine of the given numeric expression (in radians).
COSH	The hyperbolic cosine of the given numeric expression (in radians).
EXP	The exponential value of the given numeric expression.
FLOOR	The largest integer that is less or equal than the given numeric expression.
H (Heaviside)	If expression is positive or zero, it returns 1.0 else, it returns 0.0.
LN	The natural logarithm of the given numeric expression.
LOG	The base-10 logarithm of the given numeric expression.
RAND	A pseudo-random number between zero and one (both inclusive).
ROUND	The closest integer to the given numeric expression .
SIN	The sine of the given numeric expression (in radians).
SINH	The hyperbolic sine of the given numeric expression (in radians).
SQRT	The square root of the given numeric expression.
TAN	The tangent of the given numeric expression (in radians).
TANH	The hyperbolic tangent of the given numeric expression (in radians).

Table 6.1 Function specifications.

- Flow control instructions.

  Are permitted the following flow instructions like:

  - Conditional *if*
    - Format:

if *(condition)* ***then*** *instr-1* ***else*** *instr-2*

The *else* part is optional.

Instr-1 will be executed if condition is true, else *instr-2* will do.

Both, *instr-1* and *instr-2* can be instruction blocks.

- *for* and *while*
  - ***for*** *(var = init* ***to*** *end* ***step*** *s)* ***do*** *inst*

    Var: a valid variable identifier. It cannot be assigned in the instruction *inst* (it can be read, of course)

    Init and *end* must be either numeric constants or numeric constant variables, and *end* must be greater or equal than *init*. (if not, step *s* must be negative).

    Inst: an instruction or block to be executed.
  - ***While*** *(condition)* ***do*** *inst*

    Inst: an instruction or block to be executed.
- Operators.

  All the basic operators can be used for simple mathematical operations. The table bellow classifies them in three categories.

Arithmetic	Relational	Logical
Exponentiation (^)	Less than (<)	Or
Negation (-)	Less than or equal to (<=)	And
Product (*)	Greater than (>)	Xor
Division (/)	Greater than or equal to (>=)	Not
Modulus (%)	Equality (==)	
Addition subtraction (+, -)	Inequality (!=)	

Table 6.2 Operators used in lithography section.

- Drawing instruction.

The constructors of lithography session have defined a drawing instruction as bellow: ”A *drawing instruction* is an instruction that just moves the tip in the XY direction.”

So the drawing instructions available are:

1. Point, plots a point in the desired X, Y coordinates.

   ```
   Point (point = (X nm, Y nm))
   ```

   Where Xnm, Y nm are the absolute coordinates of the point in nanometers.

2. Line, draws a single line.

   ```
   Line (begin = (NanometersX1, NanometersY1), end =
   (NanometersX2, NanometersY2),InputChannels = ("IChn1",
   "IChn2",…, "IChnn" ), NumPoints = NumPoints, Smooth = bool)
   ```

   NanometersXi and NanometersYi are absolute coordinates of a point.

   IChn1,…IChnn: list with input channel names.

   NumPoints: number of points to acquire.

   Smooth: whether the acquired curve must be smoothed (optional).

3. Text, draws a single line of text defined in the pattern.

   ```
   Text (text = "Text", position = (XNm, YNm), size = Size,
   font = Font, stretch = Stretch)
   ```

   "Text": text to put in the view.

   Size: height of the text in nanometers.

   Font: name of the font used when drawing the text. If omitted, default font.

- Non-drawing instructions.

Instead the non-drawing instructions are more and differ in their use and functionality, like piezo movements, DA parameters change etc. Are defined from the constructor simply as: "A *non drawing instruction* is an instruction that perform an action different from moving the tip in the XY direction."

- `SetValue`
- `SetFeedback`
- `SetMovementSpeed`
- `SetPlaneScan`
- `Sleep`
- `ZMove`
- `DoRamp`
- `GetValue`
- `ReadDigitalBit`
- `ReadDigitalByte`
- `WriteDigitalBit`
- `WriteDigitalByte`
- `SetDynamic`
- `SetDrawingConfig`

We aren't going to describe all of them here but we would like to describe the most used.

- `SetFeedback(Index=feedback_index,active=bool,P=Pvalue,I=Ival ue,SetPoint=setpointvalue,InputChannel="IChn")`

  In this inststruction all arguments are optional.

  active (true or false): turns feedback on/off.

  Pvalue, Ivalue: feedback proportional and integral parameters.

setpointvalue: set point value in the feedback loop. Same units as in acquisition frame.

InputChannel: feedback channel name.

Index is a number specifying the feedback type.

Pvalue,Ivalue: when using feedback_index_xy.

Pvalue: represents the Power feedback parameter. In such a case, the Ivalue is ignored. When using other feedback type, these values are mutually inclusive: omit both of them or set the two values.

SetPoint: this value is ignored when using feedback_index_xy.

- `ZMove (height = nm, speed = nm/sec)`

  nm: height change of the tip from the current position. For negative values tip moves away from the sample. Positive values are allowed but should be used with care.

  speed: average movement speed in nm/sec (optional).

- `DoRamp(InputChannels=("IChn1","IChn2",…,"IChnn"), OutputChannel="OChn", NumPoints=numPoints, InitialValue=iVal, RampAmplitude=amp, Speed=speed, point=(XNm,YNm), SaveData=bool, Smooth=boolean, LimitChannel="LChn", LimitValue=lval, RelativeLimit=bool, OutputChannel2="OChn2", InitialValue2=iVal2, RampAmplitude2=amp2)`

  Applies a *ramp* through an *output* channel while acquires through an *Input* channel. Example: force vs distance (force→input, distance →output) or current vs voltage (current→input, voltage →output) where:

  numPoints: number of points that will be acquired (from 2 and 4096).

  iVal: initial ramp value in *real units* of the ramp.

  amp: ramp amplitude in *real units*. A negative value means an inversion in directions.

6.3 Automation of probe movements

While thinking over tip movement automation immediately comes in mind FZ curves. This because while using the software given by the microscope producers is normal to make FZ curves after tip approaches sample surface. This because can be present artefacts (see chapter 4.1.6).

Due to drift problems present in all piezoelectric actuators, normally isn't possible to eliminate error in positioning even when is possible to determine the correct coordinates of point. For this

reason that sometimes is interesting to make FZ curves in a ROI, that includes the desired point. There are few jobs done by different groups who have practiced this technique for determining Young's modules

6.3.1 Making Force Vs Displacement curves in a determined point

WSxM software includes a function for making FZ curves over the sample, which is under acquisition. There is an inconvenience; it isn't possible to define the exact coordinates where FZ curve is done. In this way when *FZ dialog* activates, the microscope makes a FZ curve in the middle of the line where is scanning.

This is really a big limitation for two main reasons:

- It's not possible to make FZ curve in a point different from the middle one.
- For making FZ curve, there is needed to wait until the desired line is under acquisition and later activate the FZ dialog.

In the following we have defined scrip that makes FZ curves over the sample under acquisition in the specified coordinates introduced by the AFM user in lithography section.

This is a first version of *FZcurves* function and the substrate used was Pseudomonas over gold.

Image 6.4 is acquired in AC mode and shows how it looks like the surface before applying the script. We can distinguish clearly two types of substrates: pseudomonas membranes and clean gold surface exempt form residues.

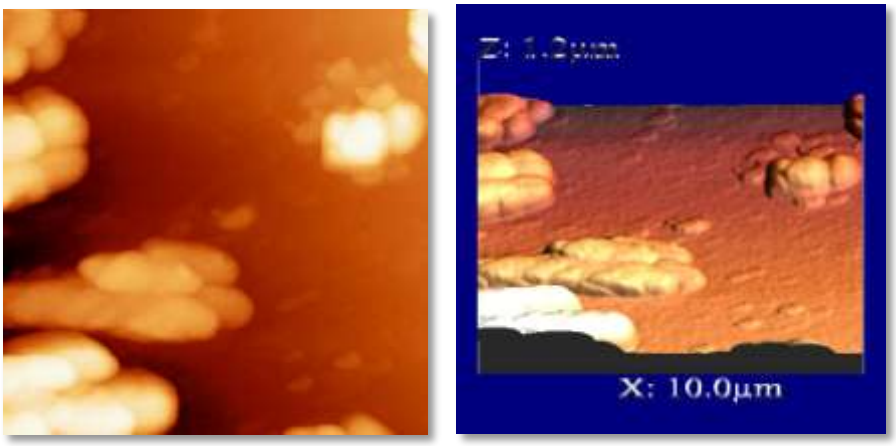

Image 6.4 Pseudomonas Au. over gold,(Left) topography (Right) 3D Reconstruction.

The related source code applied was `(See Appendix D)`. In the whole begin-end block we can distinguish three phases:

- Control instructions like: Feedback switched off and dynamic switched off.
- Effective movement composed from: Zmove and DoRamp.
- Re-establishing previous parameters like: feedback dynamic and positioning.

Over gold substrate the F-Z curve was:

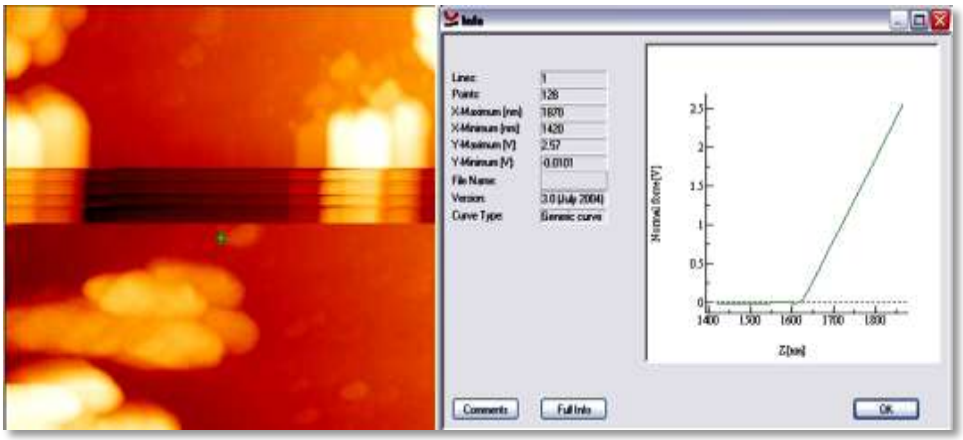

Image 6.5 (Right) FZ curve over gold substrate. (Left) Green cross showing position were FZ applied.

Over Pseudomonas au. membrane, the F-Z curve was like above. Here we note the adhesion of tip with the membrane gives the classical V shape of the curve in the final state where the tip uncouples from the membrane. This V shape isn't present in the previous image were the forces of coupling between tip and gold surface are practically inexistent.

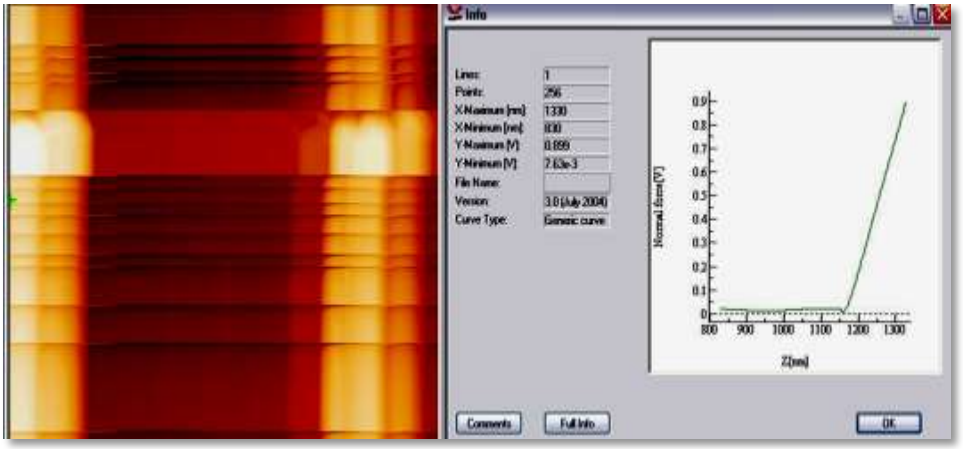

Image 6.6 (Right) FZ curve over membrane. (Left) Green cross, positioned in the left side of the picture.

Meanwhile, in another situation, we could get the FZ curve of Image 6.7.Is important to note that a possible automation could be repeatedly make FZ curves over the same substrate following some criteria like:

- FZ curves in a horizontal/vertical line.
- FZ curves over a matrix (Important for making Force Volume).

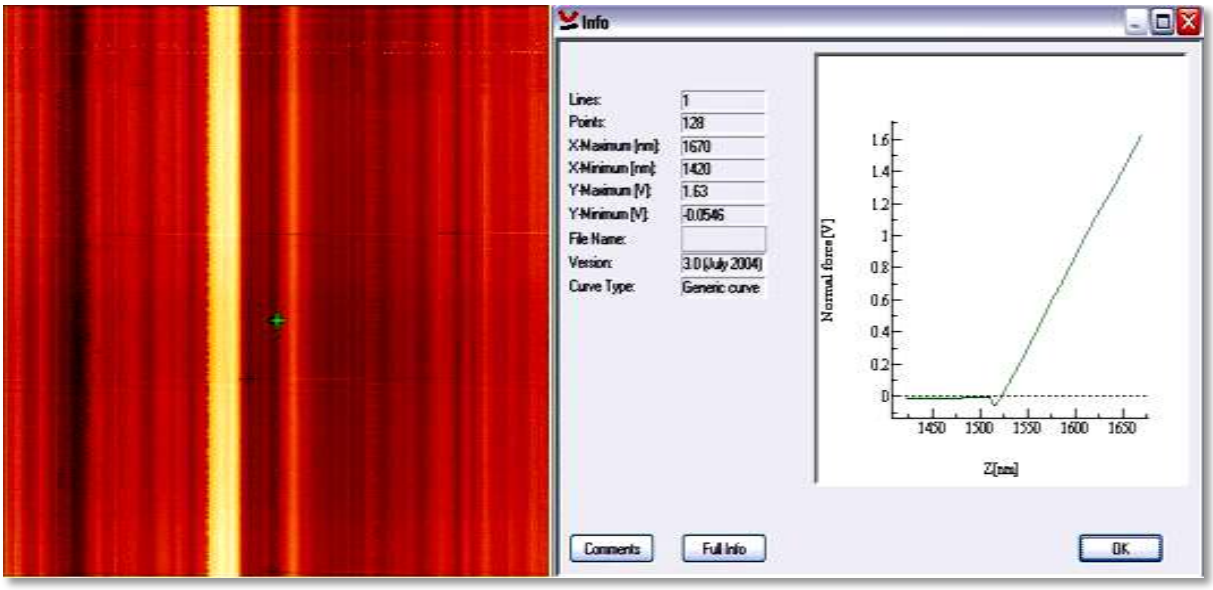

Image 6.7 Other FZ curve over membrane.

6.3.2 Multiple Force Vs Displacement curves in a line and in a matrix

As remarked before, there is the possibility to automate the process of making FZ curves even in different points. In this way are going to show a short script for making an arbitrary number of FZ curves in a line. In image 6.8 is illustrated a series of FZ curves over a PMMA grid. While over a matrix there is needed a nested loop like is shown:

```
begin
      numeric x
      numeric y
      for (x = -500 to 500 step 100) do
      begin
            for (y =-500 to 500 step 100) do
            Point (point = (x, y))
      end
end
```

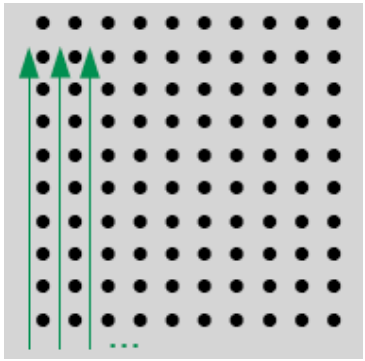

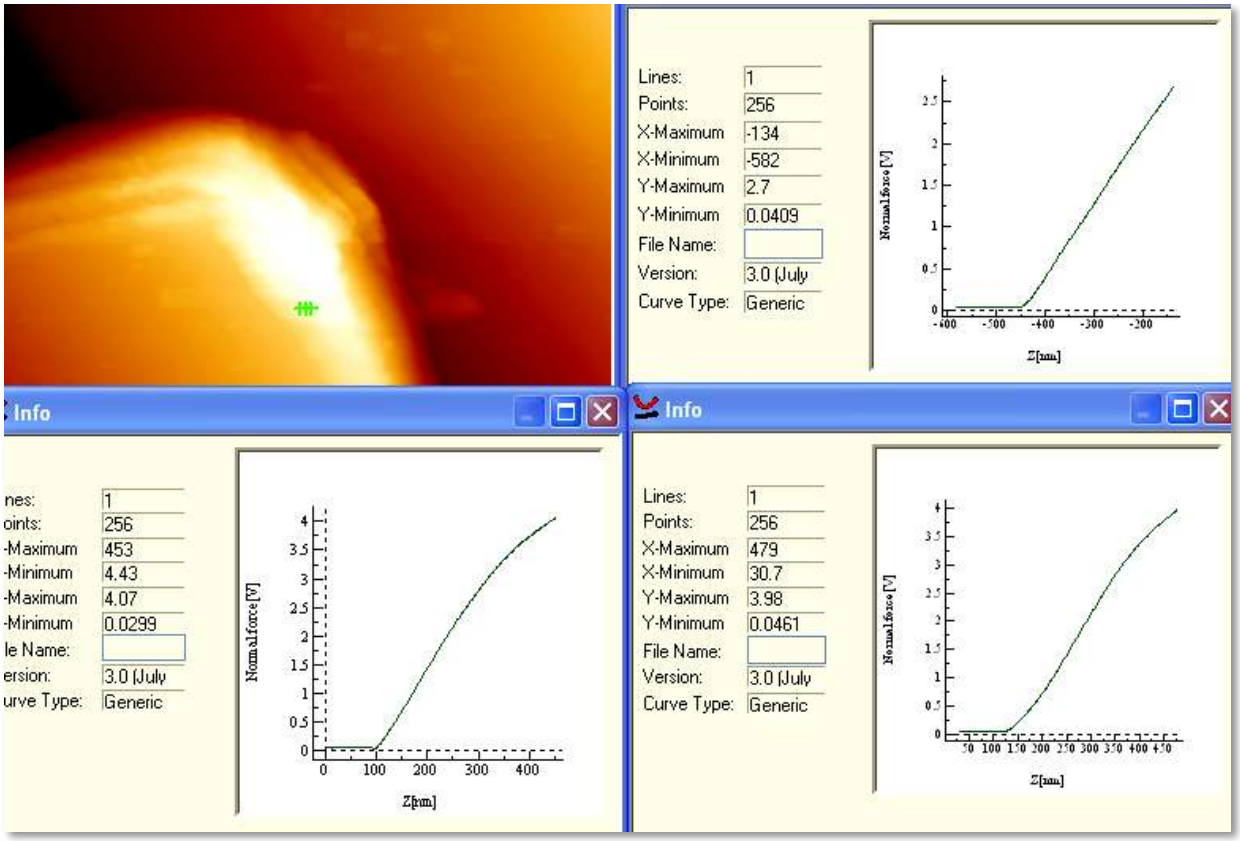

Image 6.8 Series of 3 FZ curves over a PMMA grid.

Here bellow we are going to show the associated source code. It uses a defined kind of variable named *numeric* here used for making possible *for* loop. `(See Appendix D)`

Here the tip is positioned round 700 nm from the sample surface, for this is customary to check distance (with *FZ dialog* in the WSxM) always before applying the following script. In this way it should be changed the value of height variable.

6.3.3 Modifying sample surface in Lithography mode

During this paragraph we are going to illustrate the proceedings in surface modification with AFM. The whole will be explained as a sequence of experiments, with the difficulties found meanwhile. The sample used were Pseudomonas over silicon and E.Coli over gold substrate.

- A first essay over Nanomanipulation was grasping surface closer to membrane. Here drift problems made impossible to control the exact collocation of tip, and the result is Image 6.9.

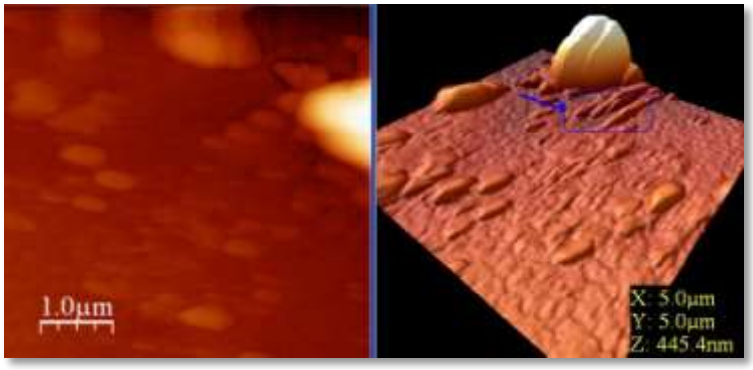

Image 6.9Grasping gold surface as evidenced in the square.

- In this experiment, we achieved scratching the surface closer to bacteria. The sequence shows: how it was before and after scratching. Right: it is a 3D reconstruction. Is important to know that at these intents, all the lines are programmed by software

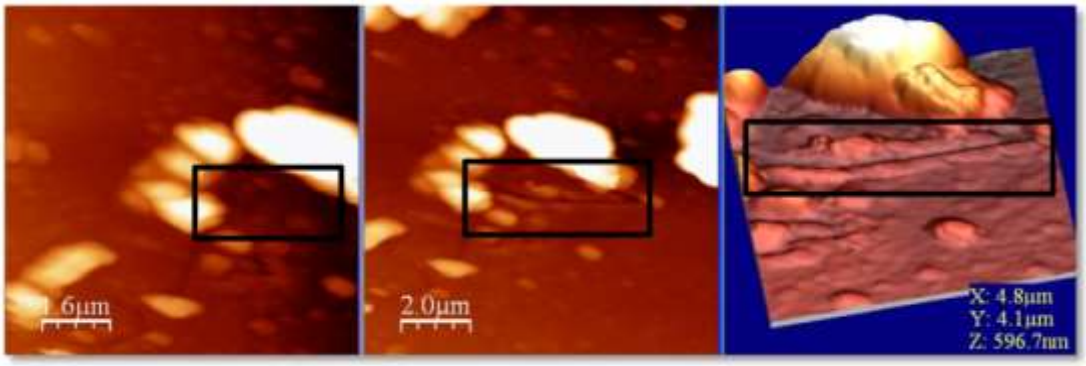

Image 6.10 Scratch closer to bacteria.

- Than we considered making other scratches over sample surface, as follows.

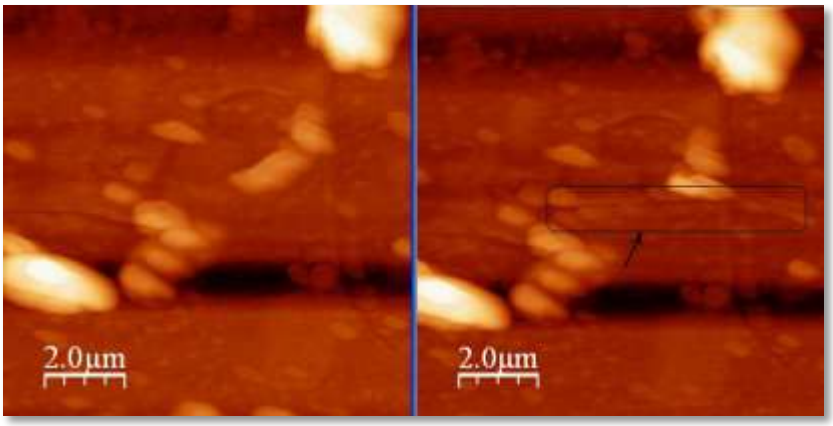

Image 6.11 Collection of horizontal and vertical scratches.

- Once familiarized, we tried making things more complicated. So here we show surface modification in two directions: *Horizontal* and *Vertical* ones. (Please note convention applied; Horizontal = **x** direction, and Vertical = **y** direction).

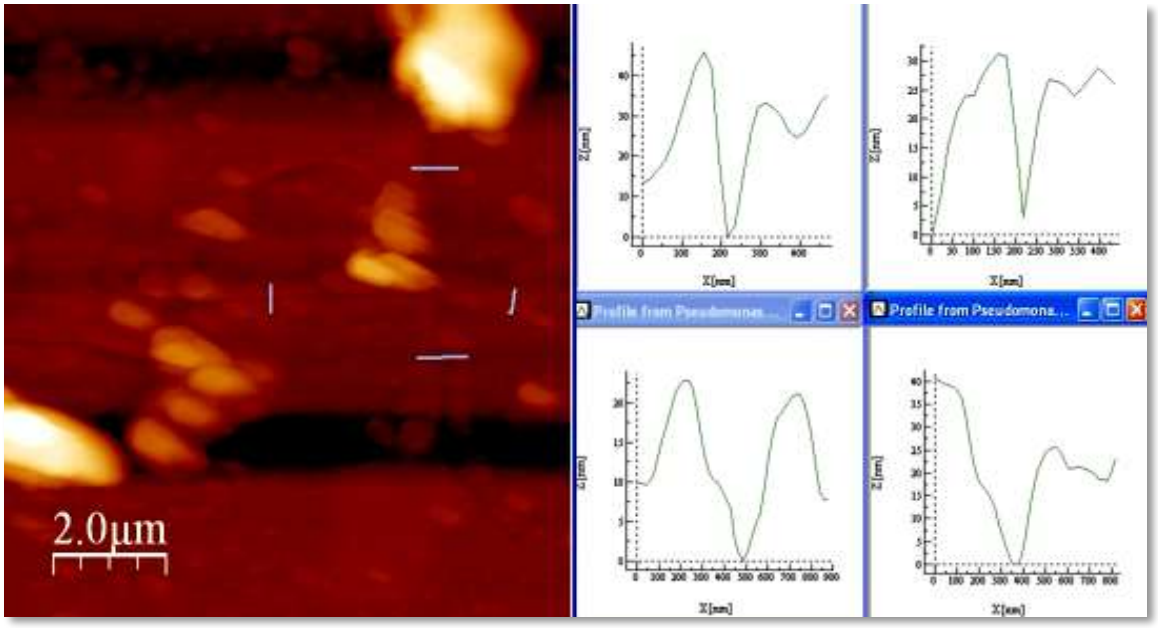

Image 6.12 Profiles of the stripes made in the surface.

- In the following we show the region of interest. A couple of bacteria are fixed at surface.

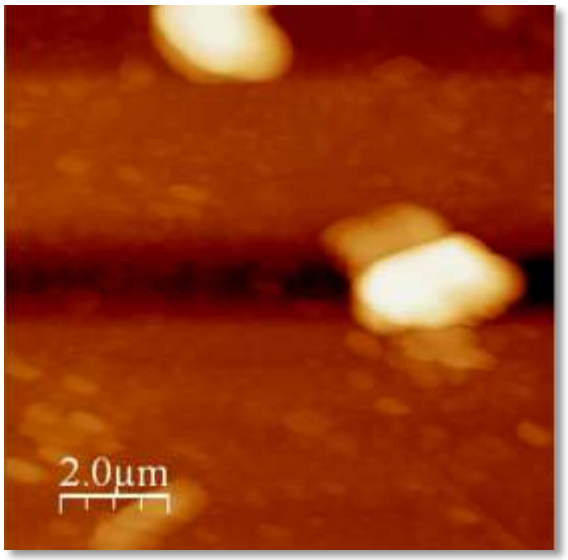

Image 6.13 Bacteria before Nanomanipulation.

- Here is a sequence of Litho sections. Previously we made a line above bacteria; as we centred tip wrongly, the result was a surface modification closer to bacteria's membrane.
  In the second intend, we achieved moving bacteria. Let's focus on surface prints remaining after lithography section; we can see the traces left from bacterial fixation in the sample surface. As a demonstration that, the relative positioning of bacteria have changed.

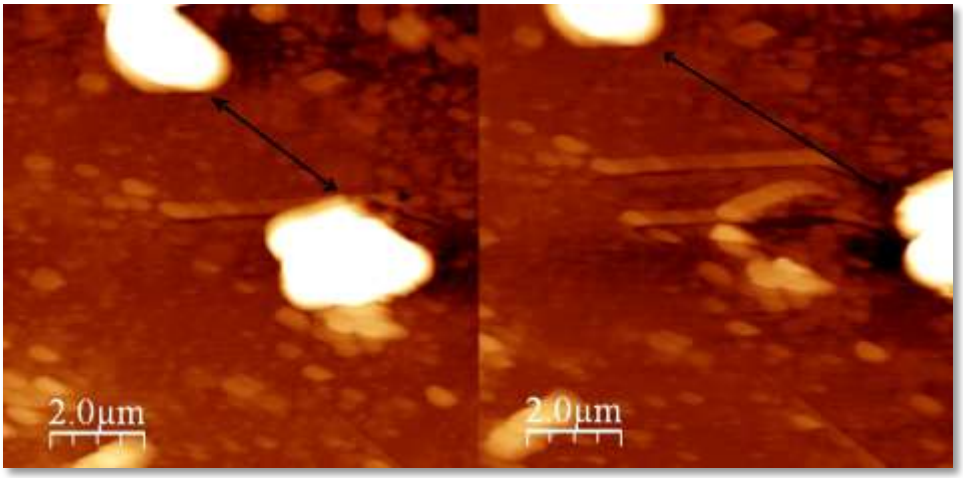

Image 6.14 Section of two scratches. (Left) just above the bacteria. (Right) Moving bacteria.

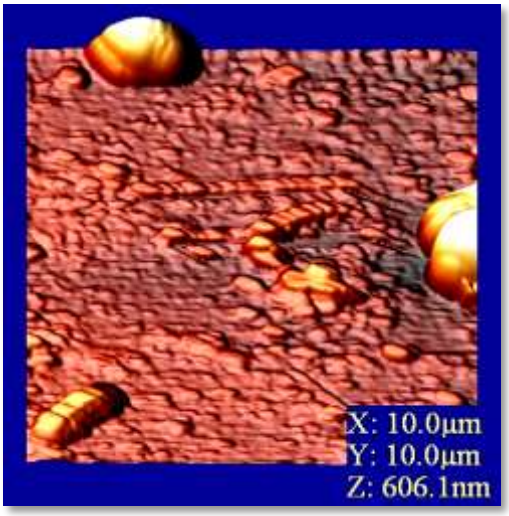

Image 6.15 3D reconstruction of zone.

- After horizontal stripes, we made few ones for getting even more familiarized with moving in horizontal direction. And we effectively moved more the bacteria. So in comparison with the previous picture, bacteria have moved even more. The incorrect centring of tip in bacteria's mass centre has induced a composed movement, which is sum of a rotation and

displacement. After this, we applied our scripts for vertical tip movement. See line passing closer to bacteria's membrane, and its 3D reconstruction in the following pictures.

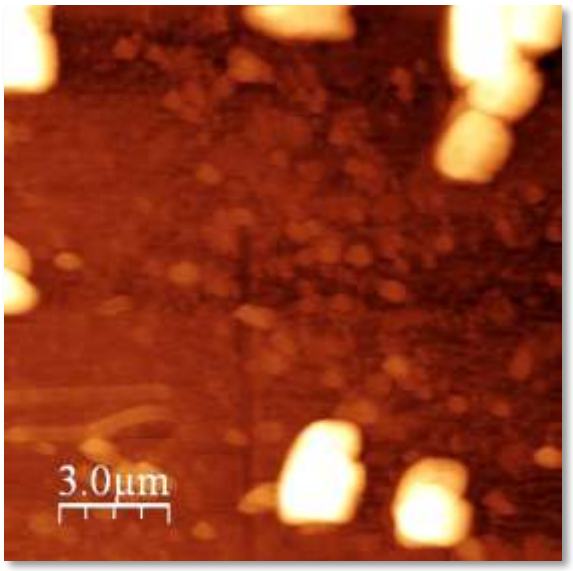

Image 6.16 Vertical stripes after displacing once again the bacteria.

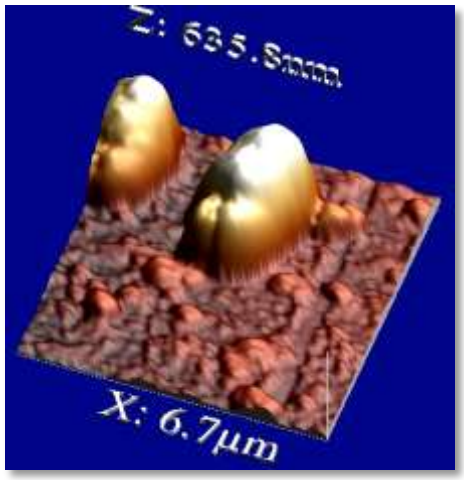

Image 6.17 3D reconstruction of vertical stripe closer to bacteria

- Here we show how we move the bacteria in vertical direction. The arrows show the relative movement in comparison with bacteria closer to the one moved.

  We notice here that we achieved controlling the force that we apply versus sample surface, and the demonstration is the absence of stripes in the sample surface. This is caused by the small contact surface between tip and bacteria membrane.

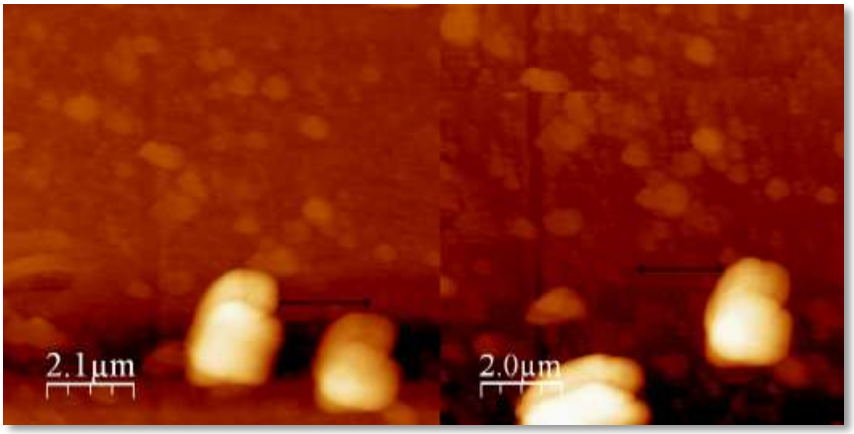

Image 6.18 Moving bacteria without scratching sample surface.

- Moving bacteria's with Litho scripts reveals a lot of problems, because of complicated circumstances in the experiments. More in specific, drift problems, lineation problems, and scan angles. Nanomanipulation improvements induced us to target "Force Measurements". Force measurements were made following two specific protocols:
    - Saving Normal & Lateral forces during one big step (round 5-7 µm) made of shorter segments (round 50~100 nm).
    - Saving Normal & Lateral forces during one big step.

  Here we present some more results obtained with our *litho scripts.*

6.3.4.1 Experiment: Breaking bacteria

During this experiment we scrape up the final part of bacteria. In the before-after sequence, we can see how the bottom of bacteria is displaced 7µm away.

The angle between cantilever and movement direction is perpendicular. We think is better to actuate in perpendicular direction, because we discard torsion and compression forces of cantilever in the resultant force. As consequence of physics behind AFM, none of them is calculable (with depreciable error).

This is basically for two factors:

1. *Cantilevers spring constant.* We used a harder one with approx. 40 N/m.
2. *Deterioration of samples.* Sample used was prepared more than one month ago. So it's not supposed to conserve membrane properties, as we will face of in the following experiments.

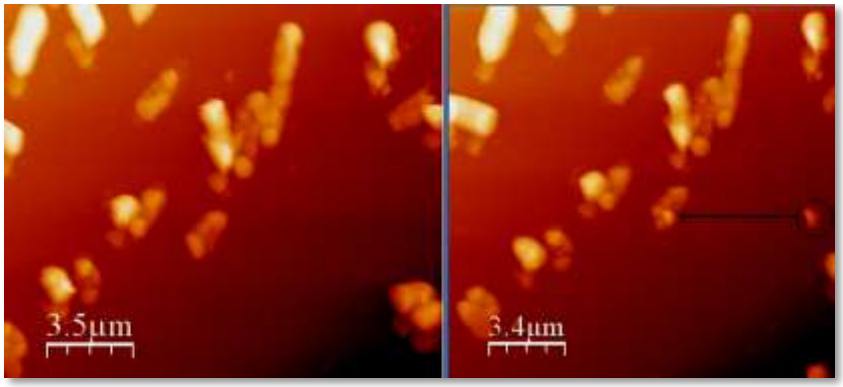

Image 6.19 Breaking bottom of E.Coli.

As we can see, while saving lateral and normal forces, we can distinguish two phases in the manipulation:

- Breaking the membrane, related with higher lateral force due to higher lateral deflection.
- Linear constant phase due to displacement of broken piece.

The MATLAB elaboration gave these results for the lateral force:

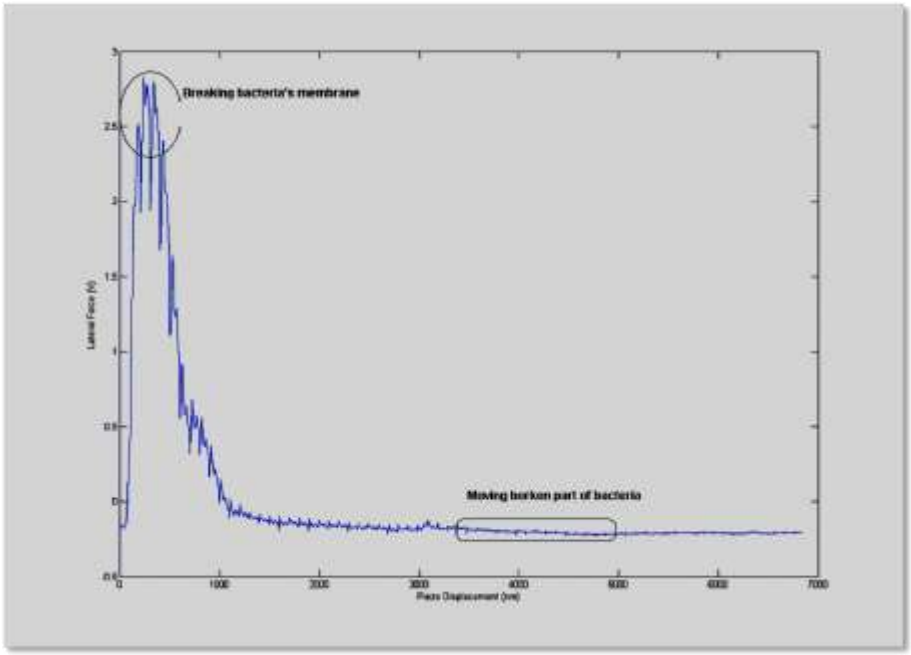

Image 6.20 Graph of lateral force. We can distinguish breaking phase and displacing phase.

We can note the nonlinearities of the graphic due to segmentation of displacement. In this case we followed the procedure 1 (Saving lateral & normal forces of step made of smaller steps).

In figure 13 is shown the nonlinearities that coincide with beginning and end of each step.

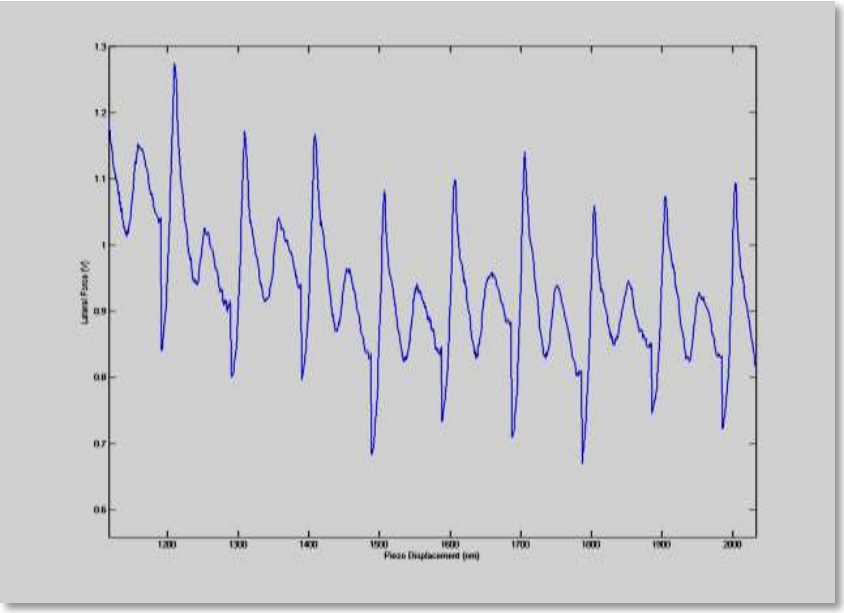

Image 6.21 Zoom in nonlinearities.

6.3.4.2 Experiment: Moving bacteria

In this case we proposed to move for entirely a bacterium, and saving lateral force. In figure 14 left, is evidenced with black circles bacterium that is centered and after litho section it "disappears" from the scan size. We augmented scan size and found the bacterium 7 μm away overlapping with another bacterium (See fig 15).

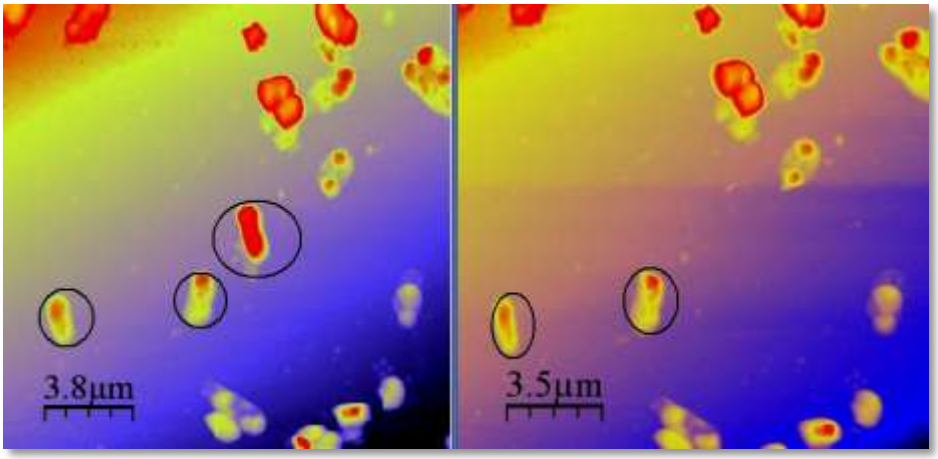

Image 6.22 Moving bacterium 7 μm in the right from centre image.

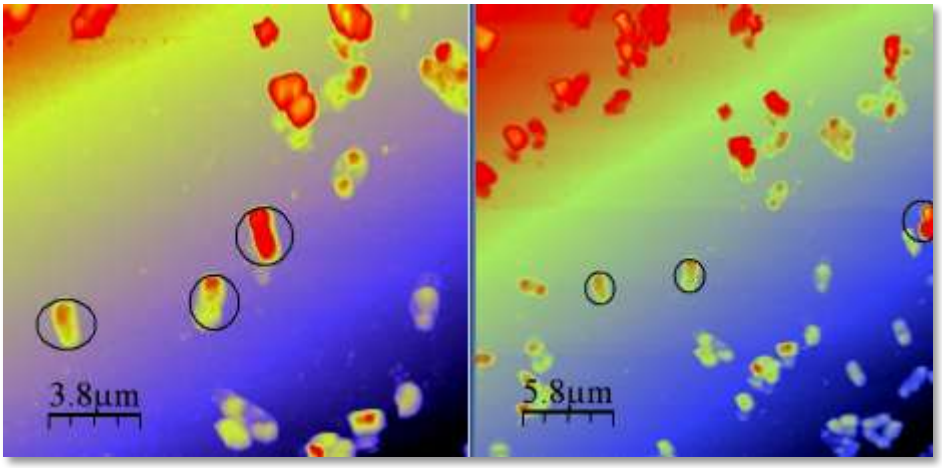

Image 6.23 Right: In centre is the bacterium that is going to be moved by the tip. Right: final coordinates of bacteria after Litho section.

While displacing bacterium, we saved normal and lateral forces (With protocol 1), and bellow we show the reconstruction with MATLAB® of the compound big step. In the same pick, is an enlargement showing the nonlinearities of this protocol. Possibly because of continuous interruptions of voltage imposed to piezoelectric actuator for moving shorter steps.

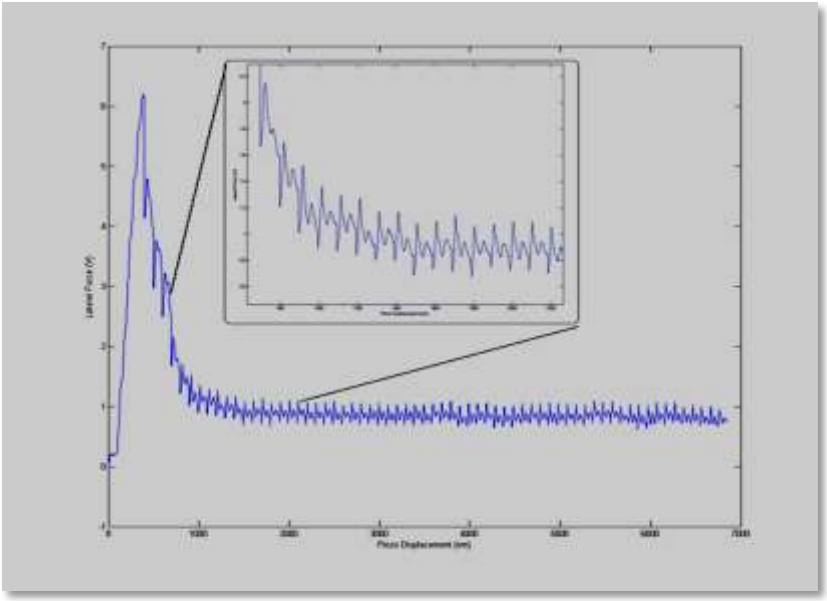

Image6.24 Lateral force saved during displacement.

6.3.4.3 Experiment: Breaking bacteria's membrane

In this experiment we collocated the tip closer to bacteria and decided to use protocol 1 while the big step is of 2 μm. Is important to emphasis once again on perpendicularity between cantilever stick and movement direction. Because the final force applied over bacterium is a combination of more forces. Few of them with unknown amplitude, which makes impossible to calculate the applied forces.

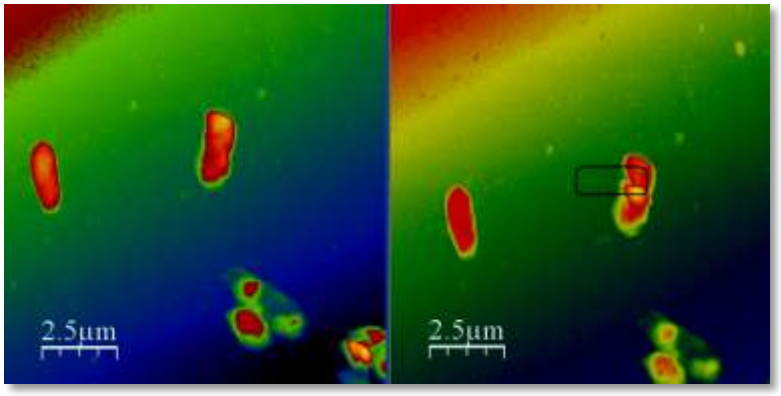

Image6.25 Breaking bacterium membrane.

Further enlargement over the broken bacterium and the stripe made over substrate:

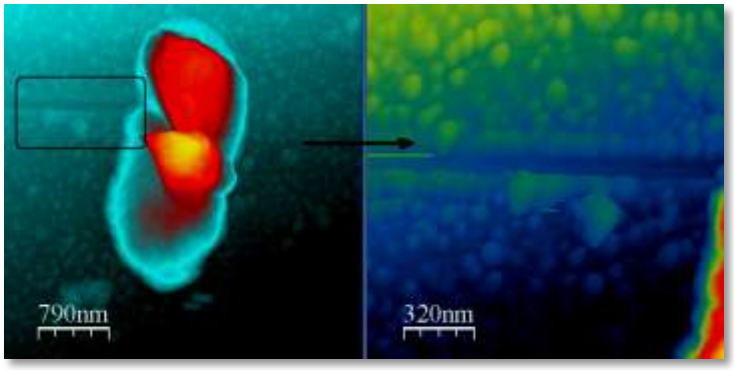

Image6.26 After Litho section.

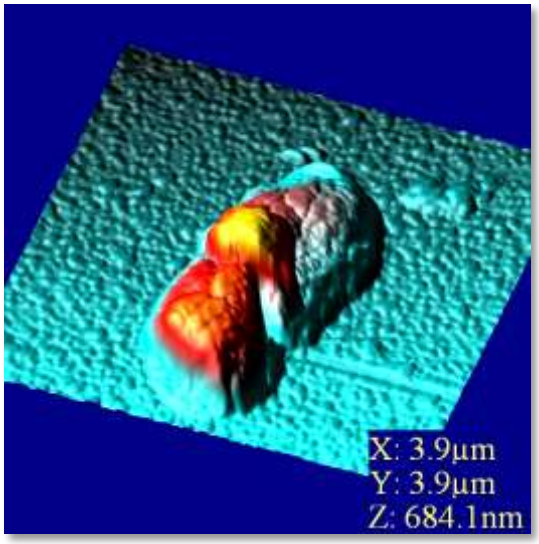

Image6.27 3D reconstruction of scratch.

MATLAB post elaboration of lateral forces saved during lithography section. Is important this kind of experiment because the pendent of the graph shows stiffness of bacterium membrane, despite the fact that here bacteria's are dry and deteriorated.

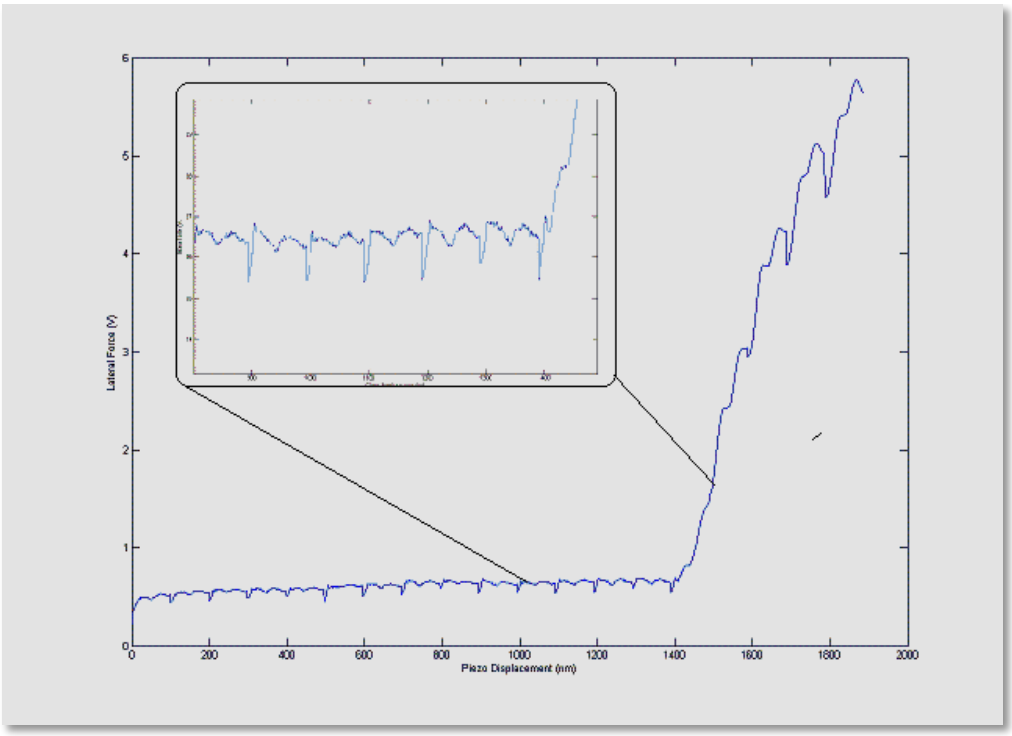

Image 6.28 Lateral force while breaking the membrane.

6.3.4.4 Experiment: Breaking through a bacteria

In this forth experiment we achieved this interesting results while breaking through a bacteria. We can see in the picture from left to right how it was before actuation and after actuation with *Litho scripting.*

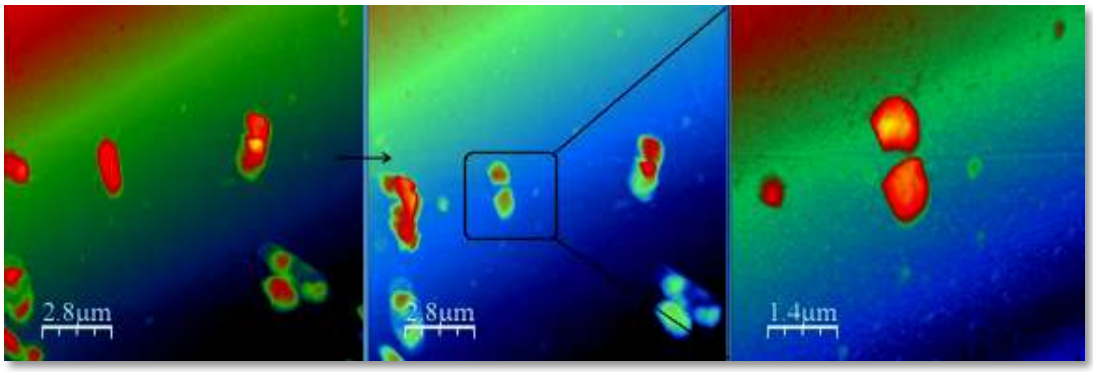

Image 6.29 Breaking through a bacterium. Left: before. Centre: after nanomanipulation. Right: zoom in.

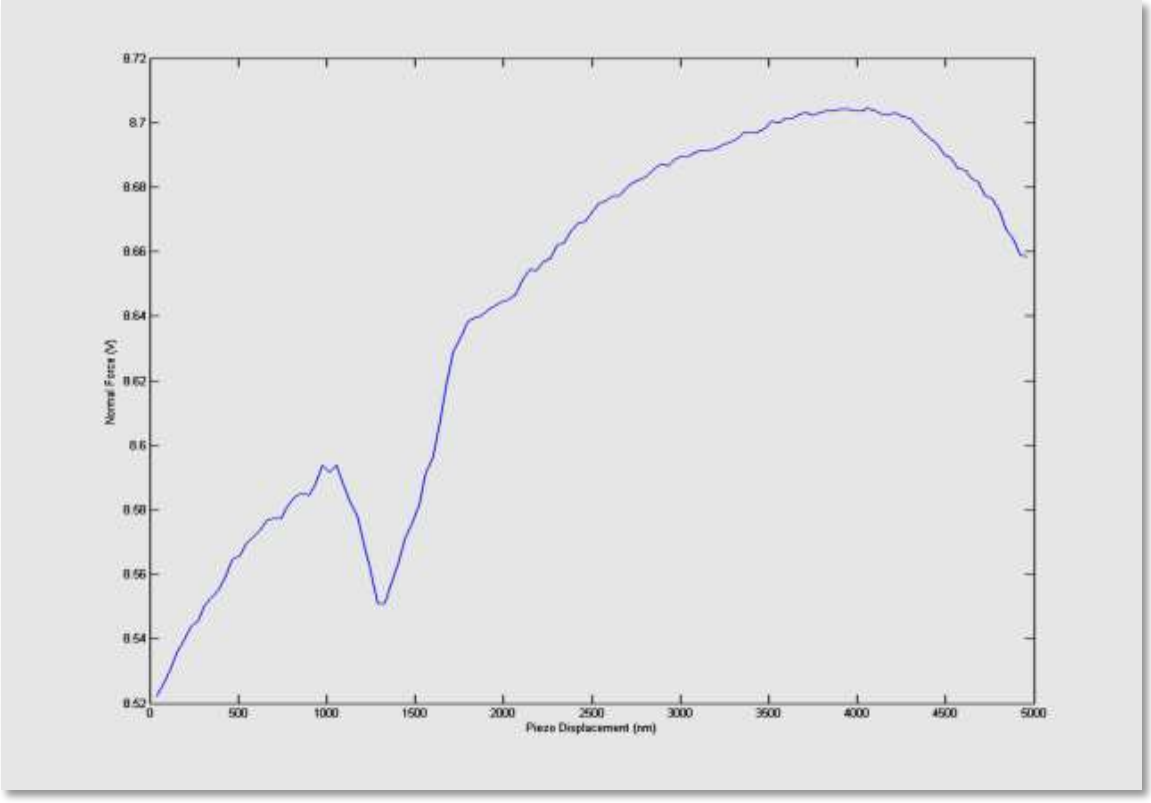

Image 6.30 Normal force saved during manipulation.

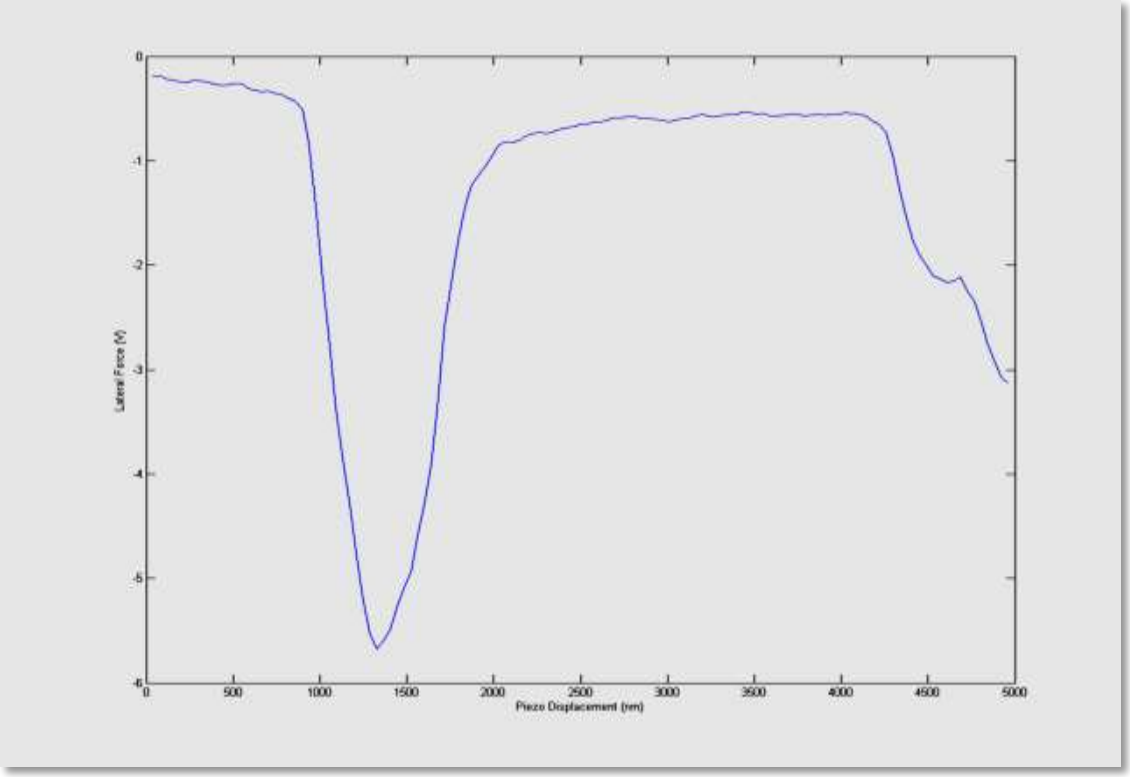

Image 6.31 Lateral force saved during manipulation.

6.3.4.5 Experiment: Force measurement while breaking a link with probe

In some scans, we saw the following links, between two bacteria. But unfortunately, due to: scan speed, oscillating amplitude, softness of the link etc. we broke the link. In the last picture is seen how it remains after zoom in, in the region of interest.

Image 6.32 First link found while scanning sample.

While scanning in the same zone (few micros away), we saw another link. This time the link was stiffer ad we decided to get closer. In the picture are shown further zooms in the region of interest.

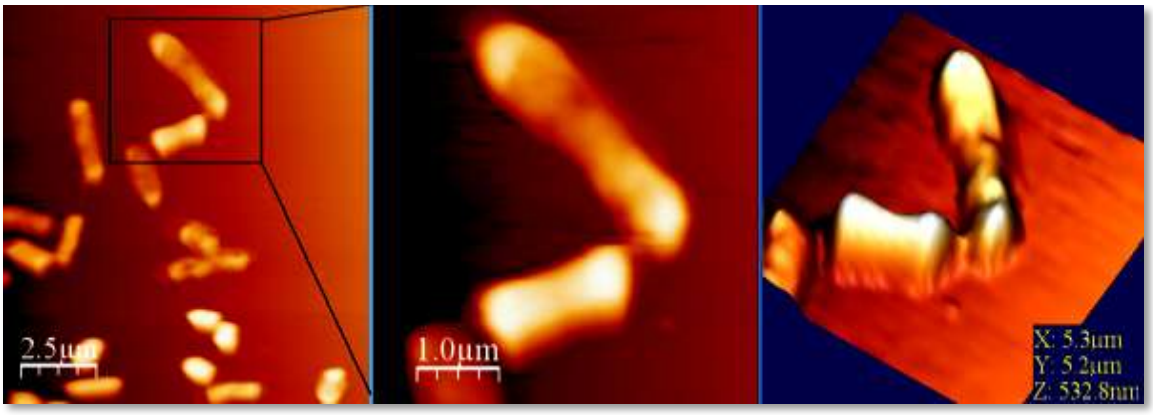

Image 6.33 Link found before litho section. (Right) 3D reconstruction of link.

In this experiment, because of angular positioning of bacteria and as a consequence of the link, we had to use a 45º angle between cantilever stick and moving direction. Is needed a further understanding of the processes that are happening between forces, which is the real influence of applying an angle different form zero at the moment of calculating applied forces. So, we placed tip by one side of the link, and in a single entire line (protocol 2), we break it. Here it is the result:

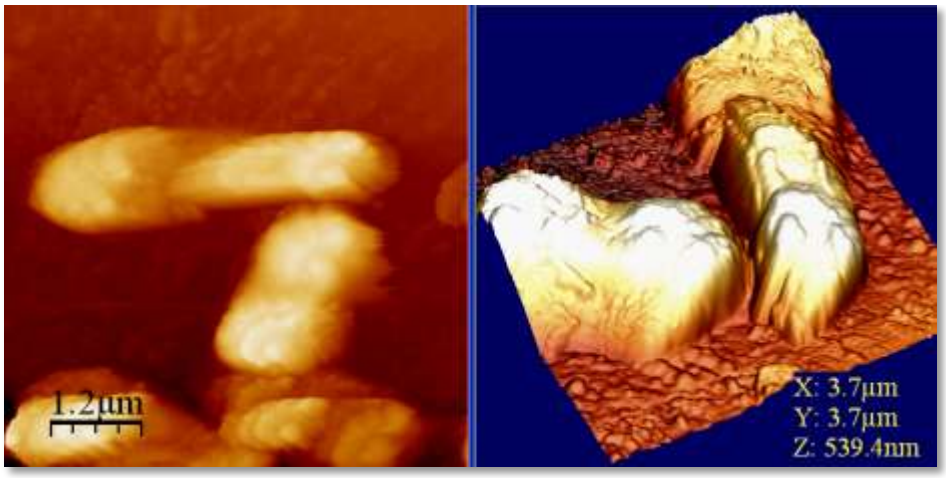

Image 6.34 Bacteria after breaking link.

We saved normal and lateral forces to have a deeper understanding of what's happening with the measured forces. We placed the markers to show the region of interest, as the link was situated approximately 1 µm far from the center of image.

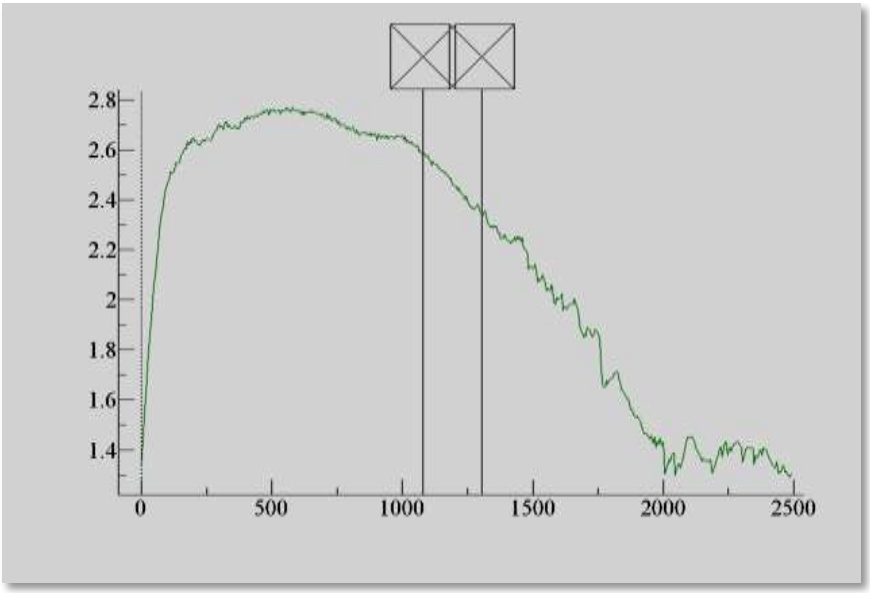

Image 6.35 Lateral force.

Is interesting to see the shape of normal force. It "notes" when the tip breaks the link. And this is confirmed by the positioning of the markers at the same distance from the beginning of graph, as the distance of the link from the center of image.

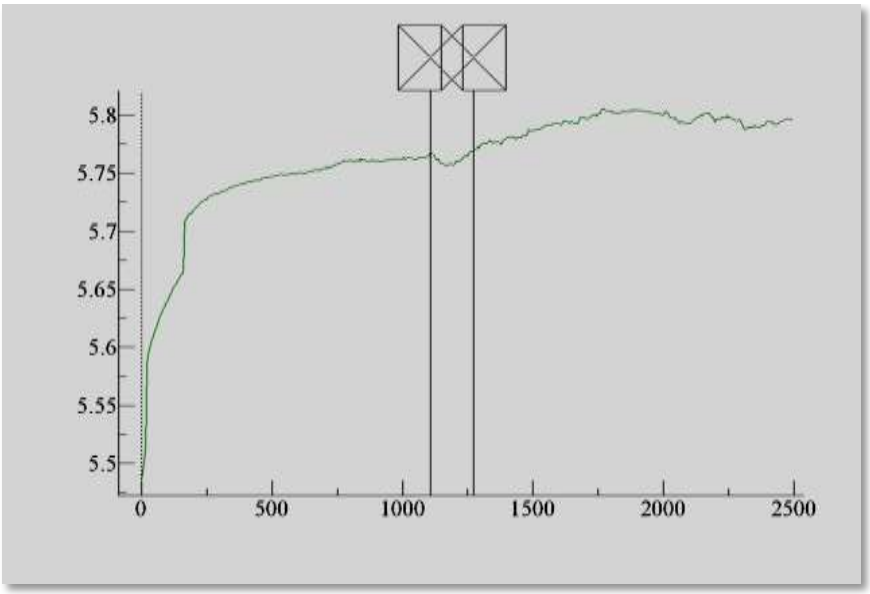

Image 6.36 Normal force.

6.3.4.6 Experiment: Force measurement while moving bacteria

Here it is another experiment. We passed trough bacterium, measured lateral and normal force, while leaving a mark over membrane without moving bacterium. Normal and lateral forces shapes are common in all similar experiments.

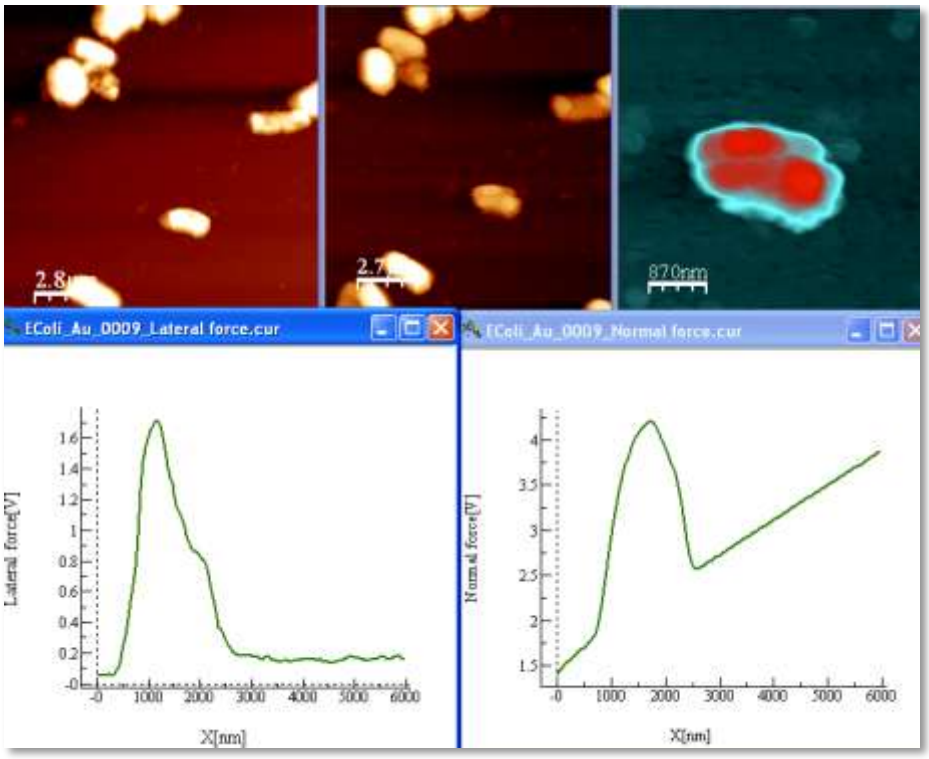

Image 6.37 Moving bacteria.

Conclusions

In this work were achieved important results like: mechanical biofilm characterization, imaging in liquid environment of bacterial biofilm. Both these results important as till now only few works have achieved these results.

We have explored the limitations of the lithography section, by developing scripts that automates tip movement. Despite these constraints, it was achieve moving, breaking, grasping the bacterial membranes and the most important thing is calculating forces exerted over cantilever. A MATLAB post elaboration of the files saved permits direct processing and visualization of the saved forces.

Finally in this work we would like to give some advices over a possible way of calibrating lateral forces in AFM.

Till now there are several works over cantilever lateral force constants calibration, some of them use their geometry for calculating these constants…etc.

Proposal:

In this work is proposed to calculate lateral constants by means of lateral forces saved during a lithography section. In this section by scripting are made several lines over a rigid surface (ex. gold), where the tip is fixed over the rigid surface by penetrating the tip over the gold surface few nanometers. In this way the tip is fixed, while the cantilever is displacing several nanometers.

The final result is absolute lateral cantilever deflection (absence of normal deflection due to rigid tip fixing over substrate surface), which can be measured. From the slopes of lateral force Vs. Horizontal cantilever displacement it can be calculated the constants.

Acknowledgments

The author of this master thesis would like to give special thanksto all of them who in a way or another sustained and collaborated in this work:

- University of Padua, for the double degree exchange program.
- Dr. Antóni Juárez and Dr. Rosa Banyos, for biological sample preparation.
- Dr. Manel Puig I Vidal for his supervision.
- Phd.thesis student Jorge Otero Díaz for its constant help during first stages in imaging with AFM, and with the optical microscopy.
- Dr. David Lewis, from Nanonics, for the images of MultiView4000.
- My family how has always supported me morally.

Appendix A

Gram staining (or **Gram's method**) is an empirical method of differentiating bacterial species into two large groups (Gram-positive and Gram-negative) based on the chemical and physical properties of their cell walls.A cell wall is: A fairly rigid layer surrounding a cell, located external to the cell membrane, which provides the cell with structural support, protection, and acts as a filtering mechanism. The cell wall also prevents over-expansion when water enters the cell. They are found in *plants*, *bacteria*, *archaea*, *fungi*, and *algae*. Animals and most *protists* do not have cell walls.

The material in a cell wall varies between species. In plants, the strongest component of the complex cell wall is a carbohydratepolymer called cellulose.

The wall gives cells rigidity and strength, offering protection against mechanical stress. In multicellular organisms, it permits the organism to build and hold its shape (morphogenesis). The cell wall also limits the entry of large molecules that may be toxic to the cell. It further permits the creation of a stable osmotic environment by preventing osmotic lysis and helping to retain water. In figure A.1 is shown in left a generic cell wall, and on the right a schematic representation of it.

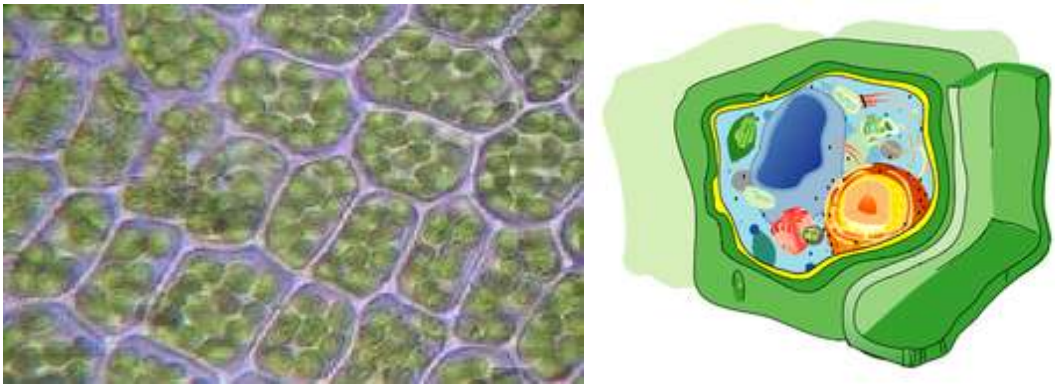

Appendix A.1 (Left) Cellular wall. (Right) Schematic representation of cell.

The Gram's method is named after its inventor, the Danish scientist Hans Christian Gram (1853 – 1938), who developed the technique in 1884 to discriminate between pneumococci and *Klebsiella pneumoniae* bacteria.

Uses in Research

The Gram stain is not an infallible tool for diagnosis, identification, or phylogeny, however. It is of extremely limited use in environmental microbiology, and has been largely superseded by molecular techniques even in the medical microbiology lab. Given that some organisms are Gram-variable (i.e. they may stain either negative or positive), and that some organisms are not

susceptible to either stain used by the Gram technique, its true utility to researchers should be considered limited and non-specific. In a modern environmental or molecular microbiology lab, most identification is done using genetic sequences and other molecular techniques, which are far more specific and information-rich than differential staining.

Medical Purposes

Gram stains are performed on body fluid or biopsy when infection is suspected. It yields results much more quickly than culture, and is especially important when infection would make an important difference in the patient's treatment and prognosis; examples are cerebrospinal fluid for meningitis and synovial fluid while detecting septic arthritis.

As a general rule (which has exceptions), Gram-negative bacteria are more pathogenic due to their outer membrane structure. The presence of a capsule will often increase the virulence of a pathogen. Additionally, Gram-negative bacteria have lipopolysaccharide in their outer membrane, an endotoxin that increases the severity of inflammation. This inflammation may be so severe that septic shock may occur. Gram-positive infections are generally less severe because the human body does not contain peptidoglycan; in fact, humans produce an enzyme (lysozyme) that attacks the open peptidoglycan layer of Gram-positive bacteria. Gram-positive bacteria are also frequently much more susceptible to beta-lactam antibiotics, such as penicillin.

Some examples of Gram's staining method results:

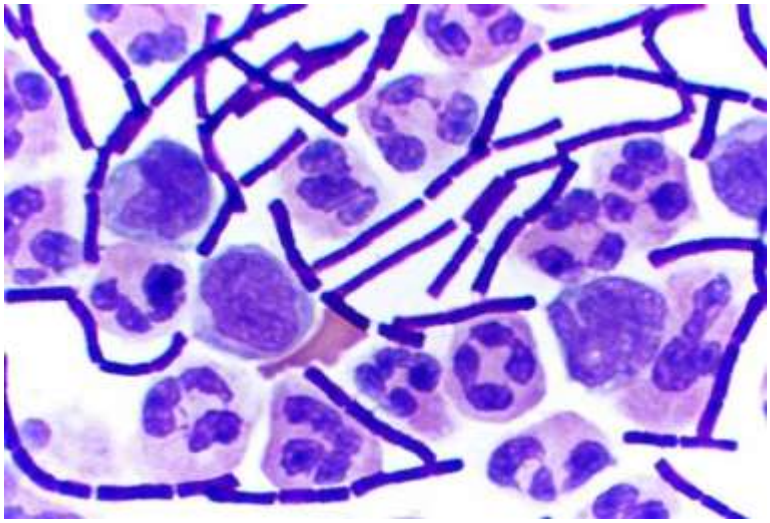

Appendix A.2Gram-positive anthrax bacteria (purple rods) in cerebrospinal fluid sample. If present, a Gram-negative bacterial species would appear pink. (The other cells are white blood cells).

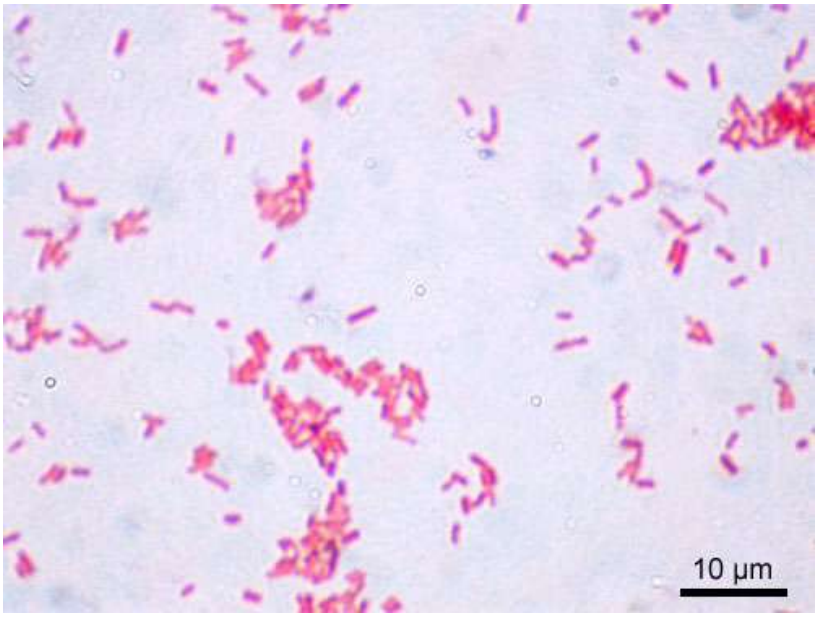

Appendix A.3 E.Coli evidenced with Gram's method. Optical microscopy.

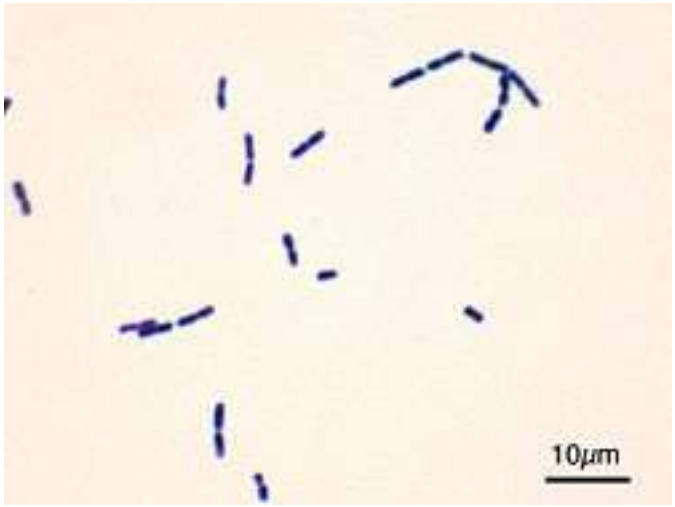

Appendix A.4 Bacilus cereus seen with optical microscopy evidenced by Gram's method.

Staining mechanism

Gram-positive bacteria have a thick mesh-like cell wall made of peptidoglycan (50-90% of cell wall), which stain purple and Gram-negative bacteria have a thinner layer (10% of cell wall), which stain pink. Gram-negative bacteria also have an additional outer membrane that contains lipids, and is separated from the cell wall by the periplasmic space. There are four basic steps of the Gram stain, which include applying a primary stain (crystal violet) to a heat-fixed smear of a bacterial culture, followed by the addition of a *mordant* (Gram's iodine), rapid decolorization with alcohol or acetone, and *counterstaining* with safranin or basic fuchsin.

Crystal violet (CV) dissociates in aqueous solutions into CV^+ and chloride (Cl^-) ions. These ions penetrate through the cell wall and cell membrane of both Gram-positive and Gram-negative cells. The CV^+ ion interacts with negatively charged components of bacterial cells and stains the cells purple. Iodine (I^- or I_3^-) interacts with CV^+ and forms large complexes of crystal violet and iodine (CV – I) within the inner and outer layers of the cell. When a decolorizing substance such as alcohol or acetone is added, it interacts with the lipids of the cell membrane. A Gram-negative cell will lose its outer membrane and the peptidoglycan layer is left exposed. The CV – I complexes are washed from the Gram-negative cell along with the outer membrane. In contrast, a Gram-positive cell becomes dehydrated from an ethanol treatment. The large CV – I complexes become trapped within the Gram-positive cell due to the multilayered nature of its peptidoglycan. The decolorization step is critical and must be timed correctly; the crystal violet stain will be removed from both Gram-positive and negative cells if the decolorizing agent is left on too long (a matter of seconds).

After decolorization, the Gram-positive cell remains purple and the Gram-negative cell loses its purple color. Counterstain, which is usually positively-charged safranin or basic fuchsin, is applied last to give decolorized Gram-negative bacteria a pink or red color.

Some bacteria, after staining with the Gram stain, yield a *Gram-variable* pattern: a mix of pink and purple cells are seen. The genera *Actinomyces*, *Arthobacter*, *Corynebacterium*, *Mycobacterium*, and *Propionibacterium* have cell walls particularly sensitive to breakage during cell division, resulting in Gram-negative staining of these Gram-positive cells. In cultures of *Bacillus*, *Butyrivibrio*, and *Clostridium* a decrease in peptidoglycan thickness during growth coincides with an increase in the number of cells that stain Gram-negative. In addition, in all bacteria stained using the Gram stain, the age of the culture may influence the results of the stain.

Gram staining protocol

1. Make a slide of tissue or body fluid that is to be stained. Heat the slide for few seconds until it becomes hot to the touch so that bacteria are firmly mounted to the slide.
2. Add the primary stain crystal violet and wait 1 minute. Rinse gently with water. This step colors all cells violet.
3. Add Gram's iodine, for 30 seconds. It is not a stain; it is a mordant. It doesn't give color directly to the bacteria but it fixes the crystal violet to the bacterial cell wall. All cells remain violet.
4. Wash with ethanol and acetone, the decolorizer. If the bacteria is Gram-positive it will retain the primary stain. If it is Gram-negative it will lose the primary stain and appear colorless.

Appendix B

Manual of Lithography

This support note shows how to use lithography section of **WSxM** *program. It will describe each one of the menus that appear in the subprogram.*

Lithography is a part of the WSxM program. In this frame you can draw on a sample, define the tip motion and write on a sample.

Introduction

WSxM Lithography section allows you to move the tip over the sample performing different actions. You can think in the tip as a pen, and the sample as a paper. If you can somehow define what does "draw" mean, you can "draw" with your tip over your sample, (like) as it was a pen. When you have a pen, you can move it far away from the paper and it will draw nothing. The same can be done with WSxM Lithography if you can define what "do not draw" means in your tip-sample system.
When you plot a simple figure, like a line or a set of concatenated lines, the tip will go to the desired starting point. Once reached that point, if you have defined what "draw" means in your system, these actions will be performed. This is what we have called **"Start drawing actions"**(we will see this feature in more detail in a few lines). In our pen-paper example, this is like moving the pen to the paper until they contact. Then, the tip will move following a path, *drawing*. When the figure is complete, the system will perform **"Finish drawing actions".** In the pen-paper example the pen goes out from the paper. Now the tip will move to the first point of the next figure, without drawing.

Drawing a new lithography pattern

There are two ways to input a lithography pattern:

1. Graphically. This is the easiest way and the one that we recommend.

   1. 1. First of all, if the *design Window* is not open, you have to open it by pressing the **Design** command in the View menu or its associated button in the toolbar.

1. 2. In the settings dialog-bar you can change the size of the drawing area. This dialog contains some figure editing and simulating information, such as the size of the drawing area, the speed of the movements during the simulation process and a check-box that allows showing or hiding the position of the tip.

1.3. Now you can plot figures by pressing the Plot menu or the appropriate toolbar command.

2**. Editing the associated code.**

2. 1. You can see the code associated to the designed pattern by opening the code Window. You can add lines by typing new code, changing the existing, coping and pasting the existing and so on.

2. 2. To make effective the changes made in the code window, you may press the Apply button (a check mark) or select this command in the Code menu.

2. 3. If you do not see the effect of the changes you did, you can verify the compilation results window. This window will tell you if there is any syntactic error in your code. You can open it by pressing the toolbar button or the command in the View menu.

You can select a background image for your lithography pattern. When you open an image from the lithography main frame, this image will be placed in the background of the design window and the size in the settings will change. If you want to auto-fit the pattern to the image, you have to check this option in the browser settings. When you go to the new lithography main frame from the acquisition main frame, the image in the selected channel will be placed in the background.

You can save your session or open a saved one with the image browser, but always in the lithography main frame.

If you are editing some code and it has syntactic errors but you want to save it, you can do this by pressing Save Code or the button in the toolbar of the code window. If you save it by pressing **Save**, it will save the pattern in the design window.

Simulating the lithography session

After you have finished drawing your lithography pattern you can simulate it. The movement speed of the tip will be the one in the settings dialog. You can execute the whole session, only a single block (i.e. a multiline) or a single simple instruction (i.e. single line in a multilane). The real tip position will not vary while simulating, but there will be a simulated tip position.

Doing a real lithography session

There is a dialog-bar in the data acquisition main frame. If you open it, you will see a button to **activate/deactivate**the lithography session (in green if it is active and in gray if it is not) and some buttons to select the execution mode, described bellow.

If there is a lithography pattern in the main lithography frame and your scan size Is different from 0, you can activate the lithography session in the acquisition main frame. To do this, press

the **On/Off** button. You will see your pattern in the selected channel.

The movement speed is the same as the simulating speed. If you change this value in the Lithography main frame, you'll see the tip movement is faster or slower.

You can execute the whole session, only a line and so on by pressing the desired button.

To continue scanning after doing your lithography session, you may press the **Stop Scanning button** in the main channel window.

General Frame (Design and Simulation)

This is the general window that appears when you get into lithography.

Menus that appear in (and belong to) this section are the following ones.

File

	Opens an image or lithography pattern to show it in the design view. Moreover, you can load an image going to acquisition, and returning to lithography. The image that you have been acquiring will appear then in the view.
	Saves in a file the lithography pattern from the design view.
	Goes to the WSxM Representation section.
	Goes to the WSxM Acquisition section.

View

Shows start drawing configuration code. A draw configuration lets you decide what is the meaning of "start to draw" on the sample and "finish to draw" on it. In this view, you can introduce instructions that will be performed before drawing each instruction (on beginning).

There is only one restriction: You cannot write here more drawing instructions[1].

Example: If you want to perform an oxidation process, you may "draw" lines by applying a Bias

Voltage. In this case, you can write here the Bias instruction and it will change automatically before plotting every line.
For more information about instructions, see Design.

Shows "finish drawing configuration" code. A draw configuration lets you decide what is the meaning of "start to draw" on the sample and "finish to draw" on it. In this view, you can introduce instructions that will be done after each drawing instruction (on finishing).

Only exists a restriction: You cannot write here more drawing instructions.
In the same example, you should set the bias to 0 or the previous value here.
For more information about instructions, see Design.

This dialog contains settings for lithography program. Here, you can choose:

- The **size** of the drawing area (or design window) (in nm)
- **Simulation speed**(in nm/s). Speed of the tip motion during simulation.
- **Drawing configuration**. (as explained before).
- You can load an existing configuration or make a new one by selecting "(new...)" configuration in list: A dialog lets you do it.
- **Show tip position**. If you don't want show it in the view, you can unmark this option. Tip position is represented in the lithography design view as a cross.
- **Auto rescale**to fit to window when opening a new image. If this option is checked and you change the background image, instructions will resize automatically, to get the full area.
- **Grid Settings**. X and Y distance between grid points in the design view. If this value is too small, the grid will not appear.
- **Font for text instructions**. This lets you select a font file from Litho directory that is included with WSxM program.

	Lets you select colors for different states of figures in the design view (normal, selected, executed), for tip, and the dot size to draw them.
	This shows the frame where the image that you are acquiring or that was opened from a file (background image) appears, mixed with lithography patterns showing tip motion (that you can simulate here too), and actions to do while moving the tip. Using "design" you can directly draw patterns (figures), or do it by means of code (see next point).
	Opens the code view, which describes the lithography pattern. You can directly edit it, or add, delete or edit figures drawn in litho design view.
	This is the view where the compilation results of the code appear. And not only this but also the result of compiling a "drawing configuration" (of starting or ending drawn).

Run

	Starts simulation. If you have selected show tip position, you can see it moving over the sample during simulation, conforming to the lithography pattern that you have designed in design frame and source code frame. Executed instructions will change the color (as you have decided in color settings).
	Starts or continues simulation, but only of the next block. When the simulation of the block finish, it will stop there.
	Starts or continues simulation, but only of the next instruction of the current block. If this instruction is a block, it will execute the first instruction of the subblock. When the simulation of the instruction finishes, it will stop there.
	Pauses simulation. This option is only available when you are running a simulation. The simulation stops where it is when you have selected this option.
	Restarts simulation. If you are running a simulation and select this option, simulation will go to the beginning of the code. If you have finished simulation by "step over" or "step into", you need to restart simulation before starting again.

Lithography Design Frame (Design and Simulation)

This is the window that appears when you select "view design". Here you can see drawing instructions and simulations of the code.

New menus that appear here now are the following:

Edit

Selects all instructions that appear in the design view. You can also select an instruction individually by clicking on it, or even select all instructions that are in a rectangle. To dothis, click once on starting selection point, and drop the mouse without unclick,to the finishing selection point, drawing the rectangle. Selection instructions will change color (as you have defined in the color settings). If you click the mouse right button over a selection, a contextual menu will appear, with actions to do with the selection.

	Deselects actual selected instructions.
	Cuts selected instructions to the clipboard (as if you pressed Ctrl+X).
	Copies selected instructions to the clipboard (as if you pressed Ctrl+C).
	Pastes in the design view instructions from the clipboard (as if you pressed Ctrl+V).
	Clears selected instructions (as if you pressed Supr).
	Undoes last action(s) done in design window (as if you pressed Ctrl+Z).
	Undoes last undo(s) done in design window (as if you pressed Ctrl+Y).

Plot

	Draws a dot in the design view. When you select it, you can click on a point of the view to select the position of the dot.
	Draws a line in the design view. When you select it, you can click on a point of the view to select the start position of the line, and click again to select the end position.
	Draws a multiline in the design view. When you select it, you can click on a point of the view to select the start position of the multiline, and click again to select the end position of each partial line.
	This option shows a dialog to write a text in the design window. You can decide the height of text. After you select OK on this dialog, the position of the text has to be defined by clicking at the corresponding location in the design view. Font can be selected in lithography settings frame.

Source Code Frame (Design and Simulation)

Here, you can see the instructions represented in the design view, and add new instructions or modify the existing ones. The language is not case sensitive, that is, you can type *LINE* or *line* and it will threat both words as if they were the same one.

Instructions available are the following ones:

Assignment Instruction

 Description

Assigns a value to a variable.

 Format

```
variable-ident = math-expression ;
```

Block

 Description

Let you organize code, and simulates it as you want, using step over and step into options.

 Format

```
begin
(....)
end
```

- Where (...) are more blocks or other instructions (without any limit).

DoRamp Instruction

Description

Acquires from the specified input channel while applying a ramp in the specified output channel. Optionally, it can apply ramps in two different output channels simultaneously.

Format

```
DoRamp(InputChannels = ("IChnList"),
OutputChannel = "OChn",
NumPoints = numPoints,
InitialValue = Unit,
RampAmplitude = Unit,
Speed = UnitPerSecond,
Point = (NanometersX, NanometersY),
SaveData = bool,
Smooth = bool,
LimitChannel = "LChn",
LimitValue = Unit,
RelativeLimit = bool,
OutputChannel2 = "OChn2",
InitialValue2 = Unit,
RampAmplitude2 = Unit)
```

- IChnList: list with input channel names.
- OChn: output channel name.
- NumPoints: number of points to acquire. It must be between 0 and 4096.
- InitialValue: initial value for acquiring the curve (optional).
- RampAmplitude: ramp amplitude.
- Speed: acquisition speed.
- NanometersX, NanometersY: coordinates where ramp will be applied.
- SaveData: whether or not the curve must be saved.

- Smooth: whether or not the acquired curve must be smoother.
- LChannel: limit channel name.
- LimitValue: limit value (in LimitChannel unit)
- RelativeLimit: whether or not the LimitValue is a relative limit
- OChn2: second output channel (optional).
- InitialValue2: initial value for the second output channel
- RampAmplitude2: ramp amplitude for the second output channel

Remarks

- The Unit for InitialValue, RampAmplitude and Speed is the one selected as default unit for the specified output channel in the Output Channels Manager. The Unit for InitialValue, RampAmplitude also applies for the second output channel, if specified. Speed is only referred to the main output channel.

- IChnList must go between parentheses.

- Channel names must be written between quotes.

- If either OChn2 or InitialValue2 or RampAmplitude2 is specified, OChn2 and RampAmplitude2 are then required. If limit channel and limit value are specified, ramp acquisition will stop when the value measured in limit channel is greater than the limit value. This limit can be either relative or absolute. These values are mutually inclusive: you must either omit both or set the two values.

For Instruction

Description

Repeats an instruction a specified number of times.

Format

```
for (var = init to end step s) do instruction
```

- Var must be a valid variable identifier.
- Both, 'init' and 'end' must be either numeric constants or numeric constant variables, and 'end' must be greater or equal than 'init'
- Instruction can be a block.
- Var cannot be assigned in instruction (it can be read, of course).
- Step is optional. If not present, its value is either 1 or -1, depending on the loop limits).

GetValue Instruction

Description

Reads a value from a channel. This instruction can be used as a numeric value (as a part of any other instruction).

Format

```
GetValue (InputChannel = "IChn", SaveData = bool)
```

- IChn: input channel name.
- SaveData: whether or not the value must be saved (optional). The value in "Saving Options" will be used if omitted.

If Instruction

Description

Executes an instruction only if a certain condition evaluates to true.

Format

```
if ( condition ) then instr-1 [else instr-2]
```

- The 'else' part is optional.
- Both, instr-1 and instr-2 can be instruction blocks.

Line Instruction

Description

Draws a single line. This is a drawing instruction.

Format

```
Line (begin = (NanometersX1, NanometersY1),
end = (NanometersX2, NanometersY2) , InputChannels = ("IChnList"),
NumPoints = NumPoints,
Smooth = bool).
```

- NanometersXi and NanometersYi are absolute coordinates of a point.
- IChn: list with input channel names.
- NumPoints: number of points to acquire. It must be between 2 and 4096.
- Smooth: whether or not the acquired curve must be smoothed (optional). This argument is false by default.

Remarks

- Begin argument is optional. If it is not specified, the beginning of the line will be the actual tip position (it can be the finishing point of the previous line).
- IChnList, NumPoints and Smooth are optional.

Point Instruction

Description

Plots a point. This is a drawing instruction.

Format

```
Point (point = (NanometersX, NanometersY))
```

- NanometersX and NanometersY are absolute coordinates of a point.

ReadDigitalBit Instruction

Description

Reads a single bit from the user input digital signals port. This instruction can be used as a numeric value (as a part of any other instruction).

Format

```
ReadDigitalBit (BitIndex = idx).
```

- idx is the bit index, from 0 to 7 (7 is the most significant bit)
- This instruction is only available to **Dulcinea Electronics** users.

ReadDigitalByte Instruction

Description

Reads the byte in the user input digital signals port. This instruction can be used as a numeric value (as a part of any other instruction).

Format

```
ReadDigitalByte ()
```

- This instruction is only available to **Dulcinea Electronics** users.

SetDrawingConfig Instruction

Description

Changes the current drawing configuration

Format

```
SetDrawingConfig (Name = "ConfigName").
```

- ConfigName is the configuration name. It must be written between quotes.

SetDynamic Instruction

Description

Activates or deactivates the oscillation on the dynamic card and changes the PLL state.

Format

```
SetDynamic (Oscillation = Bool, SwitchRelay = Bool, PLLActive = Bool,
Index = BoardIndex)
```

- Oscillation is stopped or restarted depending on the value of parameter Oscillation (false / true), if present.
- When PLLActive parameter is present, it activates / deactivates the PLL on the specified dynamic board.
- When SwitchRelay is true, the oscillation is started / stopped by changing the corresponding bit in the digital channel. When it is false, it just resets / restores the amplitude channel value. Default value for this parameter is false.
- BoardIndex determines over which dynamic board the changes are made. It can be either 1 (for the first dynamic board) or 2 (for the second dynamic board). Its default value is 1.

SetFeedBack Instruction

Description

Activates or deactivates feedback loop and set feedback parameters.

Format

```
SetFeedback (Index = feedback_index,
active = Bool, P = PValue, I = IValue,
setPoint = SetPointValue, InputChannel = iChn)
```

- All arguments are optional.
- Active (true or false) determines feedback to be turned on/off.
- PValue is the feedback proportional parameter (P).
- IValue is the feedback integral parameter (I).
- SetPointValue is value of the set point in the feedback loop. Units are the same as you have decided in the corresponding panel of the WSxM acquisition frame.
- InputChannel is the feedback channel.
- Index is a number specifying the feedback type. You can choose among the following constant values:

  feedback_index_main (1)
  feedback_index_2nd (2)
  feedback_index_3rd (3)
  feedback_index_4th (4)
  feedback_index_xy (10)
  feedback_index_z (11)

  You can use either the number or the constant.
- The meaning and need of some arguments may vary depending on the feedback chosen:
- PValue,IValue: when using either feedback_index_xy or feedback_index_z, • PValue represents the Power feedback parameter. In such a case, the IValue is ignored.

  When using other feedback type, these values are mutually inclusive: you must either omit both or set the two values.
- SetPoint: this value is ignored when using either feedback_index_xy or feedback_index_z.

- InputChannel: this argument is ignored when using feedback_index_xy.

SetMovementSpeed Instruction

Description

Sets the tip motion speed.

Format

```
SetMovementSpeed (horizontal = nm/sec, vertical = nm/sec);
```

- Units are in nm/sec.
- Both arguments are optional.

SetPlaneScan Instruction

Description

Activates or deactivates the planescan.

Format

```
SetPlaneScan(active = Bool);
```

SetValue Instruction

Description

Sets a value in a channel, as discussed below.

Format

```
SetValue (Bias = BValue); or
SetValue (OutputChannel = "OChn", Value = OValue);
```

- OChn: output channel name, between quotes. Don't use the following channels: "X scan", "Y scan", "Z".
- OValue: value to set in the specified output channel, in channel default unit.
- BValue: voltage to set in the bias output. Value must be specified in millivolts.

Sleep Instruction

Description

Waits for a specified time in milliseconds.

Format

```
Sleep (milliseconds = msec);
```

- msec is time to wait.

Text Instruction

Description

Draws a single line of text. This is a drawing instruction.

Format

```
Text (text = "Text", position = (NanometersX, NanometersY), size =
Size, font = Font, stretch = Stretch));
```

- Text is the text to put in the view.
- NanometersX and NanometersY are coordinates of the position.
- Size, is the height of the text in nanometers.
- Font is the name of the font used when drawing the text. If omitted, default.
- Stretch, is the stretching factor (optional) Its default value is 1.

Variable declaration

Description

Declares a variable with the name 'ident'.

Format

```
Float identifier;
Integer identifier;
Boolean identifier;
```

- This will declare a new variable, of the specified type.
- Variables must be declared before using them.
- You can declare variables only in the main block and before any other instruction.
- Float variables can hold rational numbers. You can use "Numeric" instead of "Float" to declare this kind of variables.

- Integer variables can hold integers in the range -2147483648 to 2147483647.
- Boolean variables can hold the logical values true and false.
- Optionally, you can declare a const variable, by writing the const. keyword before its name. In such case, you must provide its constant value as in an assignment expression.

While instruction

Description

Repeats an instruction until the specified condition is false.

Format

```
While (condition) do instr
```

- Instr can be a block.

WriteDigitalBit Instruction

Description

Writes a single bit to the user output digital signals port.

Format

```
WriteDigitalBit (BitIndex = idx, Value = val);
```

- idx is the bit index, from 0 to 7 (7 is the most significant bit).
- val can be either 0 or 1.

WriteDigitalByte Instruction

Description

Writes a byte to the user output digital signals port.

Format

```
WriteDigitalByte (Value = val);
```

- val must be in the range 0 .. 255.

ZMove Instruction

Description

Moves tip to a given height.

Format

```
Zmove (height = Nanometers, speed = nm/sec);
```

- Nanometers is height to move the tip. Positive value goes away from the sample, that is tip-sample distance is increased. Negative values are allowed but should be used with care.
- nm/sec is average movement speed (optional) .

Commands available for this frame are:

 OPEN CODE	Opens a code from a file, and puts it in the lithography code frame, but without loading. You can also load a Bitmap File (*.BMP). In this case, you will be asked to select the distance between the points of the bitmap (in nanometers). A new Lithography pattern made of Point instructions will be created. There will be points only in the dark zones of the bitmap.
 SAVE CODE	Saves code from the frame in the actual file as is, without checking it. If code is totally new, and you have not loaded it from a file, this option will ask you for a file name.
 SAVE CODE AS	Saves code from the frame in a new file, without checking it.
 APPLY	Applies code changes to the design view. Instructions are compiled, and results appear in the lithography compilation results view. If it was successful, new code will be represented in the lithography design view, and it can be simulated. During simulation the next line ready to execute will change colour. If there are errors, instruction won't appear in the view. Warnings only indicate that something can be wrong, in spite of code compile and will be shown in the view.

Lithography Dialog – Bar

	Activates/deactivates the lithography session. Activation will stop the scan (as if pressed in the selected channel acquisition window) shows the lithography pattern over the acquired image.

Appendix C

Pseudomonas aeruginosa

Member of the *Gamma Proteobacteria* class of Bacteria, it is a Gram-negative, aerobic rod belonging to the bacterial family *Pseudomonadaceae.* Since the revisionist taxonomy based on conserved macromolecules (e.g. 16S ribosomal RNA) the family includes only members of the *genus Pseudomonas,* which are cleaved into eight groups. *Pseudomonas aeruginosa* is the type species of its group containing 12 other members.

Like other members of the genus, *Pseudomonas aeruginosa* is a free-living bacterium, commonly found in soil and water. However, has become increasingly recognized as an emerging opportunistic pathogen of clinical relevance. Several different epidemiological studies track its occurrence as a nosocomial pathogen and indicate that antibiotic resistance is increasing in clinical isolates.

It exploits some break in the host defenses to initiate an infection. In fact,is the epitome of an opportunistic pathogen in humans. The bacterium almost never infects uncompromised tissues, yet there is hardly any tissue that it cannot infect if the tissue defenses are compromised in some manner. It causes: urinary tract infections, respiratory system infections, dermatitis, soft tissue infections, bacteremia, bone and joint infections, gastrointestinal infections and a variety of systemic infections, particularly in patients with severe burns and in cancer and AIDS patients who are immunosuppressed. *Pseudomonas aeruginosa* infection is a serious problem in patients hospitalized with cancer, cystic fibrosis, and burns with case fatality rate near to 50 percent, and the bacterium is the fourth most commonly isolated nosocomial pathogen accounting for 10.1 percent of all hospital-acquired infections.

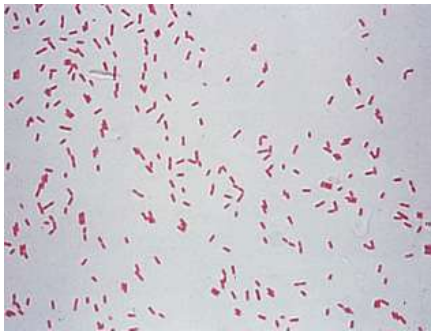

Appendix C.1Gram stain of Pseudomonas aeruginosa cells.[53]

Characteristics

Pseudomonas aeruginosa is a Gram-negative rod measuring 0.5 to 0.8 μm by 1.5 to 3.0 μm. Almost all strains are motile by means of a single polar flagellum.

Its metabolism is respiratory and never fermentative, but it will grow in the absence of O_2 if NO_3 is available as a respiratory electron acceptor.

The typical bacterium in nature might be found in a *biofilm*, attached to some surface or substrate,

or in a planktonic form, as a unicellular organism, actively swimming by means of its flagellum, is considered one of the most vigorous, fast-swimming bacteria seen in hay infusions and pond water samples.

In its natural habitat is not particularly distinctive as a pseudomonad, but it does have a combination of physiological traits that are noteworthy and may relate to its pathogenesis. Some properties:

• Has very simple nutritional requirements and it is often observed "growing in distilled water", which is evidence of its minimal nutritional needs. In the laboratory, the simplest medium for growth consists of acetate as a source of carbon and ammonium sulfate as a source of nitrogen.

• Possesses the metabolic versatility for which pseudomonads are so renowned. Organic growth factors are not required, and it can use more than seventy-five organic compounds for growth.

• Optimum temperature for growth is 37 degrees, and it is able to grow at temperatures as high as 42 degrees.

• Is tolerant to a wide variety of physical conditions, including temperature variations. It is resistant to high concentrations of salts and dyes, weak antiseptics, and many commonly used antibiotics.

• Predilection for growth in moist environments, which is probably a reflection of its natural existence in soil and water.

These natural properties of the bacterium undoubtedly contribute to its ecological success as an opportunistic pathogen. They also help explain the ubiquitous nature of the organism and its prominence as a nosocomial pathogen.

May produce three colony types. Natural isolates from soil or water typically produce a small, rough colony. Clinical samples, in general, yield one or another of two smooth colony types. One type has a fried-egg appearance, which is large, smooth, with flat edges, and an elevated appearance. Another type, frequently obtained from respiratory and urinary tract secretions, has a mucoid appearance, which is attributed to the production of alginate slime. The smooth and mucoid colonies are presumed to play a role in colonization and virulence.

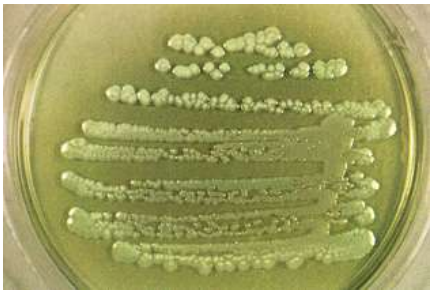

Appendix C.2Pseudomonas aeruginosa colonies on agar[54]

Its strains produce two types of soluble pigments, the fluorescent pigmentpyoverdin and the blue pigment pyocyanin. The latter is produced abundantly in media of low-iron content and functions in iron metabolism in the bacterium. Pyocyanin (from "pyocyaneus") refers to "blue pus", which is a characteristic of suppurative infections caused by *Pseudomonas.*

Appendix C.3The soluble blue pigment pyocyanin is produced by many,but not all, strains of Pseudomonas aeruginosa.[55]

Since its natural habitat is the soil, living in association with the bacilli, actinomycetes and molds, it has developed resistance to a variety of their naturally occurring antibiotics. Moreover, *Pseudomonas* maintains antibiotic resistance plasmids, both R-factors and RTFs, and it is able to transfer these genes by means of the bacterial mechanisms of horizontal gene transfer (HGT), mainly transduction and conjugation.

Only a few antibiotics are effective, and even these antibiotics are not effective against all strains. The futility of treatinginfections with antibiotics is most dramatically illustrated in cystic fibrosis patients.

Diagnosis

Infection diagnosis depends upon isolation and laboratory identification of the bacterium. It grows well on most laboratory media and commonly is isolated on blood agar or eosin-methylthionine blue agar. It is identified on the basis of its Gram morphology, inability to ferment lactose, a positive oxidase reaction, its fruity odor, and its ability to grow at 42°C. Fluorescence under ultraviolet light is helpful in its early identification.

Pathogenesis

For an opportunistic pathogen, the disease process begins with some alteration or circumvention of normal host defenses. The pathogenesis of infections is multifactorial, as suggested by the number and wide array of virulence determinants possessed by the bacterium. Multiple determinants of virulence are expected in the wide range of diseases caused, which include septicemia, urinary tract

infections, pneumonia, chronic lung infections, endocarditis, dermatitis, and osteochondritis.

Most infections are both invasive and toxinogenic and may be seen as composed of three distinct stages:

1. Bacterial attachment and colonization.
2. Local invasion.
3. Disseminated systemic disease.

However, the disease process may stop at any stage. Particular bacterial determinants of virulence mediate each of these stages and are ultimately responsible for the characteristic syndromes that accompany the disease.

Colonization

Although colonization usually precedes infections, the exact source and mode of transmission of the pathogen are often unclear because of its ubiquitous presence in the environment. The fimbriae will adhere to the epithelial cells of the upper respiratory tract and, by inference, to other epithelial cells as well. These adhesins appear to bind to specific galactose or mannose or sialic acid receptors on epithelial cells.

Colonization of the respiratory tract requires fimbrial adherence and may be aided by production of a protease enzyme that degrades fibronectin in order to expose the underlying fimbrial receptors on the epithelial cell surface.

Tissue injury may also play a role in colonization of the respiratory tract, since will adhere to tracheal epithelial cells of mice infected with influenza virus but not to normal tracheal epithelium.

The mucoid exopolysaccharide produced is a repeating polymer of mannuronic and glucuronic acid referred to as alginate. Alginate slime forms the matrix of the *Pseudomonas*biofilm that anchors the cells to their environment and in medical situations; it protects the bacteria from the host defenses such as lymphocytes, phagocytes, the cilia action of the respiratory tract, antibodies and complement. Biofilm mucoid strains are also less susceptible to antibiotics than their planktonic counterparts.

One pigment is probably a determinant of virulence for the pathogen. The blue pigment, *pyocyanin,* impairs the normal function of human nasal cilia, disrupts the respiratory epithelium, and exerts a proinflammatory effect on phagocytes. A derivative of pyocyanin, pyochelin, is a siderophore that is produced under low-iron conditions to sequester iron from the environment for growth of the pathogen. It could play a role in invasion if it extracts iron from the host to permit bacterial growth in a relatively iron-limited environment. No role in virulence is known for the fluorescent pigments.

Appendix C.4Pseudomonas aeruginosa Scanning electron micrograph.

Diseases caused by Pseudomonas aeruginosa

Endocarditis:Infects heart valves of IV drug users and prosthetic heart valves. The organism establishes itself on the endocardium by direct invasion from the blood stream.

Respiratory infections: Respiratory infections occur almost exclusively in individuals with a compromised lower respiratory tract or a compromised systemic defense mechanism. Primary pneumonia occurs in patients with chronic lung disease and congestive heart failure. Bacteremic pneumonia commonly occurs in neutropenic cancer patients undergoing chemotherapy.

Bacteremia and septicemia:*Pseudomonas aeruginosa* causes bacteremia primarily in immunocompromised patients. Predisposing conditions include hematologic malignancies, immunodeficiency relating to AIDS, neutropenia, diabetes mellitus, and severe burns. Most bacteremia is acquired in hospitals and nursing homes.

Central nervous system infections: Causes meningitis and brain abscesses. The organism invades the CNS from a contiguous structure such as the inner ear or paranasal sinus, or is inoculated directly by means of head trauma, surgery or invasive diagnostic procedures, or spreads from a distant site of infection such as the urinary tract.

Ear infections including external otitis: Is the predominant bacterial pathogen in some cases of external otitis, including "swimmer's ear". The bacterium is infrequently found in the normal ear, but often inhabits the external auditory canal in association with injury, maceration, inflammation, or simply wet and humid conditions.

Eye infections:Can cause devastating infections in the human eye. It is one of the most common causes of bacterial keratitis, and has been isolated as the etiologic agent of neonatal ophthalmia. Colonizes the ocular epithelium by means of a fimbrial attachment to sialic acid receptors. If the defenses of the environment are compromised in any way, the bacterium can proliferate rapidly through the production of enzymes such as elastase, alkaline protease and exotoxin A, and cause a

rapidly destructive infection that can lead to loss of the entire eye.

Bone and joint infections: Infections of bones and joints result from direct inoculation of the bacteria or the hematogenous spread of the bacteria from other primary sites of infection. Blood-borne infections are most often seen in IV drug users and in conjunction with urinary tract or pelvic infections.

Urinary tract infections: Urinary tract infections (UTI) caused, are usually hospital-acquired and related to urinary tract catheterization, instrumentation or surgery. The bacterium appears to be among the most adherent of common urinary pathogens to the bladder uroepithelium. As in the case of *E. coli*, urinary tract infection can occur via an ascending or descending route. In addition, *Pseudomonas* can invade the bloodstream from the urinary tract, and this is the source of nearly 40 percent of bacteremias.

Gastrointestinal infections: Can produce disease in any part of the gastrointestinal tract from the oropharynx to the rectum. As in other forms of disease, those involving the GI tract occur primarily in immunocompromised individuals.

Escherichia Coli

Theodor Escherich first described *E. coli* in 1885, as *Bacterium coli commune,* which he isolated from the feces of newborns. It was later renamed *Escherichia coli,* and for many years the bacterium was simply considered to be a commensal organism of the large intestine. It was not until 1935 that a strain of *E. coli* was shown to be the cause of an outbreak of diarrhea among infants.

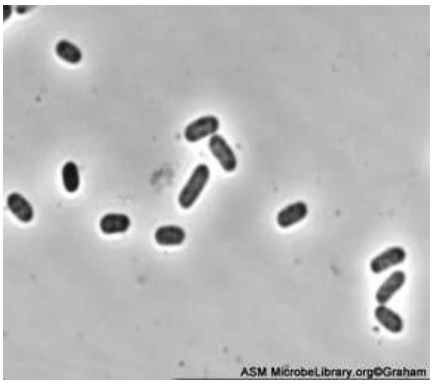

Appendix C.5E. coli O157:H7. Phase contrast image of cells immobilized on an agar-coated slide. William Ghiorse, Department of Microbiology, Cornell University, Ithaca, New York.

Colonizes the GI tract of most warm-blooded animals within hours or a few days after birth. The bacterium is ingested in foods or water or obtained directly from other individuals handling the

infant. The human bowel is usually colonized within 40 hours of birth. Can adhere to the mucus overlying the large intestine and once established, a strain may persist for months or years. Resident strains shift over a long period (weeks to months), and more rapidly after enteric infection or antimicrobial chemotherapy that perturbs the normal flora. The basis for these shifts and the ecology in the intestine of humans are poorly understood despite the vast amount of information on almost every other aspect of the organism's existence. The entire DNA base sequence of genome has been known since 1997.

E. coli is the head of the large bacterial family, *Enterobacteriaceae*, the enteric bacteria, which are facultatively anaerobic Gram-negative rods that live in the intestinal tracts of animals in health and disease. A number of genera within the family are human intestinal pathogens (e.g. *Salmonella*, *Shigella*, *Yersinia*). Several others are normal colonists of the human gastrointestinal tract (e.g. *Escherichia*, *Enterobacter*, *Klebsiella*), but these bacteria, as well, may occasionally be associated with diseases of humans. Physiologically, *E. coli* is versatile and well adapted to its characteristic habitats. It can grow in media with glucose as the sole organic constituent. A wild type has no growth factor requirements, and metabolically can transform glucose into all of the macromolecular components that make up the cell. The bacterium can grow in the presence or absence of O_2. Under anaerobic conditions it will grow by means of fermentation, producing characteristic "mixed acids and gas" as end products. However, it can also grow by means of anaerobic respiration, since it is able to utilize NO_3, NO_2 or fumarate as final electron acceptors for respiratory electron transport processes. In part, this adapts it to its intestinal (anaerobic) and its extraintestinal (aerobic or anaerobic) habitats.

E. Coli can respond to environmental signals such as chemicals, pH, temperature, osmolarity, etc., in a number of very remarkable ways considering it is a unicellular organism. For example, it can sense the presence or absence of chemicals and gases in its environment and swim towards or away from them. Or it can stop swimming and grow fimbriae that will specifically attach it to a cell or surface receptor. In response to change in temperature and osmolarity, it can vary the pore diameter of its outer membrane porins to accommodate larger molecules (nutrients) or to exclude inhibitory substances. With its complex mechanisms for regulation of metabolism the bacterium can survey the chemical contents in its environment in advance of synthesizing any enzymes that metabolize these compounds. It does not wastefully produce enzymes for degradation of carbon sources unless they are available, and it does not produce enzymes for synthesis of metabolites if they are available as nutrients in the environment.

As a consistent inhabitant of the human intestinal tract, and it is the predominant facultative organism in the human GI tract; however, it makes up a very small proportion of the total bacterial content. The anaerobic *Bacteroides* species in the bowel outnumber *E. coli* by at least 20:1. However, the regular presence of *E. coli* in the human intestine and feces has led to tracking the bacterium in nature as an indicator of fecal pollution and water contamination. As such, it is taken to mean that, wherever is found, there may be fecal contamination by intestinal parasites of humans.

Appendix C.6 Unstained cells of E. coli viewed by phase microscopy. about 1000X magnification. CDC.

Escherichia coli in the Gastrointestinal Tract

The commensal *E. coli* strains that inhabit the large intestine of all humans and warm-blooded animals comprise no more than 1% of the total bacterial biomass.

Pathogenesis of *E. coli*

Over 700 antigenic types (serotypes) of *E. coli* are recognized based on O, H, and K antigens. At one time serotyping was important in distinguishing the small number of strains that actually cause disease. Thus, the serotype O157:H7 (O refers to somatic antigen; H refers to flagellar antigen) is uniquely responsible for causing HUS (hemolytic uremic syndrome). Nowadays, particularly for diarrheagenic strains (those that cause diarrhea) pathogenic *E. coli* are classified based on their unique virulence factors and can only be identified by these traits. Hence, analysis for pathogenic *E. coli* usually requires that the isolates first be identified as *E. coli* before testing for virulence markers.

Pathogenic strains of *E. coli* are responsible for three types of infections in humans: urinary tract

infections (UTI), neonatal meningitis, and intestinal diseases (gastroenteritis). The diseases caused (or not caused) by a particular strain of *E. coli* depend on distribution and expression of an array of virulence determinants, including adhesins, invasins, toxins, and abilities to withstand host defenses.

Appendix D

For more information over the AFM source code, matlab scripts…etc. Please contact by mail at:

Ijoni.meta@gmail.com

Bibliography

Books

- V. L. Marinov, *Fundamentals of Scanning Probe Microscopy*, (NT-MDT, 2004)
- R. Howland, L. Benatar*, A practical guide to Scanning Probe Microscopy* (ThermoMicroscopes, 2000)

[1] Richard Feynman - *There's Plenty of Room at the Bottom—An Invitation to Enter a New Field of Physics.* Speech, 1959. URL:http://www.its.caltech.edu/~feynman/plenty.html (January, 2008)

[2] G. Binnig, C.F. Quate, C. Gerber - Scanning Tunneling Microscopy. *Phys. Rev. Lett*. 56 (1986) 930.

[3] G. Binnig, H. Rohrer, Ch. Gerber, E.Weibel - Tunneling through a controllable vacuum gap*. Appl. Phys. Lett*., vol. 40, p. 178 (1982).

[4] *Book:*V. L. Marinov, *Fundamentals of Scanning Probe Microscopy*, (NT-MDT, 2004)

[5] J. G. Simons – Generalized formula for the electric tunnel effect between similar electrodes separated by a thin insulating film. *J. Appl. Phys.*, 34, 1793 (1963).

[6] J. G. Simons - Electric tunnel effect between dissimilar electrodes separated by a thin insulating film. *J. Appl. Phys.*, 34, 2581 (1963).

[7] Atomic Force Microscopy

URL: http://www.chembio.uoguelph.ca/educmat/chm729/afm/firstpag.htm (12.08.2008)

[8] J.S.Barash - Van der Waals forces. *Moscow, Nauka*, 1988.

[9] Lennard-Jones, J. E. - Cohesion. *Proceedings of the Physical Society*, *43*, 461-482 (1931).

[10] M.Saint Jean, S.Hudlet, C.Guthmann, J.Berger – Van der Waals and capacitive forces in atomic force microscopies. *J. Appl. Phys.*, vol. 86 (9), p. 5245 – 5248 (1999).

[11] I.A.Birger, B.F.Shorr, G.B.Iosilevich – Calculation on strength of details of machines. *Mashinostroenie*, Moscow, 1979.

[12] D.Sarid - Exploring Scanning Probe Microscopy with mathematics. *Wiley & Sons*, 1997.

[13]A. D. L. Humphris, J. Tamayo,and M. J. Miles - Active Quality Factor Control in Liquids for Force Spectroscopy. *Langmuir*, *16,* 7891-7894.2000

[14]Tomás R. Rodríguez and Ricardo García - Theory of *Q* control in atomic force microscopy. *Appl. Phys. Lett.*82, 4821 (2003); DOI:10.1063/1.1584790

[15] V. Ph. Pastushenko, P. Hinterdorfer, F. Kienberger, C. Rankl, C. Borken, G. Kada, C. Riener, H. Schindler - Cantilever Oscillations in MAC-Mode AFM: Inertiality and Viscosity Effects of Cantilever - Sample Interaction. *Single Molecules*. Vol.3 Iss.2-3 p.155-158. 2002

[16] International SPM users meeting Scientec

URL: http://usermeeting2008.scientec.fr/

[17] Nanonics

URL: http://www.nanonics.co.il/

[18] SCIENTEC

URL: http://www.scientec.fr/

[19] NanoSurf

URL:http://www.nanosurf.com/

[20] Nanotec Electrónica

URL:http://www.nanotec.es/

[21] C. V. Raman, K. S. Krishnan - A New Type of Secondary Radiation *Nature***121**, 501-502 (31 March 1928)

[22] Manfred von Ardenne, Manfred (1938b). "Das Elektronen-Rastermikroskop. Praktische Ausführung" (in German). *Zeitschrift für technische Physik***19**: 407–416.

[23] [3.14] Futamoto, Masaaki et al., - Development of Technologies for 2-Gb/in2 Areal Density Recording. Electronics and Communications in Japan, Part II-Electronics, vol. 76, No. 3 (Mar. 1993) pp. 94-103

[24] T. Acsente - Laser diode intensity noise induced by mode hopping. *Romanian Reports in Physics, Vol. 59, No. 1, P. 87–92, 2007*

[25] H. Edwards, L. Taylor, W. Duncan and A. J. Melmed. Fast, high-resolution atomic force microscopy using a quartz tuning fork as actuator and sensor. J. Appl. Phys. **82** (3), 1997.

[26] W. H. J. Rensen, N. F. van Hulst,S. B. Kämmer - Imaging soft samples in liquid with tuning fork based shear force microscopy. Appl. Phys. Lett. 77, 1557 (2000).

[27] M. Koopman, B. I. de Bakker, M. F. Garcia-Parajo, and N. F. van Hulst - Shear force imaging of soft samples in liquid using a diving bell concept. Appl. Phys. Lett. 83, 24 (2003)

[28] Agilent Technologies.

URL:http://www.home.agilent.com/agilent/home.jspx?cc=US&lc=eng&cmpid=5443 (24.08.2008)

[29] Aist-Nt

URL: http://www.aist-nt.com/ (24.08.2008)

[30] Asylum Research

URL: http://www.asylumResearch.com/ (24.08.2008)

[31] Veeco

URL:http://www.veeco.com/Products/metrology_and_instrumentation/AFM_SPM/index.aspx (24.08.2008)

[32] Angstrom Advanced Inc.

URL: http://www.angstrom-advanced.com/ (April 2008)

[33] JPK Instruments

URL: http://www.jpk.com/index.2.html (May 2008)

[34] Tomás R. Rodríguez and Ricardo García. Theory of *Q* control in atomic force microscopy.Appl. Phys. Lett. 82, 4821 (2003)

[35] Q Control

URL:http://www.nanoanalytics.com/en/hardwareproducts/qcontrol/howitworks/index.php

[36] Q Control application from Nanoscience Instruments

URL: http://www.nanoscience.com/products/qcontrol_applications.html

[37] NT-MDT

URL: http://www.ntmdt.com/ (June 2008)

[38] Omicron

URL: http://www.omicron.de/ (May 2008)

[39] Pacific Nanotechnology

URL: http://www.pacificnanotech.com/ (June 2008)

[40] Park Systems

URL: http://www.parkafm.com/New_html/main.php(Agust 2008)

[41] RHK Technology

URL: http://www.rhk-tech.com/scanhead.php (July 2008)

[42] Surface Imaging Systems

URL: http://www.surface-imaging.com/ (Agust 2008)

[43] Gnome X Scanning Microscopy project

URL: http://gxsm.sourceforge.net/ (September 2007)

[44] The GNOME desktop environment

URL: http://www.gnome.org (Miguel de Icaza).

[45] TMS320C32 of Texas Instruments (Newer version available)

URL: http://focus.ti.com/docs/prod/folders/print/tms320c32.html (January 2008)

[46] N. Banning, S. Toze and B. J. Mee -Persistence of biofilm-associated *Escherichia coli* and *Pseudomonas aeruginosa* in groundwater and treated effluent in a laboratory model system. Microbiology 149, 47-55 (2003).

[47] G. Yang, S. H. Leuba, C. Bustamante, J. Zlatanove, K. Holde- Role of linker histones in extended chromatin fibre structure.*Nature Structural Biology*1,761-763 (1994)

[48] Carlos Bustamante, Claudio Rivetti, David J Keller - Scanning force microscopy under aqueous solutions. Current Opinion in Structural BiologyVolume 7, Issue 5, Pages 709-716,October 1997.

[49] Matthias Rief, Mathias Gautel, Filipp Oesterhelt, Julio M. Fernandez, Hermann E. Gaub - Reversible Unfolding of Individual Titin Immunoglobulin Domains by AFM.Science Vol.276 no. 5315, pp. 1109 – 1112, 16 May 1997.

[50] D. J. Müller, D. Fotiadis, S. Scheuring, Sh. A. Müller, A. Engel - Electrostatically balanced sub-nanometer imaging of biological specimens by AFM. Biophysical Journal. Volume 76, 1101–1111, February 1999.

[51] F. Moreno-Herrero, J. Colchero,J. Gómez-Herrero,A. M. Baró - Atomic force microscopy contact, tapping, and jumping modes for imaging biological samples in liquids. Physical Review. 69, 2004.

[52] NISE Network

URL: http://www.nisenet.org/publicbeta/articles/seeing_atoms/index.html (12.08.2008)

[53] www.wikipedia.com (November, 2007)

[54] Pseudomonas aeruginosas (September 4, 2008)

URL:http://www.textbookofbacteriology.net/pseudomonas.html

[55] Escherichia Coli (September 4, 2008)

URL:http://www.textbookofbacteriology.net/e.coli.html

[56] WikipediaURL: http://www.wikipedia.org/ (September 4, 2008)

[57] Liwei Chen, Xuechun Yu, Dan Wang. - Cantilever dynamics and quality factor control in AC mode AFMheight measurements. Ultramicroscopy, 107, 275–280 (2007)

[58] Y. Z. Liu, S. H. Leuba, S. M. Lindsay -Relationship between Stiffness and Force in Single Molecule Pulling Experiments. *Langmuir*, *15,* 8547-8548, 1999.

[59] P. Zahl, M. Bierkandt, S. Schröder - The flexible and modern open source scanning probe microscopy software package GXSM. Review of scientific instruments, Vol.74-3 (2003).

[60] William F. Heinz and Jan H. Hoh - Spatially resolved force spectroscopy of biological surfaces using the atomic force microscope. Nanotechnology,Vol. 17, (1999)

[61] S. M. Deupree, M. H. Schoenfisch - Quantitative Method for Determining the Lateral Strength of Bacterial Adhesion and Application for Characterizing Adhesion Kinetics. *Langmuir* 2008, *24,* 4700.

[62] R. J. Cannara, M. Eglin, R. W. Carpick -Lateral force calibration in atomic forcemicroscopy: A new lateral forcecalibration method and generalguidelines for optimization. Review of Scientific Instruments 77, 053701 (2006)

[63] Elena T. Herruzo and Ricardo Garcia - Frequency response of an atomic force microscope in liquids and air: Magnetic versus acoustic excitation. Applied Physics Letters91, 143113 (2007)

[64] A. Asenjo, M. Jaafar - Dislocation mechanisms in the first stage of plasticity of nanoindented Au (111) surfaces. Physical Review B 73, 075431 (2006)